Genosensing of CP4EPSPS DNA Segment in Genetically Modified Cereal Using Luminescent CdSe Quantum Dots

BY

Happy Mabo

A DISSERTATION SUBMITTED TO THE UNIVERSITY OF ZAMBIA IN PARTIAL FULFILMENT OF THE REQUIREMENTS FOR THE DEGREE OF MASTER OF SCIENCE IN CHEMISTRY

THE UNIVERSITY OF ZAMBIA

LUSAKA

Declaration

I, Happy Mabo, do hereby declare that this dissertation represents my own work, with all the sources acknowledged, and that it has never been previously submitted for the award of a degree in part or in full at any other Institution or University.

Signature: .....

Date: 24.06.2025

Copyright

Approval

This dissertation of Happy Mabo is approved as partial fulfillment of the requirements for the award of the degree of Master of Science in Chemistry by the University of Zambia.

Examiner's name	Signature	Date
DR. M-NYIRENDA ~~Examiner I~~ CHAIRPERSON		8/7/25
Dr. Peter M. Chewwa Examiner II		24/06/2025
Dr Evelyn Funjika Examiner III		24/6/2025
Dr. Francis Kayamba ~~Chairperson/Board of Examiners~~ EXAMINER I		24/06/2025
DR JAMES MWENDA Co-supervisor		24/6/2025
Prof. PEGGY MWANZA Co-supervisor		24/06/2025
DR. ONESMUS MUNYATI Principle Supervisor		24/06/25

Abstract

A cadmium selenide quantum dot (CdSe-QDs) based genosensor for the detection of the *CP4 epsps* DNA segment of 5-Enolpyruvylshikimate-3-Phosphate Synthase (CP4 EPSPS) in Genetically Modified Cereal was developed. The efficacy of the CdSe-QDs synthesized from cadmium chloride ($CdCl_2$) and selenium powder (Se) with polyvinyl alcohol (PVA) as a stabilizer was investigated. The QDs were characterised using UV-Vis for film thickness which affects the band gap energy and particle size and Fourier transform infrared spectrophotometry (FT-IR) for functional group analysis and potentiometric tests for determination of signal transduction and limit of detection. The UV-Vis results for the QDs showed a peak of 485 nm with an absorption edge towards 600 nm, which is attributed to the quantum confinement effect. The band gap for the QDs was found to be 3.43 electron Volts (eV) and the average diameter size was 2.82 nm, indicating the successful formation of quantized particles with very high luminescence and this was supported by the shorter absorption wavelength of the particles in the fluorescence measurements obtained. The surface modified and functionalised CdSe QDs gave a maximum binding capacity, Q_m, value of 0.0108 mg/g, and an $R^2 = 0.99902$ for the Langmuir and $R^2 = 0.81190$ for the Freundlich isotherms, indicating that the data fitted better in the Langmuir isotherm model. The FT-IR results showed characteristic absorption bands for thiourea, glutaraldehyde and the immobilized oligonucleotides indicating successful modification of the QDs. In this research the DNA containing samples were qualitatively and quantitatively determined potentiometrically yielding the following results: 92.2% (forward sample, F), 4.1% (reverse sample, R), 76.5% (positive control sample, +ve), 5.4% (negative control sample, -ve), 3.4% (cereal A sample) and 57.9% (cereal B sample) hybridizations. These results indicate that this designed method of detection based on CdSe QDs may actually work as a rapid detection method for GM soyabeans and corn, both qualitatively and quantitatively, and had a very low detection limit of 2.42×10^{-5} ng L^{-1}.

Dedication

For my late father, Deluxe Dennis Mabo, who never gave up on me and ensured that I became the man I am today. I will forever be grateful!

Acknowledgements

My sincere thanks go to my supervisor Dr. Onesimus M. Munyati for his invaluable guidance and unceasing patience. I would like to appreciate my co-supervisors Dr. James Nyirenda and Professor Phenny Mwaanga for their encouragements and support throughout my research work.

My special appreciations go to the University of Zambia, School of Natural Sciences, Department of Chemistry and the Copperbelt University (CBU), School of Mines and Mineral Sciences, Department of Environmental Engineering, for providing me with all the materials and equipment that were needed for my research.

I would like to acknowledge the support I received from my fellow researchers in the Material Sciences Research Group, Robert Singogo, Lameck Tembo, Ian Chisenga, Lilia Mposha, Nonde Kaela, Isabel Chisulo, and Henry Chalwe.

I would also like to thank Dr. Evelyn Funjika, the Head of Department of Chemistry for her assistance and expertise. I also extend my thanks to the following individuals in the Department of Chemistry, School of Natural Sciences, University of Zambia, Mr Chipo Siabbamba, Mr Adolf Lungu, Mr Oswald Musonda and Mr Edward Mweendo, for the assistance they rendered to me.

I am very grateful to the International Science Programme (ISP) through the Sustainable Chemistry and Environment Programme (SCEP) at the University of Zambia, as well as the National Science and Technology Council (NSTC), Zambia, for their patronage.

My heartfelt appreciations go to my elder brother Vincent Mabo for all the love and support he has given to me throughout my life without which this dissertation would not have been possible. I also thank all the members of the Mabo family for their continued love.

Table of Contents

List of Tables

List of Figures

List of Abbreviations

Abbreviations	
BT	*Bacillus thuringiensis*
Buffer AL	A lysis buffer
Buffer ATL	A tissue lysis buffer
Buffer AW1	A washing agent for DNA
Buffer AW2	A washing agent for DNA
Cd	Cadmium
cDNA	Complementary DNA
CdSe	Cadmium selenide
CP4EPSPS	Modified EPSPS
DNA	Deoxyribonucleic acid
ds	Double stranded DNA
EB	Elution buffer
ELISA	Enzyme-Linked Immunosorbent Assay
EPSP	5-enolpyruvylshikimate-3-phosphate
FT-IR	Fourier-Transform Infrared
GA	Glutaraldehyde
GMO	Genetically Modified Organism
HBV	Hepatitis B virus
HOMO	Highest Occupied Molecular Orbital
LOD	Limit of detection
LOMO	Lowest Occupied Molecular Orbital
LOQ	Limit of quantification
Na_2SeSO_3	Sodium selenosulphite
Na_2SO_3	Sodium sulphite
$NaBH_4$	Sodium borohydride
NaOH	Sodium hydroxide
NBA	National Biosafety Authority
PCR	Polymerase Chain Reaction
PVA	Polyvinyl alcohol
QDs	Quantum dots
RNA	Ribonucleic acid
Se	Selenium

SNP	Single Nucleotide Polymorphism
ss	Single stranded DNA
TSC	Trisodium citrate dehydrate
TU	Thiourea
UV-Vis	Ultraviolet Visible
VB	Valence band
VEGF	Vascular Endothelial Growth Factor

Symbols

mL	Milliliter
%T	Percent Transmittance
c	Centi
Eg	Band Gap Energy
g	Gram
L	Litre, volume
I	Current
^{o}C	Degrees Celsius
dm^3	Decimetre cubic
cm^3	Centimetre cubic
cm^{-1}	Per Centimetre
eV	Electron volt
h	Hour
mA	Milliamp
µA	Microamp
mV	Millivolt
ng/mL	Nano Gram Per Millilitre
β	Beta
θ	Theta
λ	Wavelength
µ	Micro
µL	Microliter
π	Pi
d	Film thickness
Δm	Number of peaks
n	Refractive index
R	Ideal gas constant
Q	Angle of incident
T	Kelvin temperature
Q_m	Adsorption capacity
Q_e	Amount of adsorbate
$h\upsilon$	Photon energy

CHAPTER 1

Introduction

1.1 Background

The drive towards growing of crops that are climate resilient in order to ensure food security for the ever increasing human population, has motivated agricultural enterprises in many parts of the world to develop new varieties of food crops through genetic engineering, a technique in which genetically modified organisms (GMOs) are created. A GMO is a plant, animal or any other living organism that has had its genetic material manipulated, often through transgenesis, in order to give the organism a certain desirable trait[1]. This may be done through the modification or introduction or elimination of one or more genes coding for agronomic input traits like agrochemical, drought, and salinity tolerance as well as pest resistance[2].

The use of GMOs in foods, however, has raised a lot of concerns world over that they may potentially cause unforeseen adverse effects. Some have argued in favour that this type of technology is very welcome as it has helped to supplement on the natural food sources[3], while others have argued against such notions as they fear modification of genes in organisms or their feed would lead to the production and expression of features that were not initially present in the organism. The modification could introduce allergenic or toxic substances into the food supply chain causing very serious mutations in either the recipient organisms or those that are made to feed on the manipulated organisms[4]. For example in the case of humans feeding on *Bacillus thuringiensis* (Bt) maize (i.e maize that has been genetically altered to produce the *Bacillus thuringiensis* bacteria, a mutated toxin which kills insects) allergic response, or undesired side effects such as toxicity, organ damage, or gene transfer may result[5].

Other concerns are on the impact that GMOs might have on the environment. Genetically modified plants may potentially cross-breed with wild relatives and create hybrid plants that cause ecological threats and, effect on non-target organisms, such as beneficial insects and birds[6]. For instance the use of glyphosate on herbicide-resistant GMOs has led to increased herbicide-resistant weeds, and this may impact the environment and human health negatively[7]. Furthermore, some other critics have often argued that there has been a lack of long-term studies on the impacts of GMOs on human health and the environment. They advocate for more independent research to assess the long-term effects of GMOs. Therefore, there is a need for monitoring of genetically modified (GM) food products so as to ensure that the contents of the foods that are available on the market are known and thereby enabling consumers to make informed decisions about what they ingest. The monitoring of GMOs and GM foods would be best done at the point of entry into a country. In the case of Zambia which

has not allowed the cultivation of genetically modified crops but has instead put in place regulations to control the import, export, development, research, contained use or placing on the market of genetically modified organisms or their feed[8], analytical laboratories designed explicitly for monitoring genetically modified foods and their products have to be situated at all points of designated entry in the country and trained experts deployed to those areas. The presence of GMOs or deoxyribose nucleic acid (DNA), constructs used in most GM foods can be detected using a genosensor, which is a type of chemical sensor that detects the presence of a biological substance(s) in a given sample[9]. At the moment, in Zambia as a country, the monitoring of GMOs and GM foods is done only by research institutions such as Zambia Agricultural Research Institute (ZARI), under Ministry of Agriculture, and Zambia National Biosafety Authority (NBA), using polymerase chain reaction (PCR) based and enzyme-linked immunosorbent assay (ELISA) based methods on certain allowed GMO containing foods. Seeing that these two methods have their own challenges in terms of cost, lack of the much needed man-power and their inability to deal with all GMO events and false positives and negatives, therefore, the monitoring of GMOs and GM foods has not been done to the full extent that it should have been[10].

The methods of GMO and GM food detection methods currently available are PCR and ELISA based[11 12]. Despite the availability and the current improvements to some of these GMO detection methods, the monitoring of the so many GM foods has not been effective due to the high costs and complexity associated with the machinery used and the protocols, and this has greatly limited the practical application of such approaches for in-field and on-site identification. For example, PCR based methods of measurement face challenges with false positives and false negatives, protein based methods have a limitation in terms of cross-reactivity and the availability of specific antibodies for all GM events[13]. Other methods use complex machines, and expensive software and technologies such as Next-Generation Sequencing (NGS) technologies.

Chemical sensors are devices that use the interaction between the analyte molecule and the sensing part of the device to cause a change in the electrochemical properties of the sensor and produce a readable response[14]. Chemical sensors have the potential to be better at detecting genetically modified (GM) crops than some traditional methods due to their sensitivity, selectivity, and portability[15]. Chemical sensors can detect even small amounts of specific substances or compounds present in GM crops, such as unique metabolites or markers associated with genetic modifications. They offer high sensitivity, allowing for the detection of trace levels of these compounds, which could help accurately identify GM crops, even when present in low concentrations. Chemical sensors can be designed to target and detect unique compounds indicative of GM crops specifically. By relying on selectivity,

these sensors can distinguish between GM crops and non-GM crops or other organisms without specific genetic modifications. This specificity helps to reduce false positives and negatives, thereby improving the chemical sensor's accuracy. Chemical sensors also have the potential to be portable. They can be miniaturised and made portable, enabling on-site or in-field analysis. This portability allows for quick and convenient testing, eliminating the need to send samples to the laboratory. Portability also enables continuous monitoring of crops during cultivation in fields, harvest and distribution, reducing the time between detection and response[15-16].

This study therefore, reports the design and development of an easier, rapid, efficient and low detection limit method for 5-enolpyruvylshikimate-3-phosphate (EPSP) synthase DNA sequence in genetically modified maize and soybeans. EPSP synthase is an enzyme produced by plants and microorganisms to catalyse the chemical reaction shown in Figure 1.1.

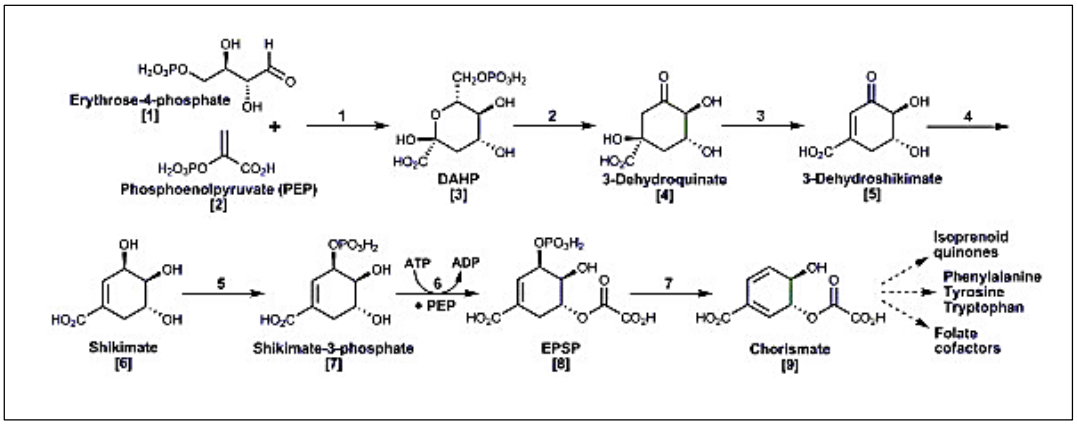

Figure 1.1: Figure shows some steps in the Shikimate Pathway[17]

The genosensor was constructed using CdSe QDs[18]. The synthesised CdSe QDs were surface modified with thiourea and then functionalised with glutaraldehyde which helped to provide them with the necessary ligands for attachment of the capture probe (a 20 base single stranded segment of DNA)[19].

1.2 Statement of the Problem

The development and widespread use of genetically modified organisms (GMOs) have raised considerable concerns regarding their potentially harmful effects on humans and the environment (on non-target organisms and ecosystems) and these concerns have been compounded by the lack of sufficient long-term data to assess their true impact. The limited research conducted on GMOs' long-term impact and the lack of exploration of CdSe QDs for CP4EPSPS gene detection in GM cereals hinder our ability to fully evaluate the potential risks and benefits associated with the use of GM crops.

There are no monitoring laboratories or testing facilities at the food entry points into the country, Zambia. The only form of GMO testing is for research purposes, and this is done by the Zambia Agricultural Research Institute (ZARI) and the Zambia National Biosafety Authority (NBA)[20]. The methods used to test GMOs and GM foods are polymerase chain reaction (PCR) and Enzyme-Linked Immunosorbent Assay, (ELISA). These methods of GMO detection face many challenges in terms of complexity of the equipment used, time-consuming which takes 10 to 12 weeks after receipt of a sample due to the complexity of the process, the high cost of the software used, and the inability of the methods to address the issue of false positives and false negatives.

Furthermore, most people do not know that some if not most of the food products they consume contain GMOs because the companies that process and package these foods do not label them correctly as is required by law. Therefore, there was a need to develop an easier, rapid, efficient and relatively cheaper means of detection which also offered a lower detection limit and this would make it easier for the authorities to enforce the law that prohibits the sale of GMOs. This would in turn compel food-producing and processing companies to label their products and ultimately allow consumers to make informed decisions about whether they would want to consume foods containing GMOs or choose non-GMO-containing foods.

1.3 Significance of the Study

The easy and speedy detection of genetically modified products is very important in that it would help to improve the GMO detection and monitoring capacity of the relevant authorities. This improved detection capacity would not only benefit Zambia, but also other countries that have taken similar stricter measures concerning cultivation, importation, exportation, or direct or indirect use of GMOs. This improved monitoring capacity will then compel all the food producers, biotechnological companies, to correctly label their food products upon packaging and as such this would in turn help consumers to decide on whether to purchase and consume such products or not. The method of detection developed in this study helps to shorten the period of detection from several weeks to several hours, cut out the time and cost associated with DNA sequencing as in the case of PCR based detection[21], Next Generation Sequencing (NGS) technologies such as Illumina Sequencing[22], Digital droplet PCR (ddPCR)[23], and High-Throughput Sequencing such as Ion Torrent Pacific Biosciences[24], for purposes of identification as well as offer high sensitivity, selectivity and a lower limit of detection of 5-enolpyruvylshikimate-3-phosphate synthase DNA segment in genetically modified maize and soybeans. This study also adds to the body of knowledge about synthesis of quantum dots using a cheaper synthetic method and development of an easier detection platform for GMOs.

1.4 Research Questions

i. What are the optimal conditions for synthesis of CdSe QDs using surfactant assisted method?

ii. What is the best architectural design of the CdSe QD-based genosensor?

iii. What are the optimal optical and morphological characteristics of CdSe QDs, and what is the lowest detectable amount of GM food product by CdSe QD-based genosensor?

1.5 Aim

To design, evaluate and optimise a CdSe QD-based genosensor for the detection of 5-enolpyruvylshikimate-3-phosphate synthase DNA sequence in genetically modified maize (*Zea mays*) and soybeans (*Glycine max*).

1.6 Specific Objectives

i. To synthesise and characterise functionalised CdSe QDs.

ii. To design a CdSe QD-based genosensor.

iii. To evaluate the designed CdSe QD-based genosensor in detecting genetically modified maize and soybeans samples, and determine the detection limit.

CHAPTER 2

Theoretical Background

2.1 Introduction

This chapter provides important background information about a sensor, biosensor in a detailed manner that highlights the salient characteristics of these types of sensors. The discussion also includes information about CdSe QDs, very tiny semi-conducting particles, chosen for the design of the genosensor in this study because of the ease with which their properties can be tuned and low cost of synthesis as well as stability when compared to nanoparticles.

2.2 Sensor

A sensor is a device designed to detect and respond to physical inputs or environmental changes, converting them into measurable signals that can be interpreted by an observer or an instrument. These electronic components play a pivotal role in various systems, ranging from everyday consumer electronics to advanced industrial applications[25].

At its core, a sensor operates based on a set of fundamental principles. The most common type is the transducer, which converts one form of energy into another[26]. For instance, a temperature sensor detects changes in temperature and converts this energy into an electrical signal. Sensors employ a variety of mechanisms to capture data, such as optical sensors that use light to sense movement or chemical sensors that react to specific substances.

The key principle behind sensor operation is the transduction process, where a physical quantity such as pressure, light, temperature, or motion is transformed into an electrical signal. This signal is then processed and analyzed by an electronic system to provide useful information (displayed digitally for instance) or trigger appropriate actions[27]. Sensors play a critical role in modern technology, enabling automation, data collection, and monitoring across numerous fields, from healthcare to aerospace and beyond. Their ability to perceive and react to the world around them continues to drive innovation and advancement in countless applications[28].

2.3 Biosensor

A biosensor is a compact analytical device that combines a biological element with a physicochemical detector to provide quantitative or qualitative information about the presence of a specific compound or analyte[29]. Typically, the biological element, such as enzymes, antibodies, or nucleic acids, interacts with the target analyte, leading to a measurable signal that is then detected by the transducer[30]. This signal can be electrical, optical, or thermal in

nature, depending on the biosensor design. Biosensors find applications in various fields, including healthcare, environmental monitoring, and food safety, offering rapid and sensitive detection capabilities that are crucial for diagnosing diseases, detecting pathogens, and monitoring environmental conditions[31]. An example of a biosensor is represented diagrammatically in Figure 2.1 below[32]. The development of biosensors has been driven by advances in nanotechnology, biotechnology, and material science[33]. Recent research has focused on improving biosensors' sensitivity, specificity, and stability. In addition, efforts have been made to integrate biosensors with microfluidics and wireless communication for real-time monitoring[34]. Biosensors have the potential to revolutionize many areas of life sciences and have significant impact on public health and environmental protection[35].

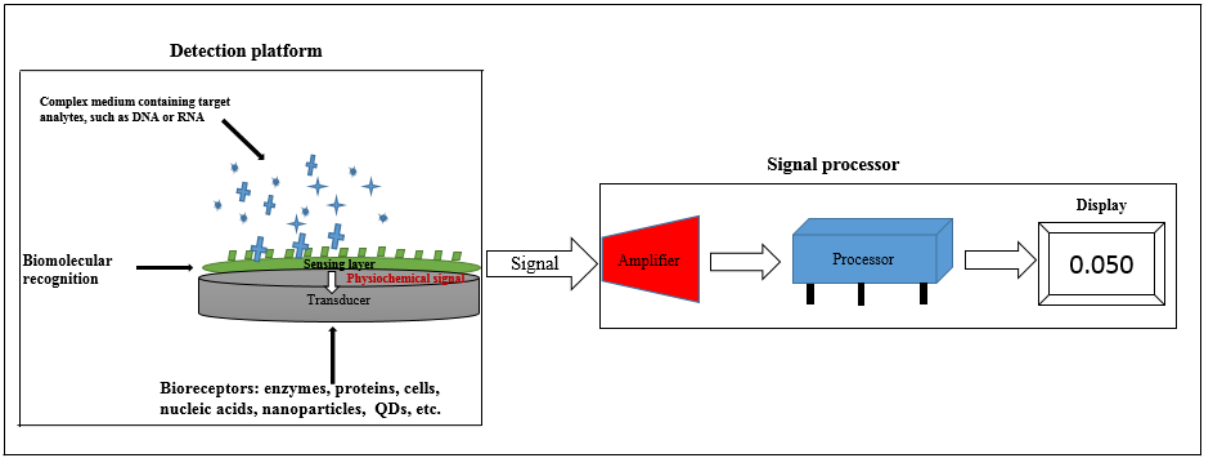

Figure 2.1: Schematic diagram shows the outlay of a biosensor and the interaction with analytes[29, 36]

2.4 Advantages and Disadvantages of Biosensors

Biosensors are powerful analytical devices that combine a biological element with a physicochemical detector to convert a biological response into a measurable signal[29]. These innovative tools offer numerous advantages in various fields, including healthcare, environmental monitoring, food safety, and security[37]. However, like any technology, biosensors also come with their own set of limitations.

One of the primary advantages of biosensors is their high sensitivity, specificity, and selectivity. Sensitivity refers to the ability of a biosensor to detect very low concentrations of analytes, making them ideal for applications requiring the detection of minute quantities of substances. Specificity enables biosensors to accurately distinguish between target analytes and other interfering compounds, ensuring reliable and precise measurements. Selectivity, on the other hand, allows biosensors to detect specific analytes in complex samples with minimal interference from other components[38].

The properties of high sensitivity, specificity, and selectivity in biosensors can be attributed to the unique recognition elements integrated into their design[39]. For instance, enzymes, antibodies, nucleic acids, or whole cells are commonly used as the biological components in biosensors. These bioreceptors interact specifically with the target analyte, triggering a signal that is then transduced by the physicochemical detector[29]. The coupling of the highly selective biological recognition element with a sensitive transducer enhances the overall performance of biosensors.

A notable example of a biosensor is the glucose biosensor used for continuous glucose monitoring in diabetes management. Enzymes such as glucose oxidase are employed to selectively detect glucose levels in blood samples with high sensitivity, enabling patients to monitor and manage their condition effectively[40]. Another example is the use of biosensors in environmental monitoring, where microbial biosensors are utilized to detect pollutants in water sources, offering a rapid and sensitive method for assessing water quality[41].

Despite their numerous advantages, biosensors also present certain disadvantages or limitations. One common limitation is the potential for interference from complex sample matrices, which can affect the accuracy and reliability of measurements[42]. Additionally, biosensors may exhibit variability in performance due to factors such as temperature fluctuations, pH changes, or sensor drift over time, requiring regular calibration and maintenance[43].

To address these limitations, ongoing research in the field of biosensors focuses on enhancing their robustness, stability, and reproducibility. Advancements in nanotechnology, material science, and signal processing have paved the way for the development of more sophisticated biosensors with improved performance characteristics[44].

2.5 Types of Biosensors

Biosensors can be classified into different types based on the transduction mechanism, such as optical, electrochemical, thermal, gravimetric, electronic, and acoustic biosensors[45]. Optical biosensors use light as the transducer to detect biological molecules [46], while electrochemical biosensors use electrodes to convert the chemical signal into an electrical signal [47]. For example the procedure can involve the measurement of the potential difference between two electrodes in contact with the sample[48], and thermal biosensors measure the heat generated or absorbed by the reaction between the biological molecule and the receptor[48-49]. Each type of biosensor

has its own advantages and limitations, and the selection of a biosensor depends on the specific application and the characteristics of the biological molecule to be detected.

2.5.1 Optical Biosensors

In Optical biosensors, which include chromogenic, luminogenic, chemiluminescence, optical fibre and surface plasmon resonance biosensors, biological molecules are detected using light, which then interacts with the transducer[50]. The optical properties of the transducer such as its absorbance or fluorescence change once there is an established interaction between the biological molecule to be detected and the capture probe[50d]. Surface plasmon resonance (SPR) and fluorescence are the two principles on which most commonly used optical biosensors operate[46, 51]. In the SPR biosensors, the biological analyte to be detected, binds to the capture probe of the detection platform and cause a change in the refractive index of the detection platform whereas for the fluorescence based optical biosensor, the biosensor detects the change in the fluorescence intensity[52]. Optical biosensors are highly sensitive and can be coupled with microfluidics for enhanced sensing capabilities [46]. This is done by controlling sample flow, reducing diffusion distances, improving mixing efficiency, and enabling multiplexed analyses in small volumes of samples[53].

2.5.2 Electrochemical Biosensors

Electrochemical biosensors are sensors that use electrodes to convert the chemical signal into an electrical signal. Examples include potentiometric, amperometric, voltametric, conductometric and impedometric biosensors. The interaction between the biological molecule and the receptor causes a change in the electrochemical properties of the electrode, such as potential, current, or impedance[54]. The most widely used electrochemical biosensors are based on amperometry, potentiometry, and impedance spectroscopy[55]. Amperometric biosensors measure the current generated by the oxidation or reduction of the electroactive species produced by the reaction between the biological molecule and the receptor, while potentiometric biosensors measure the potential difference between two electrodes in contact with the sample[56]. Potentiometric biosensors are a type of biosensor that uses a change in potential to detect the analyte of interest. They have several advantages over other types of biosensors, including high sensitivity, low cost, and ease of use. Potentiometric biosensors have been used in a variety of applications, including environmental monitoring, food safety, and medical diagnostics. Recent research has focused on the development of novel potentiometric biosensors using advanced materials such as graphene and nanowires[57]. Impedance

spectroscopy biosensors measure the change in impedance caused by the interaction between the biological molecule and the receptor. Electrochemical biosensors have high sensitivity, selectivity, and fast response time, and they can be miniaturized and integrated with microfluidics for point-of-care testing[47]. Figure 2.2 below, shows a typical example of an electrochemical biosensor.

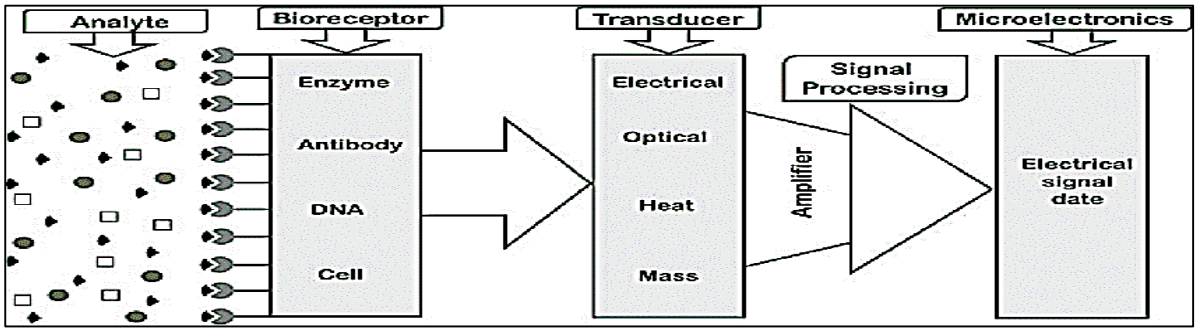

Figure 2.2: Schematic representation of an electrochemical biosensor[58].

2.5.3 Thermal Biosensors

Calorimetric biosensors are a type of thermal biosensors that measure the heat produced or consumed by a biological reaction to detect the presence of an analyte[59]. They have several advantages over other types of biosensors, including high sensitivity and the ability to detect multiple analytes simultaneously. For example in the determination of affinity constants of antibodies, calorimetric biosensors are able to provide high accurate measurements between biomolecules, offering insights into the strength of interactions of such molecules in a biological system[60]. In thermodynamic parameter determination, calorimetric biosensors have been used to accurately measure parameters such as enthalpy, entropy, and Gibbs free energy changes associated with biomolecular interactions, which helps to explain and provide a deeper understanding of reaction mechanisms and their dynamics[61]. Calorimetric biosensors have also been used in a variety of other applications, including medical diagnostics and environmental monitoring[62]. Recent research has focused on the development of novel calorimetric biosensors for the detection of specific analytes, including glucose and bacteria[63].

2.5.4 Gravimetric Biosensors

Gravimetric biosensors are a type of biosensors that detect and measure changes in mass occurring at their sensing surfaces[64]. They utilize transducers that convert the molecular interactions between the target analytes and the sensing surfaces into a measurable mass change. The sensing surfaces are typically coated with bioreceptors, such as enzymes, antibodies, or DNA, which selectively bind to the target analyte[65]. When the analytes interact

with the bioreceptors, the mass of the sensing surfaces change, leading to a shift in the resonance frequency of the transducers. The shift caused is detected and converted into signals that correspond to the concentration or presence of the target analytes. Gravimetric biosensors like Piezoelectric and Magnetoelastic find applications in fields such as environmental monitoring, medical diagnostics, and food analysis[66].

2.5.5 Electronic Biosensors

Electronic biosensors are biosensors that convert the biological recognition events into measurable electrical signals[67]. They typically consist of a biological receptor, transducer and an electronic circuitry. The biological receptor can be an enzyme, antibody, nucleic acid, or a living organism, depending on the target analyte. When the target analyte interacts with the biological receptor, it triggers a biochemical reaction or binding event, leading to the production of an electrical signal[68]. The transducer detects this electrical signal, which is then amplified, processed, and analyzed by the electronic circuitry. Electronic biosensors offer advantages such as high sensitivity, rapid response, and the ability to integrate with microelectronics for miniaturization and portability. They are commonly used in medical diagnostics, environmental monitoring, and biotechnology research[69].

2.5.6 Acoustic Biosensors

Acoustic biosensors are biosensors that utilize sound waves to detect and analyze biomolecular interactions[70]. They operate based on the principle that the binding of target analytes to specific biological receptors on a sensing surface causes changes in the acoustic wave properties. The sensing surface is usually coated with a biological receptor, such as antibodies or aptamers, which selectively recognize and bind to the target analyte[71]. When the binding event occurs, it leads to a change in the mass or elasticity of the sensing surface, resulting in the alteration of the acoustic wave characteristics, such as frequency, phase, or amplitude. These changes can be detected and quantified, providing information about the presence and concentration of the target analyte. Acoustic biosensors have advantages such as label-free detection, high sensitivity and selectivity, real-time monitoring, versatility, stability and reproducibility, as well as miniaturization and portability[72].

2.6 Applications of Biosensors in Genomic Detection

Biosensors that use DNA or RNA as the recognition element to detect specific genetic sequences are called genosensors[73]. They have several advantages over traditional DNA detection techniques, including high sensitivity, specificity, and the ability to perform real-time

monitoring. Genosensors have been used extensively in the field of genomics, including the detection of mutations and the diagnosis of genetic diseases[74]. Recent research has focused on the development of novel genosensors using advanced materials such as gold nanoparticles and graphene [75]. Currently, most genosensors use a variety of nanoscale particles, particularly quantum dots which have superior characteristics in comparison to other nanoscale particles. The properties of these particles make them excellent candidates for use in biological assays, where they can be used as labels to detect and quantify biomolecules of interest, such as proteins, DNA, and RNA. Additionally, quantum dots can be engineered with specific surface properties, allowing them to be targeted to specific biomolecules and cell types[76]. The synthesis and properties of quantum dots is explained in the sections that follow.

2.7 Quantum Dots

Quantum dots (QDs), are tiny semiconducting crystals, whose degree of conductivity depends on their size and purity[77]. The optoelectronic properties of quantum dots can be changed by manipulating the size of the quantum dots[78]. As can be seen from diagram (a) in Figure 2.3 below, the fluorescence colour emitted by quantum dots is dependent on the size of the particles. Typically very small quantum dots with a shorter wavelength have high intensity and emit blue and green fluorescence light while quantum dots with big sizes have longer wavelengths and emit red fluorescence light [79].

The size of the quantum dots also affects the band gap energy of the particles. As the size of the quantum dots decrease the band gap increases giving high energy photons, as can be seen in diagram (b) of Figure 2.3[80]. So, depending on the use of the quantum dots, the size can be tuned to give a specific fluorescence colour.

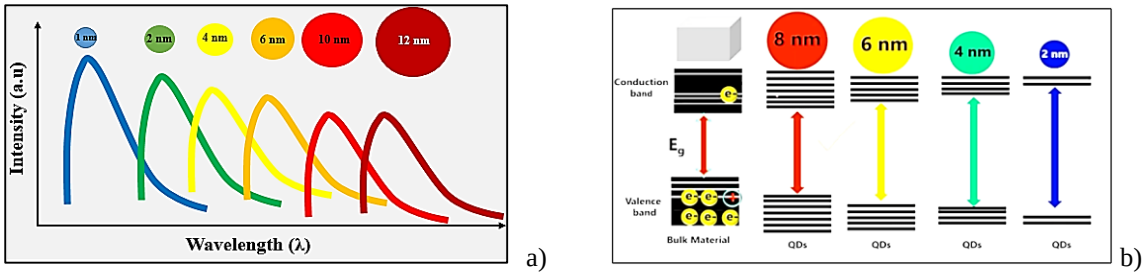

Figure 2.3: Fluorescence and band gap manipulation of quantum dots a) Diagrammatical representation of how the fluorescence colour of quantum dots depends on the size of the quantum dots b) Diagrammatical representation of how the band gap energy increases with decrease in the size of quantum dots[80].

Quantum dots are well suited for developing biosensors due to their unique optical and electronic properties, such as size-dependent fluorescence emission, high quantum yield, and photostability[81].

When quantum dots are used in sensor detection, they are typically functionalized with specific molecules that can specifically bind to the target molecules of interest[82]. This binding causes changes in the optical properties of the quantum dots, such as their fluorescence intensity or wavelength, which can be detected and measured. In sensor applications, the target molecules bind to the functionalized quantum dots on the sensor surface, leading to changes in the fluorescence properties of the quantum dots. By measuring these changes, the presence and concentration of the target molecules can be determined. This allows for highly sensitive detection of various targets, such as biomolecules, gases, or ions, with applications in fields like environmental monitoring, medical diagnostics, and food safety[36].

Specifically, the binding of a target molecule can lead to quenching (reduced fluorescence intensity) or enhancement of the fluorescence of the quantum dots, depending on the specific interactions between the quantum dots and the target molecule[83]. This change in fluorescence can be monitored to detect the presence of the target molecule. The binding of a target molecule can also cause a shift in the emission wavelength of the quantum dots. This shift can be used to identify and quantify the target molecule in the sample. Binding to a target molecule can affect the stability of the quantum dots and their resistance to aggregation or degradation[84]. Changes in stability can impact the performance and durability of the sensor. Quantum dots have a high quantum yield and photostability, which can lead to signal amplification when they bind to target molecules. This can increase the sensitivity of the sensor detection system[85].

2.8 The Band Gap Theory and Quantum Dots Particle Size Estimation

2.8.1 The Band Gap Theory

Band gap theory is a fundamental concept in solid-state physics that explains the behavior of electrons in materials[86]. It revolves around the idea of a band gap, which is an energy range in a material where no electron states can exist. This gap shows the difference between the energy levels where electrons are allowed to exist and those where they are forbidden.

In materials, electrons are arranged in energy bands that are related to the energy levels of the atoms within the material. These include the valence band (VB) or highest occupied molecular orbital (HOMO, which contains electrons at their lowest energy levels, and the conduction band (CB) or lowest unoccupied molecular orbital (LUMO), which contains electrons that can move freely within the material[87]. The gap between the highest-filled energy level and the lowest unfilled energy level is known as the band-gap (Eg)[88]. The band gap theory explains the

classification of materials into conductors, semiconductors, and insulators based on the energy separation between the valence band and the conduction band.

Conductors are materials with overlapping valence and conduction bands, allowing electrons to move freely. Insulators, on the other hand, have a large band gap that prevents electrons from moving from the valence band to the conduction band easily. Semiconductors fall between conductors and insulators; they have a smaller band gap compared to insulators, which allows them to conduct electricity under certain conditions[89].

The band gap is crucial in determining the electrical, optical, and thermal properties of materials. In terms of electrical conductivity, materials with wide band gaps are insulators because the energy required for electrons to jump from the valence band to the conduction band is high. On the other hand, materials with smaller band gaps, such as semiconductors, can conduct electricity with less energy input[90].

The band gap also influences the optical properties of materials[91]. When photons of light interact with a material, they can be absorbed if their energy matches the band gap. The absorption or emission of photons in a material is directly related to its band structure, which determines which wavelengths of light are absorbed or emitted[92].

Furthermore, the band gap theory is essential in the design and development of electronic devices. Semiconductors, with their intermediate band gap, are widely used in electronic components like transistors and diodes. By controlling the band gap through doping or other methods, engineers can manipulate the electrical behavior of these materials to create devices with specific functionalities[93].

2.8.2 Quantum Dots Particle Size Estimation

2.8.2.1 Film Thickness Determination

The formula given below (1), is used to calculate the film thickness of a glass slide coated with nanoscale particles such as QDs[94]:

$$d = \frac{\Delta m}{\sqrt[2]{n^2 - Sin^2\theta}} \times \frac{1}{\left(\frac{1}{\lambda_2} - \frac{1}{\lambda_1}\right)} \quad (1)$$

where

d= film thickness

Δm= number of peaks in the wavelength used for calculation (the number of prominent peaks that appear in the spectrum generated)

n = refractive index of the material on which the particles have been coated

θ = angle of incidence with respect to sample

$\lambda_{1 \text{ and }} \lambda_2$ = start and end wavelength used in the wavelength range used for calculations

2.8.2.2 Band Gap Calculation

The band gap measurement studies of the CdSe QDs were conducted in order to ascertain that the synthesised material was at quantum scale. The indirect band gap energy for CdSe was calculated using the Tauc's relation shown below[95].

$$(\alpha h\nu) = A(h\nu - Eg)^n \quad (2)$$

where

α = molar extinction coefficient of the material

h = Planck's constant

ν = photon's frequency

A = proportionality constant

Eg = band gap of the material

n = factor representing the type of transition of the material (equal to ½ and 2 for direct and indirect band gap respectively).

Take note that for CdSe quantum dots, n is equal to 2, which corresponds to allowed indirect transitions.

2.8.2.3 Particle Size Determination

The size of a quantum dot can be estimated using the relationship between its band gap energy and its physical dimensions, which is described by the quantum confinement effect[96]. The quantum confinement effect arises when the size of the material is reduced to a few nanometers or smaller, leading to the confinement of electrons and holes within a nanoscale volume[97]. This confinement leads to a discrete energy spectrum, and the energy difference between the highest occupied state and the lowest unoccupied state called the band gap as earlier stated above.

The relationship between the band gap energy and the size of a quantum dot can be described by the effective mass approximation and the Brus equation (3)[98]. The effective mass approximation assumes that the electrons and holes in a semiconductor material can be treated as free particles with an effective mass that depends on the size of the quantum dot. The Brus

equation relates the band gap energy to the size of the quantum dot and the effective mass of the electrons and holes[99].

$$E_g = [E_{bulk} + \frac{h^2}{8R^2}\left(\frac{1}{m_e^*} + \frac{1}{m_h^*}\right) - \frac{1.8e^2}{4\pi\varepsilon_0\varepsilon_r R}] \quad (3)$$

where

E_g = band gap energy of quantum dot,

E_{bulk} = band gap energy of the bulk semiconductor material

R = radius of quantum dot

m^*_e = effective mass of excited electron

m^*_h = effective mass of excited hole

h = Planck's constant,

ε_0 = permissivity of vacuum

ε_r = relative permittitivyt (a constant that depends on the dielectric constant and the electron-hole interaction in the material).

Rearranging the Brus equation gives:

$$\mathrm{R} = \sqrt{\left(\frac{\left[\left(\frac{h^2}{8}\right)\left(\frac{1}{m_e^*}+\frac{1}{m_h^*}\right)-\left(\frac{1.8e^2}{4\pi\varepsilon_0\varepsilon_r}\right)\right]}{(E_g - E_{bulk})}\right)} \quad (4)$$

2.8.3 Synthesis of Quantum Dots

Quantum dots (QDs) are semiconductor nanoscale particles with unique optical and electronic properties that make them attractive for a wide range of applications, including biological imaging, solar cells, and electronic devices[100]. Numerous methods have been developed for synthesizing QDs, each with its own advantages and drawbacks[77, 101].

One common method for synthesizing QDs is colloidal synthesis, in which the nanocrystals are prepared in a solution containing a precursor material and a stabilizing agent[102]. This method is relatively simple and inexpensive, and can produce high-quality QDs with narrow size distributions[103]. An example of a colloidal synthesis is shown in Figure 2.4 below, in which high quality carbon quantum dots are synthesised. However, this method of synthesising quantum dots may not be suitable for large-scale production and can result in toxic waste products.

Another method for synthesizing QDs is the solvothermal method, which involves the use of high-pressure and high-temperature conditions to promote crystal growth[104]. This method

typically results in QDs with high crystallinity and good optical properties, but it requires specialized equipment and can be time-consuming[105].

Other methods for synthesizing QDs include electrochemical synthesis, microwave-assisted synthesis, and laser ablation[106]. Each of these methods has its own advantages and drawbacks, and the choice of method will depend on the specific application and desired properties of the QDs[107].

Overall, the development of new synthesis methods for QDs is an active area of research, with the goal of producing QDs with good optoelectronic and high purity.

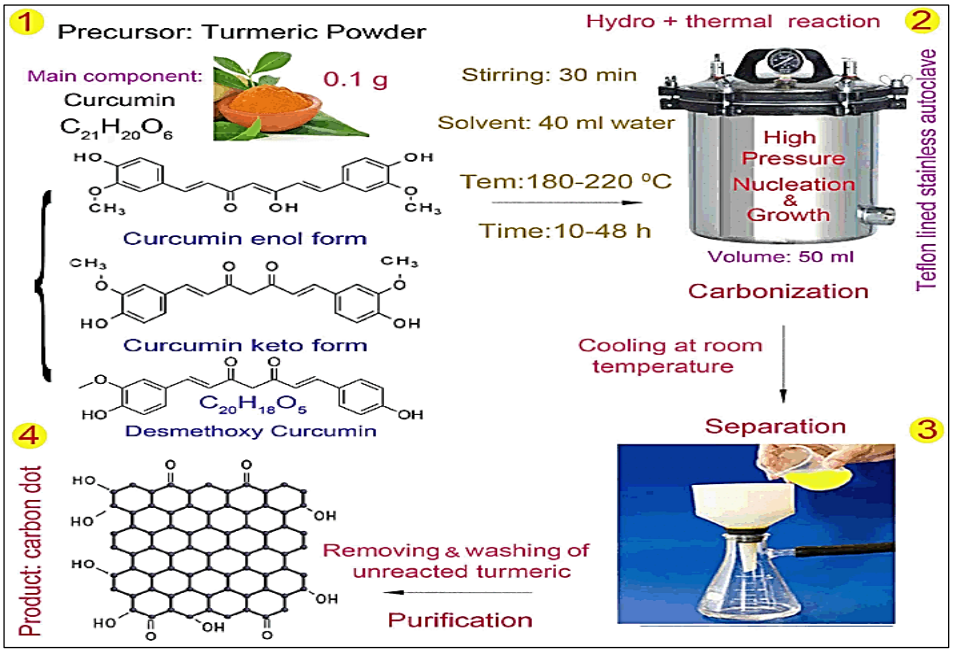

Figure 2.4: Schematic representation of synthesis of carbon quantum dots[108].

2.8.4 Proposed Reaction Steps for the Formation of CdSe QDs

The plausible mechanism of action for the formation of CdSe QDs consists of two concerted steps: (1) the formation of the CdSe QDs and, (2) the stabilization of these QDs using polyvinyl alcohol (PVA)[109].

Step 1: Formation of CdSe QDs

The first step involves the formation of CdSe QDs by reacting a solution of cadmium chloride and trisodium citrate at pH 12, which is adjusted using a 1M sodium hydroxide solution, with a solution of freshly prepared sodium selenosulphite mixed with sodium borohydride. The sodium borohydride acts as a reducing agent, which reduces the sodium selenosulphite to selenide ions. These selenide ions react with the cadmium ions in solution to form CdSe QDs[110].

$$3CdCl_{2\,(aq)} + 2Na_3C_6H_5O_{7\,(aq)} \longrightarrow Cd_3(C_6H_5O_7)_{2\,(aq.)} + 6NaCl_{(aq.)} \quad (5)$$

$$Na_2SeSO_{3\,(aq)} + 4NaBH_{4\,(aq)} + 7H_2O_{(l)} \longrightarrow Na_2Se_{\,(aq.)} + Na_2B_4O_{7\,(aq)} + 15H_{2\,(g)} + Na_2SO_{3\,(aq)} \quad (6)$$

$$Cd_3(C_6H_5O_7)_{2\,(aq)} + 3Na_2Se_{(aq)} \longrightarrow 3CdSe_{\,(aq)} + 2\,Na_3C_6H_5O_{7(aq)} \quad (7)$$

Step 2: Stabilization of the CdSe QDs using PVA

The second step involves stabilizing the CdSe QDs using PVA. Polyvinyl alcohol which is present in the reaction mixture as the QDs are forming, binds to the surface of the CdSe QDs via hydroxyl groups on the polymer. This prevents the QDs from aggregating and stabilizes them in solution in a similar manner to what is depicted in Figure 2.5 below. The PVA also acts as a capping agent, which controls the growth of the quantum dots, resulting in uniform size and shape[111].

Conclusively, the formation of CdSe QDs stabilized by PVA involves a complex series of chemical reactions that require careful control of the reaction conditions to ensure formation of well-defined quantum dots with desired optoelectronic properties[112].

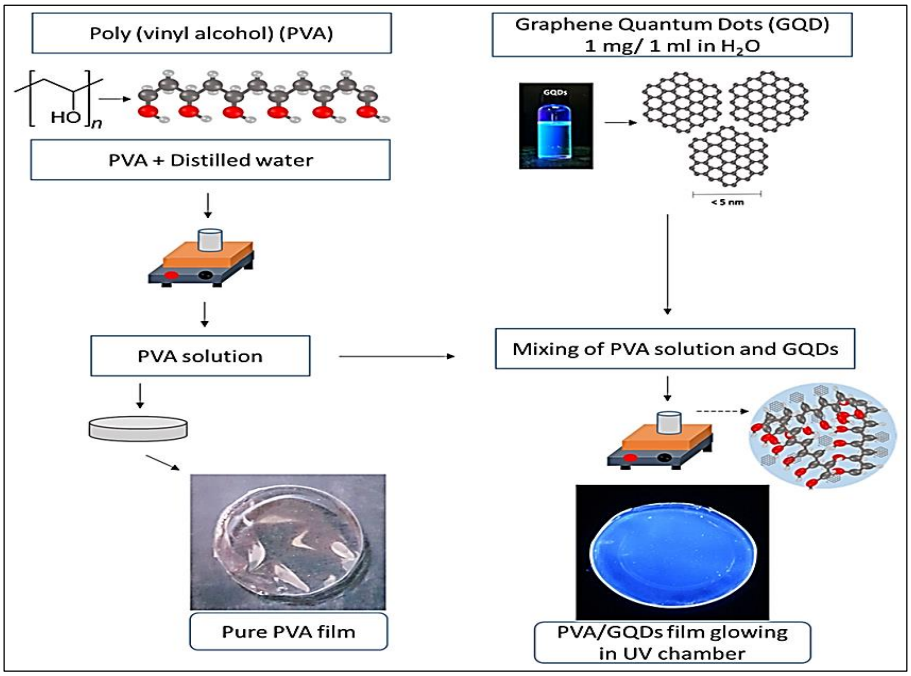

Figure 2.5: Diagrammatic representation of quantum dots stabilization using PVA[113]

2.8.5 Methods of Genosensing Using Quantum Dots

Quantum dots (QDs) are semiconductor nanoscale particles that have unique optical and electronic properties, making them attractive for genosensing applications[90a]. QDs can be functionalized with oligonucleotide probes that can bind to specific DNA sequences[114],

allowing for the detection of genetic mutations or polymorphisms. Studies have been done where QDs have been used to detect single nucleotide polymorphisms (SNPs) in the breast cancer type 1 (BRCA1) gene, which is associated with breast and ovarian cancer, as shown in Figure 2.6 [115]. In these studies, QD-based approach showed high sensitivity and specificity and was able to detect SNPs in both cell lines and clinical samples. Other studies report development of a QD-based genosensing approaches for the detection of GM crops, based on expressed proteins [12]. The QD-based approaches were able to detect GM content in samples from as low as 0.1 ng L^{-1} to as high as 13.2 ng L^{-1} of GM soybeans in non-GM soybeans and showed high selectivity and reproducibility[116]. These studies demonstrate the potential of QD-based genosensing for a variety of applications, including GMO detection and genetic disease diagnosis.

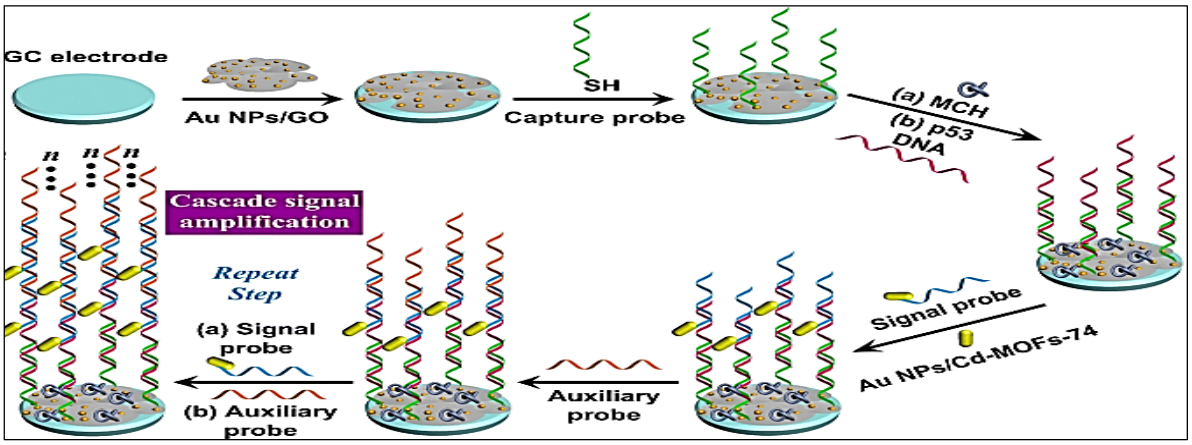

Figure 2.6: Schematic representation of single polymorphism quantum based genosensor [117]

2.9 Adsorption Isotherms

In order to gain insight into the adsorption behaviour of particles such as nano-particles and quantum dots, adsorption isotherm models are used[118]. These models help to explain the interaction between adsorbate molecules and the adsorbent surface, and they can be used to estimate important parameters such as adsorption capacity, affinity, and energetics of the resulting modified particle[119]. Such models include Langmuir, Freundlich and Temkin.

2.9.1 Langmuir Isotherm Model

The Langmuir isotherm model assumes monolayer adsorption onto a homogeneous surface with a finite number of identical adsorption sites. It is based on the assumptions that: adsorption occurs only at specific sites on the surface, each site can accommodate only one adsorbate molecule, there is no interaction between the adsorbed molecules and all adsorption sites are

identical and energetically equivalent[120]. The nonlinearized Langmuir isotherm equation is given by:

$$Q_e = \frac{Q_m K_L C_e}{(1+K_L C_e)} \quad (8)$$

where:

C_e is the equilibrium concentration of the adsorbate in the solution.

Q_e is the amount of adsorbate adsorbed per unit mass of adsorbent.

Q_m is the maximum adsorption capacity of the adsorbent.

K_L is the Langmuir constant related to the affinity of the adsorbate for the adsorbent.

The Langmuir isotherm model provides information about the maximum adsorption capacity (Q_m) and the equilibrium constant (K_L), which provides insights into the strength of the adsorbate-adsorbent interaction. The linearised form of the Langmuir equation is shown below:

$$\frac{C_e}{Q_e} = \frac{1}{(Q_m K_L)} + \frac{C_e}{Q_m} \quad (9)$$

2.9.2 The Freundlich Isotherm Model

The Freundlich isotherm model describes adsorption on heterogeneous surfaces. It assumes multilayer adsorption onto a surface with a non-uniform distribution of adsorption energies. The Freundlich model assumes that adsorption occurs on a heterogeneous surface with different adsorption energies, the adsorption capacity decreases as the surface becomes more and more occupied with adsorbates and that there are no specific adsorption sites[121].

The Freundlich isotherm equation is given by:

$$Q_e = K_F C_e^{\frac{1}{n}} \quad (10)$$

where:

Q_e is the amount of adsorbate adsorbed per unit mass of adsorbent.

C_e is the equilibrium concentration of the adsorbate in the solution.

K_F is the Freundlich constant related to the adsorption capacity.

n is the Freundlich constant related to the adsorption intensity.

The Freundlich isotherm model provides information about the adsorption capacity (K_F) and the adsorption intensity (n)[122]. The parameter n represents the linearity or nonlinearity of the adsorption process. When n is equal to 1, it indicates a linear adsorption isotherm, and the adsorption process is favourable. If n is greater than 1, it suggests a cooperative adsorption

process, meaning that the adsorption becomes increasingly favourable as the concentration of the adsorbate increases. On the other hand, if n is less than 1, it indicates a less favourable or unfavourable adsorption process, where the adsorption decreases as the concentration of the adsorbate increases[123].

In the linearized equation shown below:

$$\text{In } Q_e = \frac{1}{n}\text{In}C_e + \text{In } K_F \quad (11)$$

where Q_e and C_e are the same as in Langmuir isotherm, K_F and n are the Freundlich constants. K_F [(mg/g) (L/g) $^{1/n}$] is related to the binding energy of the adsorbent and n is the heterogeneity factor that measures the deviation from the linearity of the adsorption.

2.9.3 Temkin Isotherm Model

The Temkin isotherm model incorporates the effects of adsorbate-adsorbent interactions and assumes a linear decrease in adsorption energy with coverage[124]. The assumptions of the Temkin model are that, the heat of adsorption decreases linearly with coverage, there is a uniform distribution of binding energies and that there is no interaction between adsorbed molecules[125].

The Temkin isotherm equation is given by:

$$\frac{q_e}{q_m} = \frac{RT}{b_T}\text{In}(K_L C_e) \quad (12)$$

where:

q_e and q_m are the equilibrium and saturated adsorption amount of solute on solid surface respectively (mg/g)

R is the ideal gas constant (8.314 J/ mol·K)

T is the temperature (in Kelvin)

b_T is the adsorption to heat parameter (J/mol)

K_L is the adsorption equilibrium constant of solute on solid surface (L/mg)

Ce is the equilibrium concentration of the solute (mg/L).

The Temkin isotherm model is suitable for describing various adsorption processes, including both physical and chemical adsorptions. It can provide insights into the surface heterogeneity and the interaction between the adsorbate and the adsorbent.

CHAPTER 3

Literature Review

3.1 Introduction

This chapter gives a review of what genosensing is and how it relates to genetically modified organisms (GMOs) detection, the concerns surrounding their use and the methods that are available for their detection and the challenges associated with such existing methods. The chapter also looks at genosensing using quantum dots and the ethical considerations.

Genosensing is a technique that involves the detection of specific genetic sequences within a sample, as explained by Sanchez-Paniagua et al.[126]. In the context of genetically modified crop detection, genosensing plays a crucial role. By targeting and identifying unique genetic markers inserted into the DNA of genetically modified crops, genosensing allows for the accurate and efficient identification of these modified organisms[127]. This is essential for regulatory purposes, ensuring proper labeling and monitoring of GM crops in the food supply chain. Furthermore, genosensing can help verify the authenticity and prevent the fraudulent labeling of non-GM crops[128]. However, there is a lack of exploration of CdSe QDs for cp4epsps gene detection in GM cereals in almost if not all the current methods of GM crop detection[129].

3.2 CP4EPSPS Gene and GMO Controversy

The cp4epsps gene, also known as the 5-enolpyruvylshikimate-3-phosphate synthase gene, is a key component in genetically modified organisms. This gene is often inserted into the DNA of GMOs to confer resistance to glyphosate-based herbicides, such as Roundup. By producing an enzyme that allows the plant to continue producing essential amino acids in the presence of the hercide, crops with the cp4epsps gene are able to survive glyphosate applications while weeds are eradicated. This trait has been widely adopted in genetically modified crops, leading to increased efficiency in weed control and crop management by farmers.

Genetically modified (GM) crops, particularly soybeans and corn, have been a topic of controversy for several years[130]. The primary concern is the potential impact on human health and the environment. Soybeans and corn are two of the most widely grown GM crops in the world, with approximately 90% of soybeans and 85% of corn grown in the United States being genetically modified as reported by Qaim[131].

The primary benefit of GM soybeans and corn is their ability to resist pests and herbicides, which increases crop yields and reduces the need for pesticides[3b, 132]. However, concerns have

been raised about the potential harm to human health and the environment due to the widespread use of genetically modified crops[130a]. Studies have shown that GM crops can have unintended adverse effects on non-target organisms, such as beneficial insects and soil microorganisms as reported by Van[133].

Domingo[134] reports that there are also concerns about the potential for GM crops to cross-pollinate with non-GM crops, leading to the unintentional spread of GM traits. Additionally, there is a lack of long-term studies on the impact of GM crops on human health, which has led to controversy and debate[135].

Beeckman and Rudelsheim[136] report that regulatory frameworks for GMOs vary between countries and regions, although generally they aim to ensure the safety of GMOs for human health and the environment. These frameworks typically involve risk assessment procedures to evaluate the potential impacts of GMOs on ecosystems and human health. They also often require GMO labeling to imform consumers about the presence of GM ingridients in food products. Additionally, regulatory frameworks may involve monitoring and post-market surveillance to track the long-term effects of GMOs once they are released into the environement. The ultimate goal of these regulatory frameworks is to balance the benefits of GMO technology with potential risks, ensuring responsible development of genetically modified crops and products, as reported by Righelato[137].

Despite these concerns and the extant regualatory frameworks, the use of GM crops continues to increase due to their benefits in terms of increased crop yields and reduced pesticide use. As such, it is important to continue monitoring the potential impact of GM crops on human health and the environment[138].

There has been restricted investigation done on advanced genosensing techniques for identifying cp4epsps gene in GM crops[129a]. This study therefore, delves into developing a detection method aimed at enhancing sensitivity and realibilty of detecting cp4epsps DNA segment, a gene that codes for an enzyme linked to herbicide-resistant GM crops.

3.3 GMOs and their Prevalence in the Food Industry

Genetically modified organisms refer to organisms whose genetic material has been altered using genetic engineering techniques[139]. Amaro-Blanco et al.[140] report that in the context of food, GMOs are often created by introducing genes from one species into another to confer specific traits, such as increased resistance to pests, diseases, or herbicides.

The presence and regulation of GMOs in the market vary from country to country[141]. Some countries, such as the United States, have a relatively high adoption of GMO crops, while others have stricter regulations or limited GMO cultivation[142]. Common genetically modified crops include soybeans, corn, cotton, canola, and sugar beets. These crops are often used as ingredients in many food products, such as oils, sweeteners, and processed foods, as reported by Oguchi et al.[143]

In terms of adoption and market penetration, genetically modified crops, particularly soybeans, corn, cotton, canola, and sugar beets, have been widely cultivated and incorporated into numerous food products in many countries, as reported in (The International Service for the Acquisition of Agri-biotech Applications) ISAAA[144]. On the 23rd year of commercialization of biotech/GM crops in 2018, 26 countries grew 191.7 million hectares of biotech crops[144]. The United States, Brazil, Argentina, Canada, and India are among the leading producers of genetically modified crops. The average biotech crop adoption rate in the top five biotech crop-growing countries increased in 2018 to reach close to saturation, with USA at (93.3%) (average for soybeans, maize, and canola adoption), Brazil (93%), Argentina (~100%), Canada (92.5%), and India (95%). The number of African countries currently growing biotech crops stands at 3– South Africa at (3.4%), Sudan at (0.3%), and eSwatini at (3.9%). Two more countries – Ethiopia and Nigeria gave environmental release approvals: Ethiopia for Bt cotton, while Nigeria approved cotton and cowpea. Earlier, Kenya and Malawi also granted environmental release approvals and are working towards commercialization of biotech cotton in the short-term[145]. Figure 3.1 below shows the percentage growth of the five top biotech crops globally, while Table 3.1 shows the area allotted for cultivation of specific biotech crops.

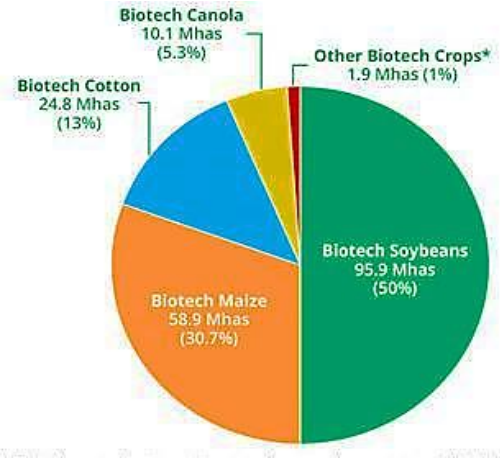

Figure 3.1: Biotech crops in 2018, eggplant (Area and adoption rate). *Sugar beets, potatoes, apples, squash, papaya, and brinjal/eggplant. Source: ISAAA, 2018[144].

Table 3.1: Global Area of Biotech Crops in 2018: by Country (Million Hectares)**

Rank	**Country**	**Area (Million Hectares)**	**Biotech Crops**
1	USA*	75.0	Maize, soybeans, cotton, canola, sugar beets, alfalfa, papaya, squash, potatoes, apples
2	Brazil*	51.3	Soybeans, maize, cotton, sugarcane
3	Argentina*	23.9	Soybeans, maize, cotton
4	Canada*	12.7	Canola, maize, soybeans, sugar beets, alfalfa, potatoes
5	India*	11.6	Cotton
6	Paraguay*	3.8	Soybeans, maize, cotton
7	China*	2.9	Cotton, Papaya
8	Pakistan*	2.8	Cotton
9	South Africa*	2.7	Maize, soybeans, cotton
10	Uruguay*	1.3	Soybeans, maize
11	Bolivia*	1.3	Soybeans
12	Australia*	0.8	Cotton, canola
13	Philippines*	0.6	Maize
14	Myanmar*	0.3	Cotton
15	Sudan*	0.2	Cotton
16	Mexico*	0.2	Cotton
17	Spain*	0.1	Maize
18	Colombia*	0.1	Cotton, maize
19	Vietnam	<0.1	Maize
20	Honduras	<0.1	Maize
21	Chile	<0.1	Maize, soybeans, canola
22	Portugal	<0.1	Maize
23	Bangladesh	<0.1	Brinjal/Eggplant
24	Costa Rica	<0.1	Cotton, soybeans
25	Indonesia	<0.1	Sugarcane
26	eSwatini	<0.1	Cotton
	Total	**191.7**	

*18 biotech mega-countries growing 50,000 hectares, or more, of biotech crops

**Rounded-off to the nearest hundred thousand.

Source: ISAAA, 2018[144].

Gaskell et al. and, Lusk and Rosan [146], report that when it comes to the issue of GMO labelling and consumer awareness, various countries have implemented different regulations. Some require mandatory labelling of GMO-containing products, while others do not. Consumer awareness and preferences for GMO labelling vary geographically, with some consumers expressing a desire for clear and transparent labelling.

Safety and health concerns of GMOs are a subject of ongoing scientific debate[147]. Based on the short-term studies that have been done, numerous scientific organizations, including the National Academy of Sciences and the World Health Organization, have concluded that genetically modified foods currently on the market are safe to consume[134, 148]. Critics, however, express concerns about potential long-term health effects, environmental impacts, and the economic implications of GMO adoption, including the consolidation of seed companies and the loss of crop diversity[147b, 149]. It should be noted that most of these studies have been conducted and funded by biotechnology companies responsible of commercializing these GM plants. Studies specifically addressing safety assessment of GM plants are still limited, published literature on GM plants over the past 4 years concerns only 3 products, therefore, more efforts are required to build confidence in the evaluation/acceptance of GM plants[149-150].

According to Kuzma and Vermaas[151], many countries have adopted different approaches in order to try and deal with the issue of GMOs . For example, some European countries like France, Germany and Italy have banned the use of GMOs completely while other countries on the other hand like the United States of America and Brazil have adopted softer measures, allowing cultivation and consumption of GMOs[144, 152]. Other countries yet still have implemented various regulatory frameworks to assess and manage GMOs' safety and environmental impacts. These frameworks involve rigorous pre-market assessments, including safety evaluations and environmental risk assessments. Regulatory approaches differ between countries, and public opinion plays a significant role in shaping the regulatory landscape[153]. However, it is important to note that scientific research and public perceptions of GMOs continue to evolve.

3.4 Previous Studies and Current Methods of GMO Detection

Detecting genetically modified (GM) soybeans and corn involves the use of various analytical methods. This section discusses some commonly used methods, along with the associated challenges.

Holst-Jensen et al.[154] report that Polymerase Chain Reaction (PCR) is a widely used method for detecting genetically modified organisms (GMOs) by amplifying specific DNA sequences that are characteristic of GM traits. It allows the identification of specific genetic elements introduced into the plant. However, PCR-based methods face challenges in terms of sensitivity, specificity, and the potential for false-positive or false-negative results. Despite its wide spread use, PCR primers may not be perfectly specific leading to non-target amplification, the presence of PCR inhibitors such as salts and humic acids can reduce its reaction efficiency, and there are cross-reactions between primers which can reduce the accuracy of the method[155].

James[145] reports that enzyme-linked immunosorbent assay (ELISA), is an immunological method that detects specific proteins or antibodies associated with GM traits. It can identify the presence of GM proteins in soybeans and corn. However, ELISA-based methods have limitations in terms of cross-reactivity, failure to identify expressed proteins in over-processed GMO containing foods, and the nonavailability of specific antibodies for all GM events[155].

Pallejà et al.[156] report that Next-Generation Sequencing (NGS) technologies can provide comprehensive genomic information, enabling the detection of GM traits by comparing the DNA sequences of a sample with a reference database. While NGS offers high-throughput and unbiased analysis, it requires expensive and sophisticated bioinformatics tools and reference databases for accurate identification.

Morisset et al.[157] report that Digital PCR (dPCR) can be used to partition DNA into thousands of small reactions, allowing quantification of target sequences. It can provide quantification of GM DNA and detect relatively low levels of GM contamination. However, dPCR has challenges related to assay design, cost, sensitivity and selectivity, and the need for specialized equipment.

Mass Spectrometry (MS)-based methods analyze protein or peptide profiles to identify GM proteins in soybeans and corn. It offers high specificity and can detect multiple GM traits simultaneously as reported by Zhang and co-authors[158]. However, MS methods require skilled operators, sophisticated equipment, and reference protein databases for accurate identification.

It's important to note that the field of GMO detection is dynamic, and new methods and technologies continue to emerge. The methods available fail to address the issue of false positives and negatives and there are no standardized detection methods and protocols to ensure consistency and accuracy across laboratories. Therefore, endeavoring to come up with new and easier methods of detection based on quantum dots due to their potential for enahanced sensitivity and specificity is crucial for accurate GM crop detection.

3.5 Quantum Dot-based Genosensing

Dong et al.[159] report that quantum dots (QDs) are nanoscale semiconductor particles, with unique optical and electrical properties that make them valuable in genosensing applications. These advantanges include hgh photosatability, tunable fluorescence, and size-dependent emission spectra. By leveraging these properties, QDs enhance the sensitivity and specificity of genosensing assays, enabling efficient detection of genetic material.

Incorporating quantum dots in genosensing opens up new possibilities for accurate and reliable genetic analysis in various fields such as medicine, environmental monitoring, and biotechnology, as reported by Zhang et al.[160]

Genosensing using CdSe quantum dots has been an area of intense research in recent decades due to its potential applications in medical diagnostics, environmental monitoring, and genetic analysis as reported by O'Connor et al[161]. The various aspects of genosensing using CdSe quantum dots, including their synthesis, functionalization, and applications are discussed here.

CdSe quantum dots have unique optical and electronic properties, making them ideal for use in genosensing applications[90a]. They have a high surface area to volume ratio, which provides a large number of binding sites for DNA molecules. CdSe quantum dots can be synthesized using various methods, including the colloidal synthesis, sol-gel synthesis, and hydrothermal synthesis, as earlier explained above[162]. Among these methods, colloidal synthesis is the most commonly used method due to its simplicity, reproducibility, and scalability[163].

Fan et al. [164] explain that functionalization of CdSe quantum dots is essential for their application in genosensing. Functionalization can be achieved through covalent or non-covalent interactions. Covalent functionalization involves the formation of a covalent bond between the CdSe quantum dots and the molecule being used to improve its surface properties. Non-covalent functionalization, on the other hand, involves the use of electrostatic, hydrophobic, or van der Waals interactions. The choice of functionalization method depends on the application and the properties of the DNA segment to be attached to them.

Genosensing using CdSe quantum dots has been demonstrated in various applications, including DNA detection and gene expression analysis[165]. DNA detection using CdSe quantum dots involves the hybridization of the target DNA with the complementary probe DNA that is attached to the surface of the CdSe quantum dots. The hybridization event leads to a change in the optical properties of the CdSe quantum dots, which can be detected using fluorescence spectroscopy. For example CdSe quantum dots have been reported to have been used in the detection of progesterone in human serum, as reported by Oh et al.[166]

Several studies have reported the use of CdSe quantum dots in genosensing applications[160, 167]. For example, Chen et al.[115] report the use of CdSe quantum dots for the detection of Mycobacterium tuberculosis DNA. The authors in this study functionalized the CdSe quantum dots with thiolated DNA probes and demonstrated the specific detection of the target DNA with a limit of detection of 2.2 nM. Fang et al.[168] report the use of CdSe quantum dots for SNP genotyping of the CYP2C19 gene, which is associated with drug metabolism. These authors functionalized the CdSe quantum dots with allele-specific probes and demonstrated the specific detection of the target SNPs with high sensitivity and selectivity. Huang et al.[169] reported the use of CdSe quantum dots for gene expression analysis of the vascular endothelial growth factor (VEGF) gene. The authors functionalized the CdSe quantum dots with DNA probes that specifically hybridize with the VEGF mRNA and demonstrated the specific detection of the target mRNA in cancer cells.

Finally, it can be said that genosensing using CdSe quantum dots has emerged as a promising technology for DNA detection, SNP genotyping, and gene expression analysis. The unique optical and electronic properties of CdSe quantum dots, combined with their high surface area to volume ratio, make them ideal for use in genosensing applications. However, to the best of the researcher's knowledge, there has been an insufficient exploration of CdSe QDs for cp4epsps detection in GM cereals.

3.6 Advances in Quantum Dot-based Genosensing

Quantum dots have emerged as a promising platform for genosensing applications due to their unique optioelectronic properties, making them ideal candidates for bioanalytical techniques. In recent years, significant advancements have been made in utilizing CdSe QD-based genosensing for various biomedical purposes, as reported by Chen et al.[170] and Meysam[171].

According to Gupta and Rajamani[172], one of the notable developments in this field is the improved sensitivity achieved through the functionalization of CdSe QDs with specific DNA

probes. By attaching complementary DNA sequences to the quantum dots, researchers have been able to enhance the selectivity and efficiency of genosensing assays. This strategy has enabled the detection of target DNA sequences with high precision, even in complex biological samples[173].

Furthermore, Lui et al.[174] report that, the integration of CdSe QDs into microfluidic devices has facilitated the miniaturization and automation of genosensing platforms. These lab-on-a-chip systems allow for the rapid and high-throughput analysis of nucleic acids, offering potential applications in point-of-care diagnostics and personalized medicine. By leveraging the unique optical properties of CdSe QDs, such as their tunable emission wavelengths and exceptional photostability, researchers have been able to develop sensitive and reliable genosensors for various genetic markers.

Moreover, the development of multiplexed genosensing assays based on CdSe QDs has enabled the simultaneous detection of multiple DNA targets in a single experiment. This capability is particularly valuable for applications requiring the parallel analysis of different genetic sequences, such as genotyping and mutation screening. By functionalizing distinct quantum dots with complementary DNA probes specific to different target sequences, researchers have achieved multiplexed genosensing with high throughput and accuracy, as reported by Vijian et al.[175]

Liu et al.[176] report that in addition to their application in DNA detection, CdSe QDs have also been explored for the detection of RNA molecules and proteins. By designing aptamer-functionalized quantum dots capable of binding to specific RNA or protein targets, researchers have expanded the utility of these nanomaterials in bioanalytical assays. This versatility highlights the potential of CdSe QD-based genosensing for a wide range of biomedical applications beyond DNA analysis.

According to Davoodi et al.[177], it has also been noted that CdSe QD-based genosensing offers significant advantages over traditional methods and other nanomaterials in DNA detection. This is because QDs possess unique optical properties, such as size-tunable emission and high photostability, making them ideal for sensitive and specific genosensing applications, as reported by Sapsford et al.[178]. In contrast to traditional methods that often rely on complicated labelling techniques or time-consuming protocols, CdSe QD-based genosensing is simpler,

faster, and more cost-effective. Additionally, their high surface-to-volume ratio allows for enhanced biomolecular interactions, leading to improved detection sensitivity.

When compared to other nanomaterials like gold nanoparticles or carbon nanotubes, CdSe QDs demonstrate superior performance in terms of signal amplification and target DNA detection. Their ability to efficiently transfer electrons and energy makes them valuable tools in genosensing applications, enabling accurate and rapid DNA analysis, according to Qiu et al.[179]

Qiu et al.[179] further report that, recent developments in CdSe QD-based genosensing as compared to other traditional detection methods have demonstrated significant progress in enhancing the sensitivity, selectivity, and multiplexing capabilities of bioanalytical techniques. As researchers continue to innovate in this field, CdSe QDs are poised to play a vital role in advancing genosensing technologies for biomedicine, biotechnology, and clinical diagnostics, as reported by Soldado et al.[180] It can also be clearly seen that the techniques discussed in this section have no methods that have been developed to deliberately detect cp4epsps DNA gene in GM crops.

3.7 Challenges and Future Directions

Cadimium selenide quantum dots have shown great promise in genosensing applications due to their unique optical properties, as reported by Liu et al.[176] However, the use of QDs in genosensing comes with its own share of challenges that need to be addressed for further improvement in the genosensing field.

Salmi and Rouabhi[181] report that, one of the main challenges associated with QDs is their potential toxicity. Therefore, this has led researchers to actively explore ways to encapsulate or modify the QDs to reduce their toxicity while maintaining their much needed optical properties[182].

Another challenge is the need for enhanced stability and sensitivity of the QDs in genosensing assays. Factors such as oxidation, photobleaching, and nonspecific binding can affect the reliability and accuracy of genosensing results. Improvements in the design of quantum QD-based sensing platforms , along with better surface modifications, are essential to overcome these stability and sensitivity isseues.

Abdoos[183], reports that the use of CdSe QDs in genosensing applications represents a cutting-edge approach in the detection and analysis of genetic materials. These nanoscale particles

offer superior sensitivity and specificity compared to conventional methods[184]. However, their use in genosensing raises a lot of significant ethical and regulatory concerns that must be carefully considered, as reported by Clift and Stone[185]. The significant ethical and regulatory concerns are toxicity and bio-compatibility, privacy and data protection, informed consent, equity and access, as well as lack of standardized regulations, safety and efficacy evaluations, environmental impact, and labelling and disclosure, respectively[186].

In summary it can be seen from the literature reviewed in this study that the existing methods of GMO detection face many challenges in terms of cost of equipment and software for identification of DNA sequences found in these genetically modified crops as well as the inability to differentiate between false positive results and false negative results. There is also a lack of advanced studies on the use of quantum dots such as CdSe QDs to detect the cp4epsps gene in GMOs. This research therefore, was focused on developing a rapid, efficient and relatively cheaper means of genosensing of cp4epsps DNA segment in genetically modified cereal using luminescent CdSe QD-based sensor which also offered a lower detection limit.

CHAPTER 4

Experimental Methods

4.1 Introduction

This chapter provides detailed descriptions of all the experiments conducted in this study, starting with the synthesis of CdSe quantum dots (QDs), which are the key components of the designed detection platform because of their ability to interact with biological molecules and change their properties even when bound with trace amounts of analytes. It also covers the surface modification and functionalization of these particles to improve their biocompatibility and sensitivity, as well as characterization. Additionally, the chapter discusses sample preparations and electrochemical analyses.

4.2 Materials Used

Cadmium chloride hemipentahydrate, ($CdCl_2 \cdot 2½H_2O$, ≥99%, Aldrich), trisodium citrate dihydrate, ($C_6H_5Na_3O_7 \cdot 2H_2O$, ≥98%), selenium powder (Se, ≥90%, Aldrich), glutaraldehyde, ($C_5H_8O_2$, ≥25%, Aldrich), polyvinyl alcohol (PVA), Sodium sulphite, (Na_2SO_3), sodium hydroxide pellets, (NaOH), sodium borohydride, ($NaBH_4$), agarose gel (Invitrogen UltraPure Agarose), ethidium bromide, (EtBr), Oligonucleotides (Inqaba Biotec., South Africa), Qiagen QIAamp DNA Mini Kit (50) (Murtaza Traders, India), ethanol (99.9%), nuclease-free water, distilled water (from the University of Zambia, School of Natural Sciences, Department of Chemistry), certified GM maize from NBA (Chilanga), suspected GM maize, soy bean-containing cornflakes, cereal containing GM soya, and non-GM local maize seeds bought from the Zambian market in Lusaka.

4.3 Instrumentation

UV-VIS measurements were recorded using a Shimadzu 2600 UV-Vis spectrophotometer. The measurements were carried out on thin films of CdSe QDs, CdSe@TU, and CdSe@TU@GA on glass slides, and solutions in cuvettes. A Perkin Elmer Spectrum RXI FT-IR Spectrometer was used to generate FT-IR data. The fluorescence spectra-of the samples were obtained using an Ossila Optical Spectrometer instrument. The measurements were carried out in solution form in cuvettes. The PCR machine was used to synthesize the target DNA segments from the whole genome sample extracts using specially designed primers.. The amplified target sequences of DNA were viewed for confirmation of successful amplification using DNA Band Imaging System (WSE-5400 Atto Printgraph Classic). Potentiometric measures on all the samples used in the research were carried out using an anapot. The samples were quantitatively

analysed using Linear Sweep Voltammetry, in the Analytical Mode of the instrument, on gold-screen-printed electrodes. Q5000 NanoDrop Spectrophotometer was used to validate the measurements done using the developed detection platform based on CdSe QDs.

4.4 Preparation of Materials

Figure 4.1 below shows the procedure used to design the detection platform. The diagram depicts the synthetic route for the CdSe QDs, their surface modification with thiourea to give them the needed ligands to interaction with the functionalization molecules, glutaraldehyde. The functionalized CdSe QDs were then immobilized with the NH_2-terminated oligonucleotides used as capture probes. This resulted into the successful design of the detection platform for of cp4epsps DNA segment incorporated into genetically modified crops.

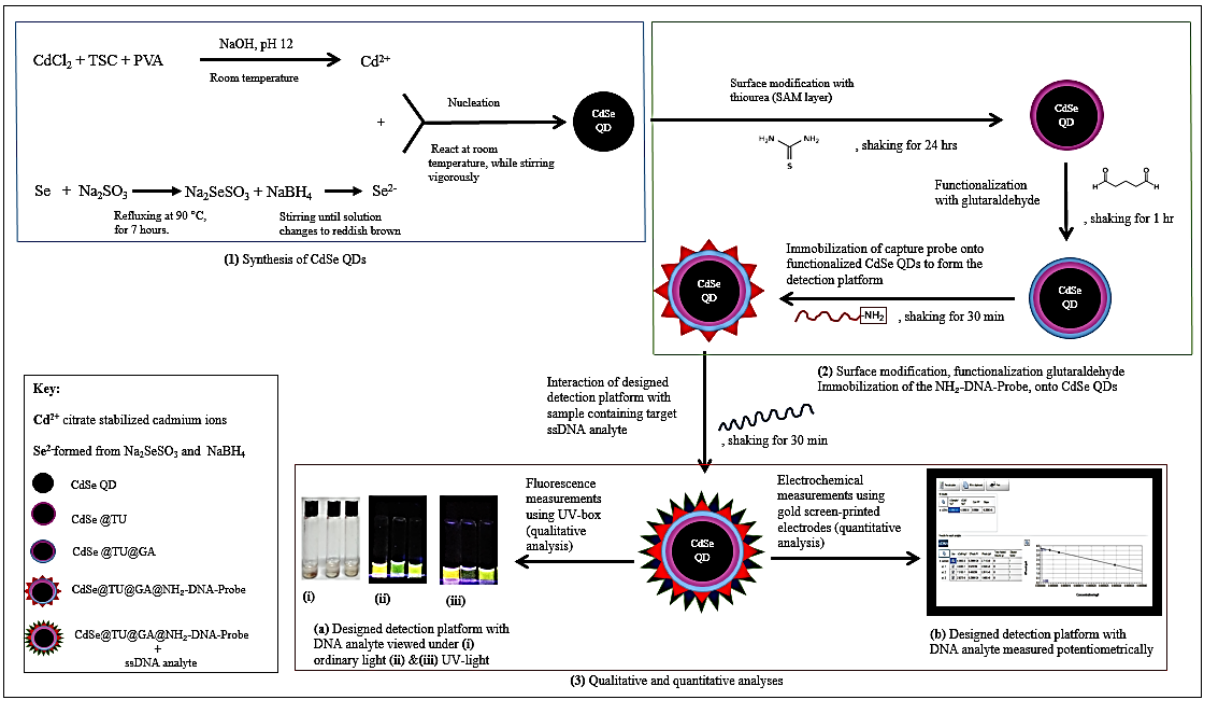

Figure 4.1: Schematic diagram shows CdSe QDs synthesis, surface modification, functionalization, immobilization with the oligonucleotide capture probe and detection of target ssDNA analyte.

4.4.1 Synthesis of CdSe QDs

The synthesis was carried out using a one-pot synthesis at room temperature without bubbling in nitrogen gas. In the procedure, 0.745 mmol of cadmium chloride hemipentahydrate, ($CdCl_2 \cdot 2½H_2O$)) was mixed with 0.442 mmol of trisodium citrate dihydrate (TSC), $C_6H_5Na_3O_7 \cdot 2H_2O$, and different concentrations of polyvinyl alcohol (PVA), 3.21×10^{-5} M, 6.42×10^{-5} M, 9.63×10^{-5} M and 1.28×10^{-4} M, in 50 mL of distilled water, to make a citrate ion stabilized precursor of Cd^{2+} ions. The pH of the solution was adjusted to 12 by 1 M NaOH solution. On the other hand, 2 g of selenium powder (Se) and 20 g of Sodium sulphite, Na_2SO_3,

were refluxed in 100 mL of distilled water at 90 °C for 7 hours, forming a solution of sodium selonosulphite, Na_2SeSO_3, which acted as the precursor for selenium. From this formed solution of sodium selonosulphite, 4 mL was then mixed with 3.44 mmol of sodium borohydride, $NaBH_4$, in distilled water making a total volume of 50 mL, and stirred until the mixture changed from colourless to red. From this freshly prepared selenium precursor, 3 mL was added drop-wise to the previously prepared cadmium precursor at room temperature and stirred for 1 hour. After 30 minutes of stirring, 5 mL of the formed product was pipetted out and it was immediately observed under UV-light, the colourless solution gave a very deep green luminescence. As the mixture was allowed to continue stirring, the solution changed slightly to a pale yellow solution which still gave deep green luminescence under UV-light. The product also gave a characteristic CdSe-QDs ultraviolet-visible excitation peak at 485 nm[187].

4.4.2 Synthesis of CdSe@TU

Thiourea was used to modify the surface of the CdSe QDs. The following concentrations of thiourea were prepared and used in the surface modification step: 0.0540 mg mL^{-1}, 0.1100 mg mL^{-1}, 0.1600 mg mL^{-1}, 0.2200 mg mL^{-1}, 0.2700 mg mL^{-1}, 0.3300 mg mL^{-1}, 0.3800 mg mL^{-1}, 0.4300 mg mL^{-1}, 0.4900 mg mL^{-1} and 0.5400 mg mL^{-1}. From each of the ten different concentrations, 1 mL was measured out and mixed with 0.1 mL (added to 0.90 mL of nuclease-free water) of a solution of cadmium selenide, synthesised using 9.36×10^{-4} M of PVA. The mixtures were vortexed for 15 seconds to ensure that the thiourea was well dispersed in the solutions. The mixtures were then mounted onto the oscillating flask shaker and allowed to run for 24 hours.

This was immediately followed by centrifugation for 5 minutes. The supernatants were separated from the CdSe quantum dots and analysed using the UV-VIS spectrophotometer.

4.4.3 Synthesis of CdSe@TU@GA

From the previously prepared CdSe@TU, 1.0 mL was measured out and reacted with 0.2 µL of glutaraldehyde while shaking for 1 hour, per each required preparation. The synthesised composites were separated from the unreacted glutaraldehyde by centrifugation. The residue was washed several times using nuclease-free water and then stored securely at -4 °C for characterisations.

4.4.4 Synthesis of CdSe@TU@GA@NH_2-Probe-DNA

In the synthesis of CdSe@TU@GA@NH_2-Probe-DNA, 1 mL of the previously prepared CdSe@TU@GA was reacted with 5 µL of the 5.0 ng L^{-1} NH_2-Probe-DNA (oligonucleotide, diluted using nuclease free-water) and shaken for 30 minutes, followed by centrifugation at 10,000 rpm for 15 minutes. The supernatant was carefully removed and discarded. The remaining particles, which settled at the bottom of the vial, were washed using nuclease free water to remove the unbound oligonucleotides. The designed detection particles with the capture probes were then stored at -20 °C to be used later in the electrochemical analyses.

4.4.5 Extraction of DNA Samples

The following steps were taken in the extraction and preparation of cp4epsps DNA segment from GM corn and soy beans containing cereal, locally grown maize seed and certified GM soy beans, adopted from the method reported by Pacheco et al [188].

A water-bath was setup, at 65 °C. A 100 mg sample was weighed out and added to a 2-mL Eppendorf tube followed by addition of 1 mL Lysis Buffer and 10 µL proteinase K solution, mixed thoroughly by vortexing for 15 seconds and incubated at 65 °C for 30 minutes with occasional vortexing. After incubation, the mixture was allowed to cool to room temperature (20 °C). The tube was centrifuged at 8,000 rpm for 5 minutes and 500 µL of supernatant was further transferred into a new 2 mL Eppendorf tube. After adding 500 µL of chloroform to the supernatant, the tube was vortexed for 15 seconds and centrifuged at 8,000 rpm for 15 minutes at 4 °C. The upper phase was carefully collected, mixed with 500 µL chloroform and centrifuged again at 8,000 rpm for 15 minutes at 4 °C. The supernatant was collected in a 2-mL Eppendorf tube and mixed carefully with 1 mL phosphate buffer. Then 600 µL of this solution was transferred to a QIAquick spin column and centrifuged at 9,500 rpm for 1 minute and filtrate was discarded. Then 500 µL of AW2 (99.9% ethanol to wash the salts out) was added to the QIAquick spin column and centrifuged at 9,500rpm for 1 minute. After discarding the filtrate, the column was again centrifuged at 8,500 rpm for 1 minute. The DNA was eluted into a fresh 2-mL Eppendorf tube by adding 100 µL elution buffer to the QIAquick spin column and incubating it for 5 minute at room temperature and then centrifuging at 8,500 rpm for 1 minute. The procedure was repeated for the other three samples. This modified extraction method took 1 hour 30 minutes for all samples.

4.4.6 Synthesis of CP4ESPSP DNA Segment from the Extracted DNA Samples

Using a PCR machine, cp4epsps DNA containing segments were synthesized by reacting a mixture of the genomic DNA extracted from GM cereal and specially designed primers as described below.

From the extracted genomic DNA, 1 µg was measured out and added to a clean microcentrifuge tube containing 0.5 µM of each of the designed forward and reverse primers, 200 µM of each dNTP, appropriate amounts of DNA polymerase and the PCR buffer, based on the manufacturer's instructions. The containts of the tube were mixed gently by pipetting up and down 5 times and then carefully loaded onto the wells of min-PCR machine. A 60.20 °C temperature was set, a 60 minutes duration and 40 cycles for the targeted segment of the research conducted. After setting the program, the PCR reaction was started to amplify the target DNA sequence.

After the synthesis process was done, the target DNA segment sample was put in a clean vial and stored at -20 °C for further use.

4.4.7 Agarose Gel Electrophoresis

Given that PCR reactions generate a large number of DNA segments, the amplified DNA molecules with the expected length, as per the designed primers, was analyzed by agarose gel electrophoresis using 1% agarose gel (Invitrogen UltraPure Agarose). Electrophoresis was performed using 1× Tris–acetate–EDTA (TAE) buffer containing 1 µg/mL of ethidium bromide (EtBr) and at a constant voltage of 100 V for 30 minutes. The DNA bands were visualized and images were acquired using an Imaging system (WSE-5400 Atto Printgraph Classic).

4.5 Characterization of Materials

The synthesized and functionalized CdSe QDs were interrogated for their optical properties. UV-Vis measurements were obtaied using a Shimadzu 2600 UV-Vis spectrophotometer. The measurements were carried out on thin films of CdSe QDs, CdSe@TU, and CdSe@TU@GA on glass slides, and solutions in cuvettes. The FT-IR spectra were recorded using KBr powder on a Perkin Elmer Spectrum RXI FT-IR spectrometer. The samples were scanned over a range of 500 cm^{-1} to 4000 cm^{-1}. The fluorescence intensities of the samples were analysed using an Ossila Optical Spectrometer instrument. The measurements were carried out in solution form in cuvettes. The electrochemical analyses of all the samples were carried out using an AnaPot

(a potentiometer). The samples were quantitatively analysed using Linear Sweep Voltammetry, in the Analytical Mode of the instrument.

4.6 Band Gap Measurements

4.6.1 Determination of Band Gap Energy and Calculation of Particle Size of CdSe QDs

In the procedure for determination of the band gap energy and the subsequent calculation of the size of the synthesized CdSe QDs. Thin glass films were spin-coated with the CdSe QDs and using the UV-Vis spectrophotometer, absorption spectral data were generated from a wavelength range of 1400 nm to 200 nm. The UV-Vis spectral data obtained were used to calculate the film thickness, using equation (1), and the value found was used to determine the band gap energy. The value of the anlge θ used in calculating the film thickness was obtained from the Shimadzu 2600 UV-Vis spectrophotometer. The Tauc's Relation was used to determine the band gap energy of the CdSe QDs.

Using the Tauc's relation, the plotting of $(\alpha h\upsilon)^{1/2}$ versus the photon energy ($h\upsilon$) gave a straight line in a certain region and the extrapolation of the straight line intercepted the ($h\upsilon$)-axis to give the value of the indirect optical energy gap (E_g) for the synthesized CdSe QDs[189].

From the estimated energy band gap of the CdSe QDs of 3.43 eV and the shift in the energy band gap between the bulk CdSe (1.74 eV, as the standard value), the size of the CdSe QDs was calculated by using the Brus equation (3). The sample calculation is given in Appendix D: D.1.

4.7 Adsorption Isotherm Studies

The binding properties of the synthesised CdSe QDs were studied using adsorption isotherms. In the procedure employed, four standard concentrations of thiourea of 0.1000 mg mL^{-1}, 0.200 mg mL^{-1}, 0.4000 mg mL^{-1} and 0.6000 mg mL^{-1}were used to plot a calibration curve, using the Linear Sweep Voltametric function of the Anapot, in the Analytical Mode, on gold-screen-printed electrodes. The gold electrodes were thoroughly cleaned using absolute ethanol. Initial concentrations of thiourea of 0.0540 mg mL^{-1}, 0.1100 mg mL^{-1}, 0.1600 mg mL^{-1}, 0.2200 mg mL^{-1}, 0.2700 mg mL^{-1}, 0.3300 mg mL^{-1}, 0.3800 mg mL^{-1}, 0.4300 mg mL^{-1}, 0.4900 mg mL^{-1} and 0.5400 mg mL^{-1} were measured against the plotted calibration curve and recorded in Table 5.1. 1 mL of the above stated concentrations of thiourea were then added to 10 separate vials containing 0.1 mL of the synthesised CdSe QDs and the mixtures were allowed to react while shaking at 1,000 rpm for 24 hours. This was followed by centrifugation at 4,000 rpm for 5

minutes. The supernatant was collected and then used to determine how much of the thiourea had bound to the CdSe QDs.

4.8 Assessment and Evaluation of Detection Platform

4.8.1 Detection Platform Evaluation and Specificity Determination

4.8.1.1 Detection of Complementary Probe-DNA and Uncomplimentary DNA

In order to evaluate the designed CdSe QD-based detection platform, standard solutions of 1.0 ng L^{-1}, 2.0 ng L^{-1}, 4.0 ng $L^{-1}$and 6.0 ng L^{-1} probe-DNA, bound to the QDs, were prepared and calibration curves plotted on the Anapot, using gold-screen-printed electrodes. Then five different concentrations of the single stranded probe cDNA (F) of 2.0 ng L^{-1}, 2.5 ng L^{-1}, 3.0 ng L^{-1}, 3.5 ng L^{-1}, 4.0 ng L^{-1}, and five of the uncomplimentary ssDNA (R) of 2.0 ng L^{-1}, 2.5 ng L^{-1}, 3.0 ng L^{-1}, 4.0 ng L^{-1}, and 5.0 ng L^{-1}, were prepared. 0.01 mL of each of these solutions was reacted with 0.01 mL of the designed detection platform (in 1.98 mL of nuclease free water) for 30 minutes while shaking. The vials were centrifuged at 8,000 rpm for 15 minutes. The supernatant was carefully removed from each vial, the remaining QDs with attached analytes were carefully resuspened and measured against the plotted standard concentrations on the Anapot.

4.8.2 Binding Ability of Designed Detection Platform

4.8.2.1 Binding Ability of CdSe@TU@GA@NH_2-Probe-DNA and CdSe@TU@GA for cp4epsps DNA Segment

The binding ability of the designed CdSe QD-based detection platform, for the cp4epsps DNA sequence, was evaluated by reacting the probe cDNA with both CdSe@TU@GA@NH_2-Probe-DNA and CdSe@TU@GA. In the procedure, a concentration of the probe cDNA of 2.5 ng L^{-1} was prepared and reacted with CdSe@TU@GA@NH_2-Probe-DNA and CdSe@TU@GA separately, for 30 minutes while shaking. The vials were centrifuged at 10 000 rpm for 15 minutes. The supernatant was carefully removed from each vial, the remaining QDs with attached analytes were carefully resuspended and measured against the plotted standard concentrations on the AnaPot.

4.8.2.2 False Positive and False Negative Measurements

Further experiments were done in order to deal with the problem of false negatives and false positives. In the procedure used, the designed CdSe QD based detection platform was allowed to interact with both a non-GM DNA sequence containing sample and a GM DNA sequence containing sample, prepared as described in section 4.4.5. In the preparation procedure 100 mg

of non-GM locally grown maize and GM soy beans (certified to be genetically modified by ZARI) were used. The extracted DNA segments were treated with the primers used to synthesize cp4epsps DNA segments from the suspected samples, and the electrochemical analysis was done as described in section 4.9.11 above.

4.8.3 Determination of Detection Limit

In order to determine the lowest amount of targeted sample DNA that could be detected using the designed detection platform, the concentrations of the probe cDNA were reduced by dividing the lowest concentration used in the generation of the calibration curve by 10 which resulted into concentrations of 2.42 ng L^{-1}, 2.42 × 10^{-1} ng L^{-1}, 2.42 × 10^{-2} ng L^{-1} , 2.42 × 10^{-3} ng L^{-1}, 2.42 × 10^{-4} ng L^{-1}, 2.42 × 10^{-5} ng L^{-1}, 2.42 × 10^{-6} ng L^{-1}, 2.42 × 10^{-7} ng L^{-1}, 2.42 × 10^{-8} ng L^{-1}, and 2.42 × 10^{-9} ng L^{-1}. These concentrations were measured against the calibration curve and the results reported. The result obtained was validated theoretically, using linear regression.

4.8.4 Detection of DNA Samples

A 1 µL volume was taken from each of the 40× amplified extracted DNA samples and added to 9 µL of nuclease free water to make a total volume of 10 µL. 1 mL of CdSe@TU@GA@ NH_2-Probe-DNA was pipetted into two different Eppendorf tubes and a 2 µL of the above prepared suspected samples was added to each tube, shaken for 30 minutes and then centrifuged at 8,000 rpm for 15 minutes at room temperature (25 °C). The supernatant was taken out carefully, the remaining QDs with attached analytes were carefully resuspened and then measured against the previously plotted calibration curves. The determined concentrations of the DNA in the samples were then calculated using the dilution factor and the PCR amplification factor.

4.9 Validation of Methods

The validation of the developed method was done using a Q5000 NanoDrop Spectrophotometer. The Q5000 Nanodrop Spectrophotometer had a detection limit of 1 ng/µL as per the manufacturer's specifications. Therefore, in order to make sure that the samples that were tested using this instrument were in the detectable range, the amounts of the designed detection particles were increased 1000 fold from 0.01 mL to 10 mL and the concentrations of the analytes were increased 1, 000, 000 fold. The increased number of particles of the designed detection platform ensured availability of an increased number of hybridization points for the then increased number of analyte molecules[190].

The Nanodrop Spectrophotometer was prepared by turning it on to allow it to warm up. Using a lint free-cloth, the sample pedestal (pin) of the instrument was cleaned with an optical cleaning solution to ensure accurate measurements. The wavelength was set to 260 nm, corresponding to the absorbance maximum for DNA. 1 µL of each of the DNA samples was pipetted onto the sample pedestal of the instrument using a fresh pipette tip in order to prevent contamination. The lid of the instrument was closed and 10 s were allowed to pass to ensure stabilization. The instrument measured the absorbance of the DNA sample at a wavelength of 260 nm and it was recorded. The procedure was repeated for all the DNA samples. The concentration of the DNA sample was automatically computed by the software of the instrument installed onto a computer, and gave a numerical figure with the appropriate units of ng/µL.

CHAPTER 5

Results and Discussion

5.1 Introduction

This chapter presents and discusses the results of the characterisation experiments carried out in this study. These include, UV-VIS analyses, band gap energy determination, particle size estimation via calculations, adsorption studies, fluorescence determination as well as FT-IR analyses of the CdSe QDs and the surface modified and functionalized particles. The chapter also presentst the DNA extraction data from samples and electrochemical analyses of the extracted and prepared DNA samples, determination of the limit of detection as well as validation of the study conducted.

5.2 Ultraviolet/Visible (UV-Vis) Spectroscopy Studies

5.2.1 UV-Vis Spectrum of the Synthesised CdSe QDs

The synthesised CdSe QDs solution had a colourless appearance in ordinary light but when viewed under UV-light, the particles showed a deep green luminescence. Figure 5.1, below, shows the appearance of the synthesised CdSe QDs in **a)** ordinary light while **b)** under UV-light.

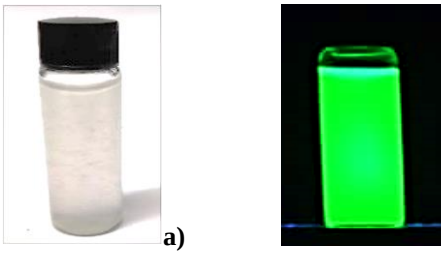

a) **b)**

Figure 5.1: CdSe-QDs solutions in a) ordinary light and b) under UV-light at 366 nm.

To determine the optical properties of the synthesized CdSe QDs, the UV-Vis Spectrum was collected using Shimadzu 2600 spectrophotometer, and is shown in Figure 5.2.

In Figure 5.2, the CdSe QDs showed an absorption peak of 485 nm, with an absorption edge towards 600 nm. The absorption was in agreement with what has been reported in literature for CdSe QDs[191].

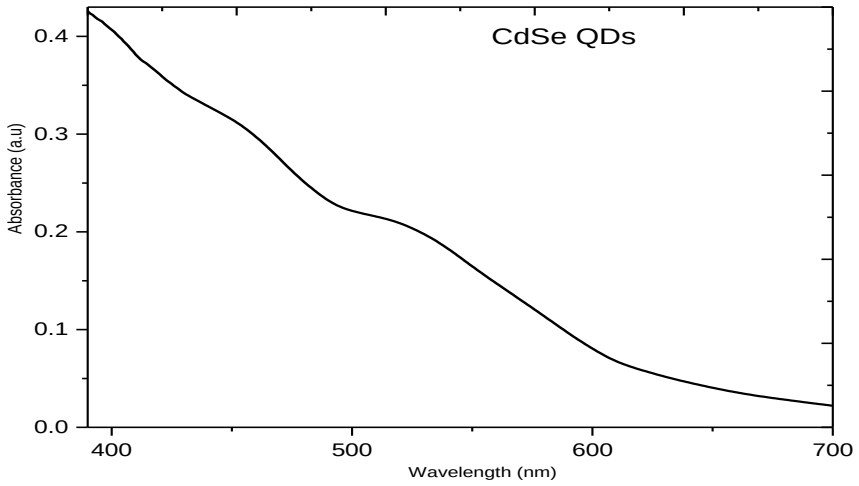

Figure 5.2: UV-Vis spectrum of the synthesised CdSe QDs**.**

The interrogation of the CdSe QDs using UV-Vis analysis, helped to validate their optical properties. The particles showed an absorption peak around 485 nm[192], with an absorption edge towards 600 nm, due to their large band gap energy. The band gap energy of semiconductor QDs is inversely proportional to its size, and CdSe QDs with a diameter of around 2-4 nm have a band gap energy that corresponds to absorption in the visible region of the electromagnetic spectrum[193]. The absorption band around 485 nm corresponds to the energy required to excite an electron from the valence band to the conduction band of the quantum dot, which is determined by the band gap energy[194]. Therefore, the size of the CdSe QDs determines its band gap energy and hence the wavelength of light required to excite it[195].

5.2.2 UV-Vis Spectrum of CdSe, CdSe@TU, and CdSe@TU@GA

The interaction of the thiourea with the CdSe QDs was also confirmed by the red shift in the UV-Vis absorption spectrum as can be seen from Figure 5.3 below. This is due to the formation of a new surface state that is energetically higher than the original surface state. This new state can lead to a decrease in the band gap energy and an increase in the absorption wavelength, as can be seen in Figure 5.3, the absorption peak has shifted from 485 nm to 584 nm. This result was in agreement with what has been reported in literature[196].

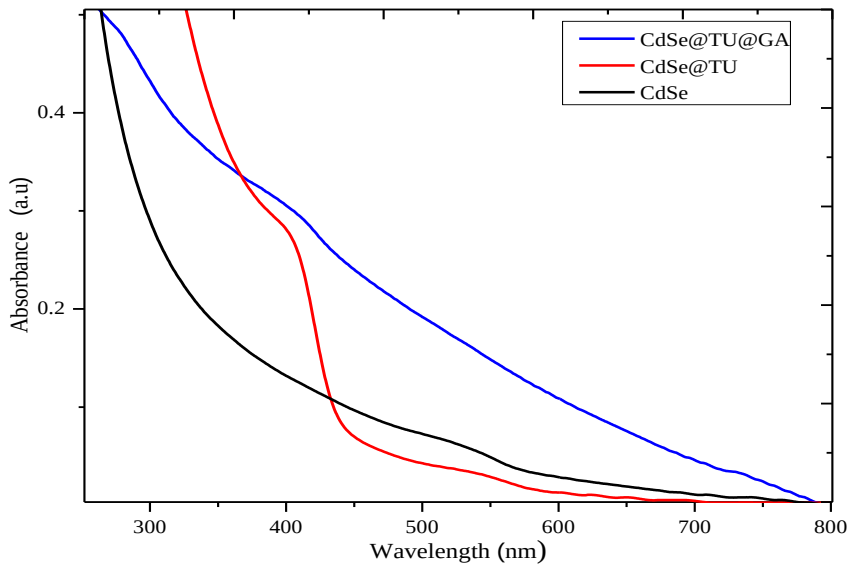

Figure 5.3: UV-Vis spectra of the synthesised CdSe QDs, CdSe QDs@TU and CdSe QDs@TU@GA

Coating CdSe QDs with thiourea leads to a red shift in the UV-Vis spectrum due to the formation of a thin layer of thiourea molecules on the surface of the quantum dots. This layer can alter the electronic structure and energy levels of the QDs, leading to a 99 nm shift in the absorption and emission spectra[197].

The spectrum for CdSe@TU@GA, indeed confirms the modification and functionalization of the CdSe QDs. The huge red shift shown in Figure 5.3 shows that new electronic states were created in the QDs as the particles became covered with a layer of thiourea and glutaraldehyde molecules[196c].

In addition, the UV data helped to confirm that the particles were forming according to the design shown in Figure 4.1. For example, in Figure 5.3, the absorption bands are attributed to functional groups present in thiourea. This data can also be complimented with that from FT-IR shown in Figure 5.5.

5.3 Optical Band Gap Determination of CdSe QDs

The graph in Figure 5.4, below shows the plot of $(\alpha h\upsilon)^{1/2}$ versus the photon energy ($h\upsilon$) which gives a straight line in a certain region. The extrapolation of this straight line intercepts the ($h\upsilon$)-axis to give the value of the indirect optical energy gap (Eg).

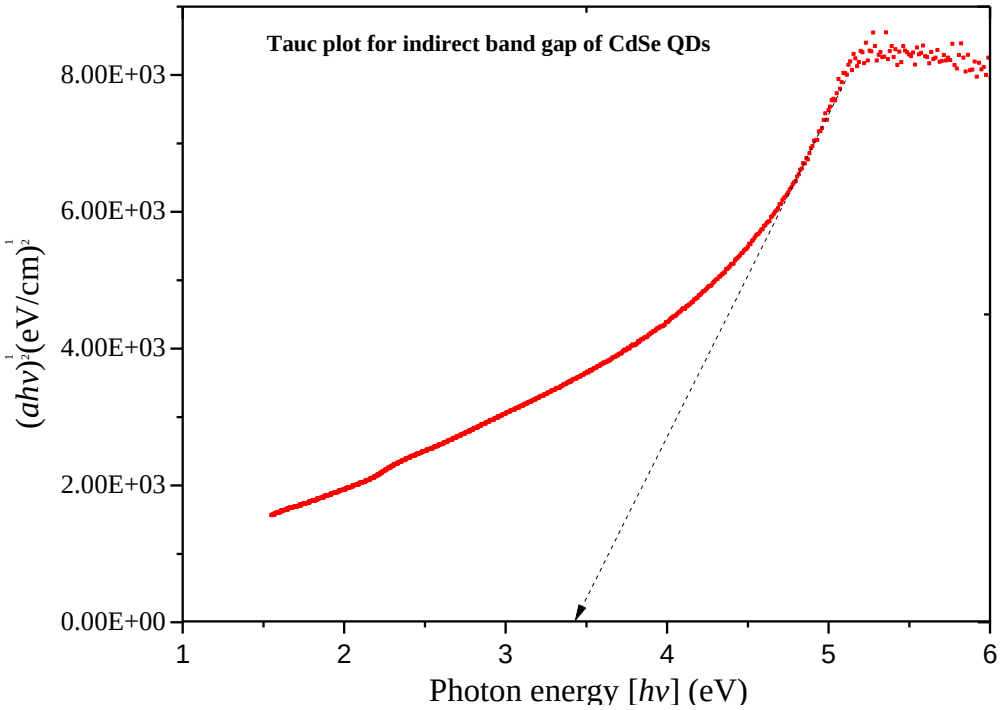

Figure 5.4: Tauc plot for indirect band gap of the synthesised CdSe QDs

Determining the band gap energy and size of quantum dots is crucial due to their direct impact on the optical and electronic properties of the particles[198]. This energy gap dictates the type of light they absorb and emit, which is critical for application in genosensors[199]. Knowing the exact band gap makes it easier to tailor quantum dots for specific uses, optimizing their efficiency and performance. Tuning the band gap also influences their conductivity and electron behavior. Fundamentally, accurate band gap energy determination is important for customizing quantum dots with desired optical and electrical characteristics, paving the way for better genosensor design[200].

In this study, from Figure 5.4 above, the band gap value for the synthesised CdSe QDs was estimated to be 3.43 eV. This value showed that the CdSe particles were of quantum dot size (i.e. with closer electron holes; higher kinetic energy). The reported band gap for CdSe QDs from literature is 2.28 eV and a relative red shift to the band gap of bulk cubic CdSe of 1.74 eV[201]. This obtained big value of the band gap energy of the synthesised CdSe QDs conforms to the fluorescing properties observed in the material produced.

The radius was calculated to be equal to 1.410 nm giving an average diameter size of the synthesised CdSe QDs of 2.82 nm, a result that fell within the reported diameter range for quantum dots of 2 nm to 10 nm[202]. Example calculations of the radius are reported in Appendix D: D.1.

5.4 Fourier Transform-Infrared (FT-IR) Spectral Studies

5.4.1 FT-IR Spectral Analyses of CdSe QDs, CdSe@TU and CdSe@TU@GA@Probe

Fourier Transform-Infrared (FT-IR) spectroscopic studies were done to confirm successful coating of thiourea onto the quantum dots as well as the subsequent functionalization of the surface modified particles using glutaraldehyde.

The FT-IR plots in Figure 5.5 show the detected characteristic absorption bands of the thiourea and glutaraldehyde and the probe oligonucleotides onto the surface of the CdSe QDs.

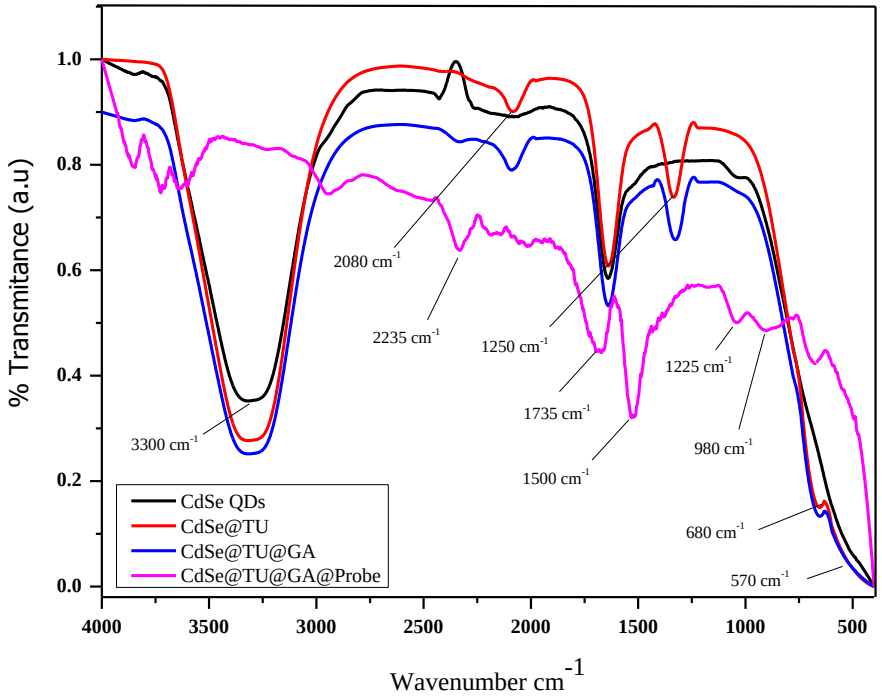

Figure 5.5: FT-IR Spectra of CdSe QDs, CdSe@TU, CdSe@TU@GA and CdSe@TU@GA@Probe

In the FT-IR plot shown in Figure 5.5 above, the characteristic broad absorption band of Cd-Se bond[203] appears at 570 cm^{-1}. The OH band[204] at 3300 cm^{-1} from the particle stabilizer PVA, is characteristic of the stretching vibration of the hydroxyl groups on the surface of the CdSe QDs. Introducing thiourea as a surface modifier led to the appearance of bands associated with thiocarbonyl (-C=S) stretch[205] around 2080 cm^{-1}. The presence of thiourea was confirmed by observing characteristic bands around 1250 cm^{-1} for C-N stretching and 680 cm^{-1} for C-S stretching[206]. Functionalizing the thiourea-modified CdSe QDs with glutaraldehyde introduced aldehyde groups that would react with amino groups present in the oligonucleotides. The appearance of a band around 1730 cm^{-1} corresponded to the C=O stretching of the aldehyde group[206a, 207]. The immobilization of oligonucleotides onto the surface-functionalized QDs

involved the interaction between amino groups of the oligonucleotides and the aldehyde groups on the CdSe QD surface. This interaction led to the formation of imine bonds. In the FT-IR spectrum, the formation of imine bonds[208] was observed at 2235 cm^{-1}. Additionally, characteristic bands related to the oligonucleotide structure, such as phosphate bands appeared around 1235 cm^{-1} and sugar-phosphate backbone vibrations[209] around 980 cm^{-1} were observed.

5.5 Fluorescence Studies

The fluorescence results in Figures 5.6 and 5.7 below show emission of CdSe QDs at shorter wavelength which confirms that indeed the particles synthesized were of very small size[210].

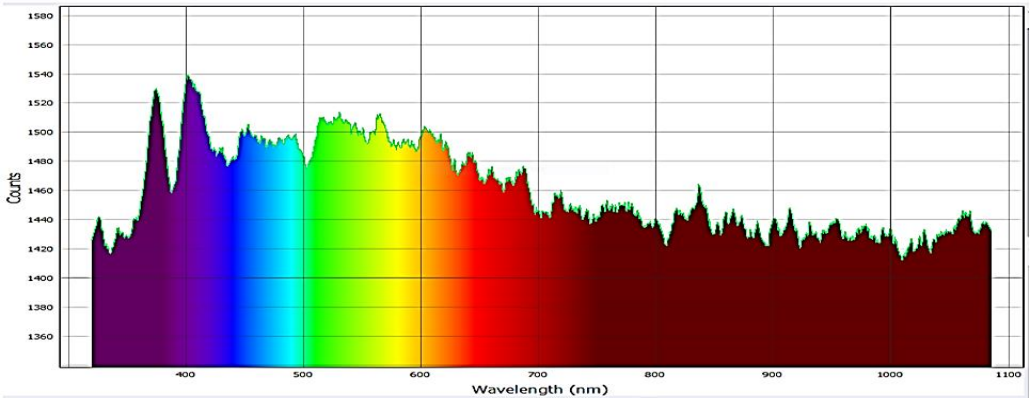

Figure 5.6: Fluorescence spectrum for CdSe QDs (Ossila spectrometer generated)

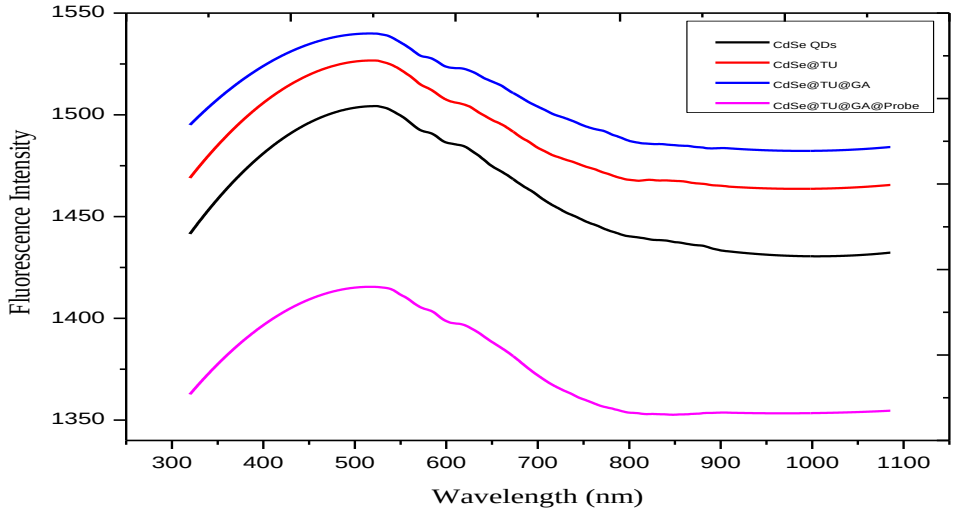

Figure 5.7: Fluorescence intensity of CdSe, CdSe@TU, CdSe@TU@GA and CdSe@TU@GA@Probe

The CdSe QDs show a well-defined spectrum. The fluorescence intensity of the CdSe@TU was higher than that of the CdSe QDs, which indicated that the surface modification of the particles had taken place successfully, resulting in change of the surface chemistry of the CdSe QDs. Functionalizing the surface modified CdSe QDs with glutaraldehyde further modified

their fluorescence properties as can be seen from Figure 5.7 above. The immobilization of the oligonucleotides onto the surface modified and functionalized CdSe QDs appeared to have affected the intensity of the particles, by reducing it[211]. The results helped to comfirm the desired modifications of the particles.

5.6 Adsorption Isotherm Models

The adsorption isotherm models are widely used to describe and analyze the adsorption process, particularly in the field of surface chemistry and material science. These models provide insights into the interaction between adsorbate molecules and the adsorbent surface, and they can be used to estimate important parameters such as adsorption capacity, affinity, and energetics[212]. A full discussion and equations for adsorption isotherm models are given in **chapter 2, section 2.9**, while the results for all experiments on the surface modification and functionalization of the CdSe QDs can be found in Appendix B: B.1.

5.7 Sample Extraction Data

5.7.1 DNA Extraction Data from Negative Control, Positive Control, and the Two Suspected GM DNA Sequence Containing Samples and PCR Amplicons

Using a modified Mericon extraction method, the amounts of the DNA concentrations obtained and reported in Table 5.1 below, were consistent with what has been reported and recommended except for one sample, sample A, which consistently gave very low amounts each time the extraction was carried out[213].

Table 5.1: Determination of concentration and purity of DNA extracted Samples

No.	Sample ID	Description	Sample Type	SW (nm)	SW Abs	260 Abs (10 mm)	280 Abs (10 mm)	260/280 (DNA Purity)	260/230	Conc. (ng/µL)
1	My Sample 1 (-)	(-) (Negative control, local maize seeds)	dsDNA	260	2.059	2.059	1.132	1.82	0.49	102.94
2	My Sample 2 (A)	Bokomo cornflakes	dsDNA	260	0.251	0.251	0.135	1.75	0.24	12.53
3	My Sample 3 (B)	Bokomo ProNutro Original Cereal	dsDNA	260	1.597	1.597	0.854	1.87	0.53	79.47
4	My Sample 4 (+)	Positive control, Certified GM soya	dsDNA	260	2.376	2.376	1.322	1.80	0.48	118.79

Take note that in Table 5.1 above, SW stands for "specific wavelength", SW Abs is the "absorption at the specified walength", 260/280 is the "ratio of the absorption wavelength for DNA to RNA", which is used as a measure of the purity of DNA, and 260/230 ratio is "a measure of contamination of the DNA". A 260/280 ration range of 1.8 – 2.0 indicates that the DNA sample is relative pure while a 260/230 ratio range of 2.0 – 2.2 indicates that the DNA sample is free of contamination from salts, phenols or other organic compounds[214]. From the results presented in the table, the low 260/230 ratios gotten were due to the fact that the DNA samples were extracted using strong salts and no subsequent DNA purification experiments were conducted as this was not necessary for the procedure used in the research.

5.7.2 Agarose Gel Electrophoresis

The extracted DNA samples were amplified and analyzed by agarose gel electrophoresis using 1% agarose gel (Invitrogen UltraPure Agarose). Electrophoresis was performed using 1× Tris–acetate–EDTA (TAE) buffer containing 1 μg/mL of ethidium bromide (EtBr) and a constant voltage of 100 V for 30 minutes. The DNA bands were visualized and images were acquired using an imaging system (Atto Printgraph Classic), as shown in Figure 5.8 below.

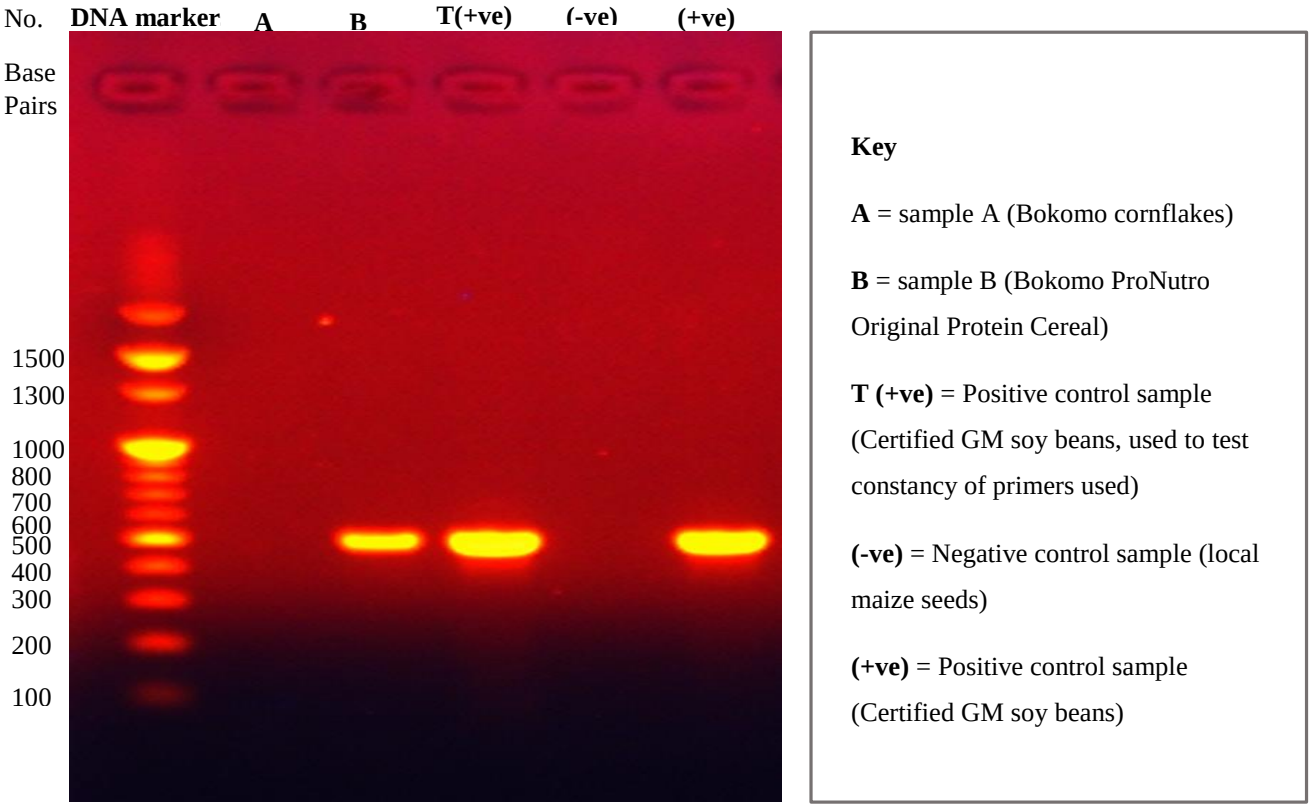

Figure 5.8: Agarose gel electrophoresis for the amplified negative control, positive control and the two suspected GM DNA containing samples (1% agarose)

5.8 Assessment and Evaluation of Detection Platform

5.8.1 Platform Evaluation and Specificity Determination

DNA hybridization is a fundamental concept in molecular biology and genetics that involves pairing of complimentary DNA strands. Given that DNA is composed of four nucleotide bases: adenine (A), thymine (T), cytosine (C) and guanine (G), therefore, if two strands of DNA have bases that are complimentary to each other, then hybridization (alignment of respective bases) would take place forming a double stranded duplex of DNA. Specifically, adenine (A) pairs with thymine (T), via two hydrogen bonds and cytosine (C) pairs with guanine (G) via three hydrogen bonds[215].

On the other hand non-complimentary strands refer to strands that do not align properly with each other due to mismatched bases. This therefore then indicates that if the hybridization percentage is more than 50%, then the level of complementarity is very high in the strands that are being aligned[216].

Therefore, in this research, in order to try and evaluate the workability of the designed detection platform based on CdSe QDs, five known concentrations of the complimentary DNA to the capture probe DNA sequence as well as five known concentrations of the opposite strand to the complimentary strand were prepared and subjected to the detection platform. The concentrations of the samples containing the complimentary strand to the capture probe had a higher degree of hybridisation with an average value of 94.4% hybridization while that of the non-complimentary strand was relatively lower with an average hybridization value of 5.0%, from the data shown in Table 5.2. These results obtained indeed helped to prove that detection platforms based on the use of a specific sequence of DNA strands can have a high level of selectivity, seeing that the hybridization percentage was higher than the recommended hybridization threshold of 50% and this proved that no other DNA sequence could bind to the devised capture probe DNA other than the intend target sequence.

Table 5.2: Specificity evaluation of the designed CdSe QD-based genosensor

Sample ID	**F**	**F**	**F**	**F**	**F**	**R**	**R**	**R**	**R**	**R**
Initial Conc. (ng L^{-1})	2.0	2.5	3.0	3.5	4.0	2.0	2.5	3.0	4.0	5.0
Final Conc. (ng L^{-1})	0.032	0.083	0.117	0.298	0.424	1.876	2.360	2.847	3.840	4.805
Used Conc. (ng L^{-1})	1.968	2.417	2.883	3.203	3.576	0.124	0.140	0.153	0.160	0.195
% Hybridisation	98.4	96.7	96.1	91.5	89.4	6.2	5.6	5.1	4.0	3.9

5.8.2 Binding Ability of CdSe@TU@GA@NH_2-Probe-DNA and CdSe@TU@GA for the cp4epsps DNA Segment

The binding ability of the designed detection platform was tested by subjecting known concentrations of the probe complimentary DNA (cDNA) to both CdSe@TU@GA@NH_2-Probe-DNA and CdSe@TU@GA respectively and the results obtained are as shown in Table 5.3. Figure 5.9 shows the vials containing the detecting particles under both ordinary light and UV-irradiation for the selectivity experiments carried out.

Table 5.3: Binidng ability determination of the detection platform

Sample ID	CdSe@TU@GA@NH_2-Probe-DNA	CdSe@TU@GA
Initial Conc. (ng L^{-1})	2.5	2.5
Final Conc. (ng L^{-1})	0.0625	2.395
Used Conc. (ng L^{-1})	2.438	0.105
Hybridisation percentage	97.5 %	4.2%

It can be seen clearly from the large hybridization percentage of the CdSe@TU@GA@NH_2-Probe-DNA of 97.5% compared to that of the CdSe@TU@GA of only 4.2% that the designed detection platform indeed had very high selectivity. This result was confirmed by the physical changes of the fluorescence of the CdSe@TU@GA@NH_2-Probe-DNA and that of CdSe@TU@GA.

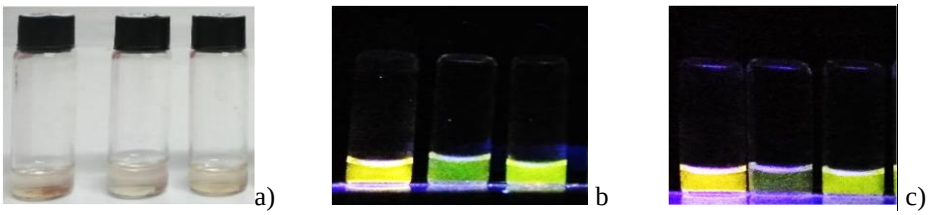

Figure 5.9: CdSe QDs, CdSe@TU@GA@NH_2-Probe-DNA and CdSe@TU@GA solutions, from left to right, a) in ordinary light and b) under UV-light at 366 nm before interaction with the analyte and c) after interaction with the analyte containing the target DNA segment.

Figure 5.9 shows that the solutions in ordinary light had a colourless appearance and when viewed under UV-light, they showed luminescence ranging from light yellow for the CdSe QDs, green for CdSe@TU@GA@NH_2-Probe-DNA and greenish-yellow for CdSe@TU@GA and after interaction with the analyte. The observed differences in the fluorescence intensity of the modified QDs with the capture probe and the QDs without the capture probe DNA sequences can actually be used to signal if the analyte of interest is present in the sample or not. The luminescence of the surface modified and functionalized CdSe QDs immobilized with the capture probe reduced very significantly compared to the particles without the capture probe. This change in fluorescence of the QDs before and after interaction with the analyte

sample was used to propose a qualitative method of detection for the sample containing the targeted DNA segment. Seeing from all the experimental results presented, it can said that the detection platform is highly selective and specific, therefore, the change in the intensity or almost disappearance of the fluorescence of the detecting particles after hybridization with the sample analyte cannot be mistaken for anything else.

5.8.3 Determination of Detection Limit

In order to determine the lowest amount of targeted sample DNA that could be detected using the designed detection platform, the concentrations of the probe cDNA were reduced by dividing the lowest concentration of 2.42 ng L^{-1}, used in the generation of the calibration curve by 10 which resulted into concentrations of 2.42×10^{-1} ng L^{-1}, 2.42×10^{-2} ng L^{-1}, 2.42×10^{-3} ng L^{-1}, 2.42×10^{-4} ng L^{-1}, 2.42×10^{-5} ng L^{-1}, 2.42×10^{-6} ng L^{-1} , 2.42×10^{-7} ng L^{-1} , 2.42×10^{-8} ng L^{-1} and 2.42×10^{-9} ng L^{-1}. These concentrations were measured against the calibration curve and the lowest detectable amount of target DNA was found to be 2.42×10^{-5} ng L^{-1}. DNA concentrations smaller than 2.42×10^{-5} ng L^{-1} could not be detected.

Further more, the theoretical determination of the limit of detection was done using *I*peak readings of concentrations, shown in Table 5.4 below. The *I*peak readings are maximum current readings that were obtained from the potentiometer after allowing the current to pass through the above stated conecntrations of the samples. The readings were used to plot a graph of concentration against *I*peak, as shown in Figure 5.10 below. Using the linear regression equation y = 5654.54545 × + 1.372 (r^2 = 0.99506), the limit of detection (LOD) and limit of quantification (LOQ) were computed from their following respective equations LOD =3.3 σ/s and LOQ = 10 σ/s, where σ is residual of standard deviation of regression or standard deviation (SD) of the y-intercept and s is the slope from the regression analysis. The limit of detection from these calculations was found to be 0.0228 µg L^{-1} (2.28×10^{-5} ng L^{-1}), a result that was comparable with that obtained in the first set of experiments, of 2.42×10^{-5} ng L^{-1}, discussed earlier. The limit of quantification was found to be 0.0692 µg L^{-1} ($6.92\ 10^{-5}$ ng L^{-1}). The results obtained therefore, showed that indeed the designed detection platform had low limit of detection.

Table 5.4: Theoretical limit of detection for cp4epsps DNA gene segment

Conc. (µg L^{-1})	1.0×10^{-1}	9.0×10^{-2}	8.0×10^{-2}	7.0×10^{-2}	6.0×10^{-2}	5.0×10^{-2}	4.0×10^{-2}	3.0×10^{-2}	2.0×10^{-2}	1.0×10^{-2}
*I*Peak (µA)	1.95	1.86	1.82	1.78	1.70	1.67	1.62	1.51	1.49	1.43

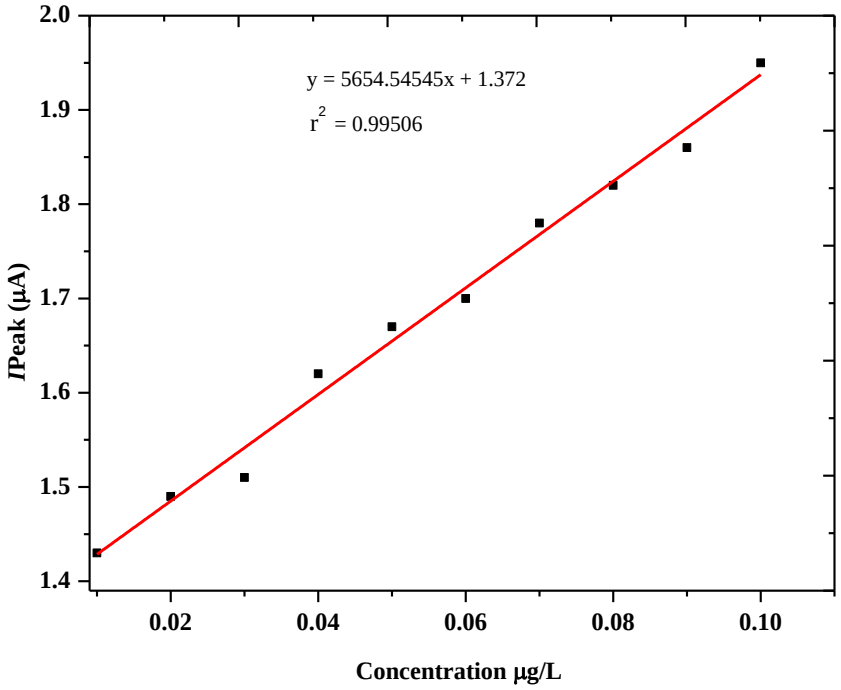

Figure 5.10: Linear regression analysis of *I*peak and concentration

5.8.4 Normality Tests

Normality tests are used in statistics to calculate the likelihood that a random variable underlying a data collection will be normally distributed and to assess whether a data set is well-modelled by a normal distribution. The Shapiro-Wilk Test and the Normal Q-Q Test were used to test the theoretical limit of detection determination data obtained in this study for normality[217].

5.8.4.1 Shapiro-Wilk Test

The Shapiro-Wilk Test, is a test of normality that is commonly used for testing the normality assumption in parametric statistics[218]. Table 5.5 shows the results obtained from a Shapiro-Wilk normality test on the data that was used to determine the theoretical limit of detection.

Table 5.5: Shapiro-Wilk Tests of Normality

	Kolmogorov-Smirnov[a]			Shapiro-Wilk		
	Statistic	df	Sig.	Statistic	df	Sig. (p-value)
*I*Peak (µA)	0.143	10	0.200*	0.966	10	0.853

a. Lilliefors Significance Correction

*. This is a lower bound of the true significance.

Shapiro-Wilk Test assumes that the data is normally distributed, and this is referred to as the Null hypothesis. The p-value is the probability of obtaining the observed test statistic if the null hypothesis is true (thai is if the data is normally distributed)[218].

A p-value > 0.05 indicates that the data is normally distributed and therefore, the null hypothesis can not be rejected, while a p-value ≤ 0.05 indicates that the data does not follow a normal distribution and the null hypothesis should be rejected[219].

The data obtained from the experiments done in this study gave a p-value = 0.853 which means that the data was normally distributed and therefore the null hypothesis has been accepted.

5.8.4.2 Normal Q-Q Plot

A Normal Q-Q Plot is used to test the normal distribution of data graphically. The data points will be near the diagonal line if they are normally distributed; they will deviate from the line in a non-linear way if they are not[220]. The normal Q-Q plot in Figure 5.11 below shows that the data was normally distributed and therefore the null hypothesis must not be rejected for these experiments done on determination of the theoretical limit of detection.

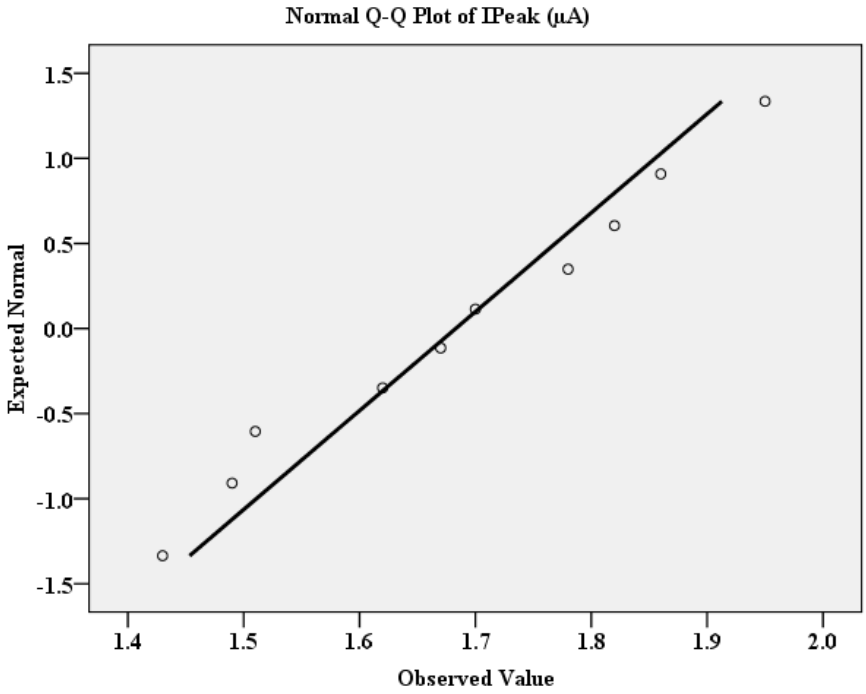

Figure 5.11: Normal Q-Q Plot of *I*peak **(µA)** data

5.8.5 Detection of DNA Samples

The electrochemical detection of DNA strands involves the use of electrochemical methods to identify and quantify DNA molecules. It is a sensitive and very useful technique that has gained significant attention in DNA analysis and diagnostics. The detection process typically involves the measurement of the electrical potential of the electrode with the DNA capture probe molecule attached to it before and after hybridization with the target DNA sequence of interest. The binding then induces specific changes in the properties of the system which can then be detected and measured[221].

In the electrochemical analyses performed, using the Anapot, the concentrations of the samples were measured before and after interaction with the designed CdSe QD-based nanosensor and the obtained values were assessed based on the earlier mentioned 50% recommended hybridization percentage[216]. Sample **F**, which was a complimentary strand to the capture probe oligonucleotide had a 92.2% hybridisation, while the opposite strand sample **R** only gave a 4.1% hybridisation. The positive control sample **(+ve)** gave a 76.5% hybridisation with the capture probe, while the negative control sample **(-ve)** only gave 5.4% interaction. These results were consistent with the agarose gel electrophoresis analysis showed in Figure 5.8, which indicated that the control sample did not contain the target DNA segment that was present in the positive control sample. Of the two suspected samples that were analyzed, sample **A** and sample **B**, sample **A** had a relatively lower yield of DNA and the electrochemical analysis results only gave a 3.4% hybridisation, while sample **B** gave a fairly higher hybridisation percentage of 57.9%, as shown in Table 5.6 below. These results proved that sample **A** had no target DNA sequence while sample B had the targeted DNA sequence.

Table 5.6: Determination of concentrations of analytes using the CdSe DQ-based genosensor

Sample ID	**F**	**R**	**(+ve)**	**(-ve)**	**A**	**B**
Initial conc. (ng L^{-1})	5.027	1.857	1.189	1.597	2.270	1.491
Final conc. (ng L^{-1})	0.394	1.781	0.279	1.511	2.193	0.628
Used conc. (ng L^{-1})	4.633	0.076	0.910	0.086	0.077	0.863
% of Hybridisation	92.2%	4.1%	76.5%	5.4%	3.4%	57.9%

This method of measurement showed that even if all the samples had DNA in them, only the ones with DNA of specific sequence interacted with the designed detection platform, hence, therein lies the specificity of the detection platform itself.

5.9 Validation of Methods

The results of the samples obtained from the electrochemical measurements, using the Anapot, were authenticated using the NanoDrop Spectrophotometer. Despite the discrepancies in the actual figures in the results measured using the devised CdSe QD-based nanosensor and the NanoDrop Spectrophotometer, as can be seen from Tables 5.6 above and 5.7 below (due to the very high concentrations used in the later procedure), there was perfect agreement in the nature of the data obtained in the study and therefore, this designed detection platform for detection of 5-enolpyruvylshikimate-3-phosphate (CP4EPSP) gene in GM cereal can be used to act as a prototype for devising detection platforms for all varieties of GM crops.

Table 5.7: Determination of concentrations of analytes using the NanoDrop Spectrophotometer

Sample ID	**F**	**R**	**(+ve)**	**(-ve)**	**A**	**B**
Initial conc. (ng/µL)	5.140	5.110	5.200	5.317	5.004	5.010
Final conc. (ng/µL)	1.521	4.788	2.012	4.955	4.719	2.500
Used conc. (ng/µL)	3.619	0.322	3.188	0.362	0.285	2.510
% of Hybridisation	70.4%	6.3%	61.3%	6.8%	5.7%	50.1%

CHAPTER 6

6.1 Conclusion

In this study, it has been shown that quantum dots can be synthesised using an easier and cheaper method that does not need the use of nitrogen, high temperatures and toxic organic solvents as is reported in most papers, but only needs the use of an appropriate surfactant, stabilizer and the right pH[222]. This method gave soluble and highly luminescent CdSe QDs whose degree of luminescence and stability depended on the concentration of the stabilizing urgent, PVA, used. The CdSe QDs had an absorption peak around 485 nm and the band gap energy was calculated to be 3.43 eV. The average diameter of the synthesised CdSe QDs was found to be 2.82 nm, a result that fell within the range of diameters for quantum dots of 2 nm to 10 nm reported in literature[223].

The surface modified and functionalized CdSe QDs gave a Q_m value of 0.0108 mg/g, and an $R^2 = 0.99902$ for the Langmuir and $R^2 = 0.81190$ for the Freundlich isotherms, indicating that the data fitted better in the Langmuir isotherm model. The successful coating with thiourea onto the QDs and the functionalization with glutaraldehyde and the subsequent immobilization of the oligonucleotides used as capture probes, was confirmed using FT-IR. The attachment of these molecules onto the QDs affected the luminescence efficiency and this was observed through fluorescence measurements. This property of CdSe QDs to change their fluorescence intensity when ligands are attached to them was used as a qualitative method of measurement, besides the electrochemical method, to develop a rapid detection platform for a segment of DNA incorporated into genetically modified corn and soybeans. In this research an NH_2 terminated sequence of DNA at the 5′ end was immobilized onto the CdSe@TU@GA to make CdSe@TU@GA@NH_2Probe-ssDNA and the concentration of DNA containing samples were qualitatively and quantitatively determined potentiometrically, via a potentiometer (Anapot), yielding the following results: 92.2%, 4.1%, 76.5%, 5.4%, 3.4% and 57.9% hybridizations for the samples forward sample (F), reverse sample (R), positive control sample (+ve), negative control sample (-ve), cereal A and cereal B, respectively. The surface-modified and functionalized CdSe QDs, immobilized with the capture probe single-stranded DNA had their fluorescence quenched after interaction with a sample containing the target DNA sequence. Therefore, this means that this developed method of detection based on CdSe QDs can actually work as a rapid detection method for GM soybeans and corn, both qualitatively and quantitatively and had a very low detection limit of 2.42×10^{-5} ng L^{-1}.

6.2 Recommendations

The proposed future works should try to focus on designing a detection platform with highly sensitive quantum dots to make sure that detection of the target DNA segment is achieved without amplification of the extracted DNA sample. Future works should also look at developing a standardized detection protocol and a catalogue to be used to detect all GMO crop events.

References

1. (a) Pirondini, A.; Marmiroli, N., Environmental risk assessment in GMO analysis. *Riv Biol* **2008,** *101* (2), 215-46; (b) Pirondini, A.; Marmiroli, N., Environmental risk assessment in GMO analysis. *Riv Biol* **2010,** *103* (2-3), 371-402.

2. Akiyama, H.; Nakamura, F.; Yamada, C.; Nakamura, K.; Nakajima, O.; Kawakami, H.; Harikai, N.; Furui, S.; Kitta, K.; Teshima, R., A screening method for the detection of the 35S promoter and the nopaline synthase terminator in genetically modified organisms in a real-time multiplex polymerase chain reaction using high-resolution melting-curve analysis. *Biol Pharm Bull* **2009,** *32* (11), 1824-9.

3. (a) Potrykus, I., The GMO-crop potential for more, and more nutritious food is blocked by unjustified regulation. *Journal of Innovation & Knowledge* **2017,** *2* (3), 90-96; (b) Abraham, A., Toward a workable biosafety system for regulating genetically modified organisms in Ethiopia: balancing conservation and competitiveness. *GM Crops Food* **2013,** *4* (1), 28-35.

4. (a) Krayer von Krauss, M. P.; Casman, E. A.; Small, M. J., Elicitation of expert judgments of uncertainty in the risk assessment of herbicide-tolerant oilseed crops. *Risk Anal* **2004,** *24* (6), 1515-27; (b) Ricroch, A. E.; Guillaume-Hofnung, M.; Kuntz, M., The ethical concerns about transgenic crops. *Biochem J* **2018,** *475* (4), 803-811; (c) Robbins, P. B., GMO Reignited in Science but Not in Law: A Flawed Framework Fuels France's Stalemate. *Food Drug Law J* **2014,** *69* (3), 429-46, ii; (d) Yang, Y. T.; Chen, B., Governing GMOs in the USA: science, law and public health. *J Sci Food Agric* **2016,** *96* (6), 1851-5; (e) In *Genetically Engineered Crops: Experiences and Prospects*, Washington (DC), 2016.

5. (a) Kwiatek, K.; Mazur, M.; Sieradzki, Z., Current issues connected with usage of genetically modified crops in production of feed and livestock feeding. *Pol J Vet Sci* **2008,** *11* (4), 411-4; (b) Hicks, D. J.; Millstein, R. L., GMOs: Non-health Issues' Encyclopedia of Food and Agricultural Ethics. *Springer, Dordrecht* **2016**; (c) National Toxicology, P., NTP toxicology studies of acesulfame potassium (CAS No. 55589-62-3) in genetically modified (FVB Tg.AC Hemizygous) mice and carcinogenicity studies of acesulfame potassium in genetically modified [B6.129-Trp53(tm1Brd) (N5) Haploinsufficient] mice (feed studies)mice. *Natl Toxicol Program Genet Modif Model Rep* **2005,** (2), 1-113; (d) Culp, S. J.; Beland, F. A.; Heflich, R. H.; Benson, R. W.; Blankenship, L. R.; Webb, P. J.; Mellick, P. W.; Trotter, R. W.; Shelton, S. D.; Greenlees, K. J.; Manjanatha, M. G., Mutagenicity and carcinogenicity in relation to DNA adduct formation in rats fed leucomalachite green. *Mutat Res* **2002,** *506-507*, 55-63.

6. Haslberger, A. G., Need for an "integrated safety assessment" of GMOs, linking food safety and environmental considerations. *J Agric Food Chem* **2006,** *54* (9), 3173-80.

7. (a) Alcantara-de la Cruz, R.; Dominguez-Martinez, P. A.; da Silveira, H. M.; Cruz-Hipolito, H. E.; Palma-Bautista, C.; Vazquez-Garcia, J. G.; Dominguez-Valenzuela, J. A.; De Prado, R., Management of Glyphosate-Resistant Weeds in Mexican Citrus Groves: Chemical Alternatives and Economic Viability. *Plants (Basel)* **2019,** *8* (9); (b) Ashworth, M. B.; Walsh, M. J.; Flower, K. C.; Powles, S. B., Identification of the first glyphosate-resistant wild radish (Raphanus raphanistrum L.) populations. *Pest Manag Sci* **2014,** *70* (9), 1432-6; (c) Bonny, S., Genetically Modified Herbicide-Tolerant Crops, Weeds, and Herbicides: Overview and Impact. *Environ Manage* **2016,** *57* (1), 31-48; (d) Ferrante, M.; Rapisarda, P.; Grasso, A.; Favara, C.; Oliveri Conti, G., Glyphosate and environmental toxicity with "One Health" approach, a review. *Environ Res* **2023,** *235*, 116678.

8. Zambian Government, S. I. o., Biosafety (Genetically Modified Organisms for Food, Feed and Processing) Regulations, 2010. *Statutory Instrument 42 of 2010. The Biosafety Act, 2007* **2010,** *42* (Statutory Instrument 42 of 2010).

9. (a) Kaushik, M.; Khurana, S.; Mehra, K.; Yadav, N.; Mishra, S.; Kukreti, S., Emerging Trends in Advanced Nanomaterials Based Electrochemical Genosensors. *Curr Pharm Des* **2018,** *24* (31), 3697-3709; (b) Liu, A.; Wang, K.; Weng, S.; Lei, Y.; Lin, L.; Chen, W.; Lin, X.; Chen, Y., Development of electrochemical DNA biosensors. *TrAC Trends in Analytical Chemistry* **2012,** *37*, 101-111.

10. (a) Waithaka, M.; Belay, G.; Kyotalimye, M.; Karembu, M., Progress and Challenges for Implementation of the Common Market for Eastern and Southern Africa Policy on Biotechnology and Biosafety. *Front Bioeng Biotechnol* **2015,** *3*, 109; (b) Nuss, E. T.; Arscott, S. A.; Bresnahan, K.; Pixley, K. V.; Rocheford, T.; Hotz, C.; Siamusantu, W.; Chileshe, J.; Tanumihardjo, S. A., Comparative intake of white- versus orange-colored maize by Zambian children in the context of promotion of biofortified maize. *Food Nutr Bull* **2012,** *33* (1), 63-71.

11. Stobiecka, M.; Cieśla, J. M.; Janowska, B.; Tudek, B.; Radecka, H., Piezoelectric Sensor for Determination of Genetically Modified Soybean Roundup Ready (R) in Samples not Amplified by PCR. *Sensors* **2007,** *7* (8), 1462-1479.

12. Zeng, H.; Yang, Q.; Liu, H.; Wu, G.; Jiang, W.; Liu, X.; Wang, J.; Tang, X., A sensitive immunosensor based on graphene-PAMAM composites for rapid detection of the CP4-EPSPS protein in genetically modified crops. *Food Chemistry* **2021,** *361*, 129901.

13. (a) Ahmed, W.; Simpson, S. L.; Bertsch, P. M.; Bibby, K.; Bivins, A.; Blackall, L. L.; Bofill-Mas, S.; Bosch, A.; Brandao, J.; Choi, P. M.; Ciesielski, M.; Donner, E.; D'Souza, N.;

Farnleitner, A. H.; Gerrity, D.; Gonzalez, R.; Griffith, J. F.; Gyawali, P.; Haas, C. N.; Hamilton, K. A.; Hapuarachchi, H. C.; Harwood, V. J.; Haque, R.; Jackson, G.; Khan, S. J.; Khan, W.; Kitajima, M.; Korajkic, A.; La Rosa, G.; Layton, B. A.; Lipp, E.; McLellan, S. L.; McMinn, B.; Medema, G.; Metcalfe, S.; Meijer, W. G.; Mueller, J. F.; Murphy, H.; Naughton, C. C.; Noble, R. T.; Payyappat, S.; Petterson, S.; Pitkanen, T.; Rajal, V. B.; Reyneke, B.; Roman, F. A., Jr.; Rose, J. B.; Rusinol, M.; Sadowsky, M. J.; Sala-Comorera, L.; Setoh, Y. X.; Sherchan, S. P.; Sirikanchana, K.; Smith, W.; Steele, J. A.; Sabburg, R.; Symonds, E. M.; Thai, P.; Thomas, K. V.; Tynan, J.; Toze, S.; Thompson, J.; Whiteley, A. S.; Wong, J. C. C.; Sano, D.; Wuertz, S.; Xagoraraki, I.; Zhang, Q.; Zimmer-Faust, A. G.; Shanks, O. C., Minimizing errors in RT-PCR detection and quantification of SARS-CoV-2 RNA for wastewater surveillance. *Sci Total Environ* **2022,** *805*, 149877; (b) Auvray, F.; Lecureuil, C.; Dilasser, F.; Tache, J.; Derzelle, S., Development of a real-time PCR assay with an internal amplification control for the screening of Shiga toxin-producing Escherichia coli in foods. *Lett Appl Microbiol* **2009,** *48* (5), 554-9.

14. Das, R.; Nag, S.; Banerjee, P., Electrochemical Nanosensors for Sensitization of Sweat Metabolites: From Concept Mapping to Personalized Health Monitoring. *Molecules* **2023,** *28* (3).

15. Holst-Jensen, A., Testing for genetically modified organisms (GMOs): Past, present and future perspectives. *Biotechnol Adv* **2009,** *27* (6), 1071-1082.

16. Kamle, S.; Ali, S., Genetically modified crops: detection strategies and biosafety issues. *Gene* **2013,** *522* (2), 123-32.

17. Zucko, J.; Dunlap, W.; Shick, J.; Cullum, J.; Cercelet, F.; Amin, B.; Hammen, L.; Lau, T.; Williams, J.; Hranueli, D.; Long, P., Global genome analysis of the shikimic acid pathway reveals greater gene loss in host-associated than in free-living bacteria. *BMC genomics* **2010,** *11*, 628.

18. (a) Campuzano, S.; Yanez-Sedeno, P.; Pingarron, J. M., Carbon Dots and Graphene Quantum Dots in Electrochemical Biosensing. *Nanomaterials (Basel)* **2019,** *9* (4); (b) Jin, T.; Sasaki, A.; Kinjo, M.; Miyazaki, J., A quantum dot-based ratiometric pH sensor. *Chem Commun (Camb)* **2010,** *46* (14), 2408-10.

19. Abu Elgoud, E. M.; Abd-Elhamid, A. I.; Aly, H. F., Adsorption behavior of Mo(VI) from aqueous solutions using tungstate-modified magnetic nanoparticle. *Environ Sci Pollut Res Int* **2024**.

20. (a) Kemp, L.; Adam, L.; Boehm, C. R.; Breitling, R.; Casagrande, R.; Dando, M.; Djikeng, A.; Evans, N. G.; Hammond, R.; Hills, K.; Holt, L. A.; Kuiken, T.; Markotic, A.;

Millett, P.; Napier, J. A.; Nelson, C.; OhEigeartaigh, S. S.; Osbourn, A.; Palmer, M.; Patron, N. J.; Perello, E.; Piyawattanametha, W.; Restrepo-Schild, V.; Rios-Rojas, C.; Rhodes, C.; Roessing, A.; Scott, D.; Shapira, P.; Simuntala, C.; Smith, R. D.; Sundaram, L. S.; Takano, E.; Uttmark, G.; Wintle, B.; Zahra, N. B.; Sutherland, W. J., Bioengineering horizon scan 2020. *Elife* **2020,** *9*; (b) Bohn, T.; Aheto, D. W.; Mwangala, F. S.; Fischer, K.; Bones, I. L.; Simoloka, C.; Mbeule, I.; Schmidt, G.; Breckling, B., Pollen-mediated gene flow and seed exchange in small-scale Zambian maize farming, implications for biosafety assessment. *Sci Rep* **2016,** *6*, 34483.

21. Hougs, L.; Gatto, F.; Goerlich, O.; Grohmann, L.; Lieske, K.; Mazzara, M.; Narendja, F.; Ovesna, J.; Papazova, N.; Scholtens, I. M. J.; Zel, J., Verification of Analytical Methods for GMO Testing When Implementing Interlaboratory Validated Methods. 2019; pp 245-266.

22. Willems, S.; Fraiture, M.-A.; Keersmaecker, S.; Roosens, N., Next Generation Sequencing to identify GMO in food and feed products. *LabInfo* **2015,** *13*.

23. Corbisier, P.; Pinheiro, L.; Mazoua, S.; Kortekaas, A. M.; Chung, P. Y.; Gerganova, T.; Roebben, G.; Emons, H.; Emslie, K., DNA copy number concentration measured by digital and droplet digital quantitative PCR using certified reference materials. *Anal Bioanal Chem* **2015,** *407* (7), 1831-40.

24. Churko, J. M.; Mantalas, G. L.; Snyder, M. P.; Wu, J. C., Overview of high throughput sequencing technologies to elucidate molecular pathways in cardiovascular diseases. *Circ Res* **2013,** *112* (12), 1613-23.

25. Sawde, S.; Patil, R.; Moharil, S., *Basic principles of some sensors and their applications: A review*. 2024; p 020027.

26. Korotcenkov, G.; Atashbar, M.; Krishnamurthy, S., Basic principles of chemical sensors operation. 2010; pp 1-62.

27. Vyacheslav, L.; Svitlana, S., Analysis of Basic Principles for Sensor System Design Process Mobile Robots. *Journal La Multiapp* **2020,** *1* (4), 1-6.

28. Janata, J., *Principles of Chemical Sensors*. 2009.

29. Abuzeid, H.; Abdelaal, A.; Elsharkawy, S.; Ali, G., Basic Principles and Applications of Biological Sensors Technology. 2023.

30. Koyun, A.; Ahlatcioglu Özerol, E.; İpek, Y., Biosensors and Their Principles. 2012.

31. Perumal, V.; Hashim, U., Advances in biosensors: Principle, architecture and applications. *Journal of applied biomedicine* **2014,** *12*.

32. (a) Afsarimanesh, N.; Mukhopadhyay, S. C.; Kruger, M., Molecularly Imprinted Polymer-Based Electrochemical Biosensor for Bone Loss Detection. *IEEE Trans Biomed Eng*

2018, *65* (6), 1264-1271; (b) Aftim, N.; Istamboulie, G.; Piletska, E.; Piletsky, S.; Calas-Blanchard, C.; Noguer, T., Biosensor-assisted selection of optimal parameters for designing molecularly imprinted polymers selective to phosmet insecticide. *Talanta* **2017,** *174*, 414-419; (c) Ahmad, R.; Ahn, M. S.; Hahn, Y. B., ZnO nanorods array based field-effect transistor biosensor for phosphate detection. *J Colloid Interface Sci* **2017,** *498*, 292-297; (d) Aigner, M.; Preissegger, P.; Kalcher, K.; Mehmeti, E.; Macheroux, P.; Edmondson, D.; Ortner, A., Biosensor for the characterisation of hMAO B inhibitors and the quantification of selegiline. *Talanta* **2017,** *174*, 696-702; (e) Wasik, D.; Mulchandani, A.; Yates, M. V., Point-of-Use Nanobiosensor for Detection of Dengue Virus NS1 Antigen in Adult Aedes aegypti: A Potential Tool for Improved Dengue Surveillance. *Anal Chem* **2018,** *90* (1), 679-684.

33. (a) Deng, W.; Goldys, E. M., Chemical sensing with nanoparticles as optical reporters: from noble metal nanoparticles to quantum dots and upconverting nanoparticles. *Analyst* **2014,** *139* (21), 5321-34; (b) Mahato, K.; Kumar, A.; Maurya, P. K.; Chandra, P., Shifting paradigm of cancer diagnoses in clinically relevant samples based on miniaturized electrochemical nanobiosensors and microfluidic devices. *Biosens Bioelectron* **2018,** *100*, 411-428; (c) Wang, Y.; Howes, P. D.; Kim, E.; Spicer, C. D.; Thomas, M. R.; Lin, Y.; Crowder, S. W.; Pence, I. J.; Stevens, M. M., Duplex-Specific Nuclease-Amplified Detection of MicroRNA Using Compact Quantum Dot-DNA Conjugates. *ACS Appl Mater Interfaces* **2018,** *10* (34), 28290-28300.

34. (a) Fernandes, A. C.; Gernaey, K. V.; Kruhne, U., "Connecting worlds - a view on microfluidics for a wider application". *Biotechnol Adv* **2018,** *36* (4), 1341-1366; (b) Fernandes, A. C.; Semenova, D.; Panjan, P.; Sesay, A. M.; Gernaey, K. V.; Kruhne, U., Multi-function microfluidic platform for sensor integration. *N Biotechnol* **2018,** *47*, 8-17; (c) Giouroudi, I.; Kokkinis, G., Recent Advances in Magnetic Microfluidic Biosensors. *Nanomaterials (Basel)* **2017,** *7* (7); (d) Go, D. B.; Atashbar, M. Z.; Ramshani, Z.; Chang, H. C., Surface acoustic wave devices for chemical sensing and microfluidics: A review and perspective. *Anal Methods* **2017,** *9* (28), 4112-4134; (e) Han, D.; Chand, R.; Kim, Y. S., Microscale loop-mediated isothermal amplification of viral DNA with real-time monitoring on solution-gated graphene FET microchip. *Biosens Bioelectron* **2017,** *93*, 220-225; (f) Hu, L.; Ge, A.; Wang, X.; Wang, S.; Yue, X.; Wang, J.; Feng, X.; Du, W.; Liu, B. F., Real-time monitoring of immune responses under pathogen invasion and drug interference by integrated microfluidic device coupled with worm-based biosensor. *Biosens Bioelectron* **2018,** *110*, 233-238; (g) Huang, L.; Luo, Y.; Sun, X.; Ju, H.; Tian, J.; Yu, B. Y., An artemisinin-mediated ROS evolving and dual protease light-

up nanocapsule for real-time imaging of lysosomal tumor cell death. *Biosens Bioelectron* **2017,** *92*, 724-732.

35. (a) Abi, A.; Mohammadpour, Z.; Zuo, X.; Safavi, A., Nucleic acid-based electrochemical nanobiosensors. *Biosens Bioelectron* **2018,** *102*, 479-489; (b) Adachi, T.; Kaida, Y.; Kitazumi, Y.; Shirai, O.; Kano, K., Bioelectrocatalytic performance of d-fructose dehydrogenase. *Bioelectrochemistry* **2019,** *129*, 1-9; (c) Adegoke, O.; Park, E. Y., The use of nanocrystal quantum dot as fluorophore reporters in molecular beacon-based assays. *Nano Converg* **2016,** *3* (1), 32.

36. Abdelrasoul, G. N.; Anwar, A.; MacKay, S.; Tamura, M.; Shah, M. A.; Khasa, D. P.; Montgomery, R. R.; Ko, A. I.; Chen, J., DNA aptamer-based non-faradaic impedance biosensor for detecting E. coli. *Anal Chim Acta* **2020,** *1107*, 135-144.

37. Wang, D. L., P.; Jiang, Y.; Liu, P.; Miao, B.; Hao, W.; Huang, X., Open external circuit for microbial fuel cell sensor to monitor the nitrate in aquatic environment. *Biosens Bioelectron* **2018,** *111*, 97-101.

38. van Grinsven, B.; Eersels, K.; Peeters, M.; Losada-Perez, P.; Vandenryt, T.; Cleij, T. J.; Wagner, P., The heat-transfer method: a versatile low-cost, label-free, fast, and user-friendly readout platform for biosensor applications. *ACS Appl Mater Interfaces* **2014,** *6* (16), 13309-18.

39. Kumar, V.; Bhatt, D.; Saruchi; Pandey, S., Luminescence nanomaterials for biosensing applications. *Luminescence* **2023,** *38* (7), 1011-1025.

40. Palomino-Asencio, L.; Chigo-Anota, E.; Garcia-Hernandez, E., Insights on alpha-Glucose Biosensors/Carriers Based on Boron-Nitride Nanomaterials from an Atomistic and Electronic Point of View. *Chemphyschem* **2022,** *23* (24), e202200310.

41. D'Souza, S., Microbial Biosensors. *Biosensors & bioelectronics* **2001,** *16*, 337-53.

42. Carpenter, A.; Paulsen, I.; Williams, T., Blueprints for Biosensors: Design, Limitations, and Applications. *Genes* **2018,** *9*, 375.

43. Phumlani, T.; Poslet Morgan, S.; Zikhona, N.-T., Biosensors: Design, Development and Applications. In *Nanopores*, Sadia, A.; Akhtar, M. S.; Hyung-Shik, S., Eds. IntechOpen: Rijeka, 2021; p Ch. 3.

44. Fatima, A.; Younas, I.; Ali, M., An Overview on Recent Advances in Biosensor Technology and its Future Application. *Archives Of Pharmacy Practice* **2022,** *13*, 5-10.

45. (a) Pundir, C. S.; Deswal, R.; Narwal, V., Quantitative analysis of hydrogen peroxide with special emphasis on biosensors. *Bioprocess Biosyst Eng* **2018,** *41* (3), 313-329; (b) Yu, J.; Li, Z.; Chen, C.; Chen, Y.; Zhu, Z., [Research Progress of Implantable Biosensors for

Continuous Glucose Monitoring]. *Sheng Wu Yi Xue Gong Cheng Xue Za Zhi* **2016,** *33* (5), 991-7.

46. Benito-Pena, E.; Valdes, M. G.; Glahn-Martinez, B.; Moreno-Bondi, M. C., Fluorescence based fiber optic and planar waveguide biosensors. A review. *Anal Chim Acta* **2016,** *943*, 17-40.

47. Artigues, M.; Oh, S.; Gilabert-Porres, J.; Abella, J.; Borros, S.; Colominas, S., Novel grafted electrochemical interface for covalent glucose oxidase immobilization using reactive pentafluorophenyl methacrylate. *Colloids Surf B Biointerfaces* **2019,** *175*, 1-9.

48. Lee, J.; Wipf, M.; Mu, L.; Adams, C.; Hannant, J.; Reed, M. A., Metal-coated microfluidic channels: An approach to eliminate streaming potential effects in nano biosensors. *Biosens Bioelectron* **2017,** *87*, 447-452.

49. Chen, H.; Rim, Y. S.; Wang, I. C.; Li, C.; Zhu, B.; Sun, M.; Goorsky, M. S.; He, X.; Yang, Y., Quasi-Two-Dimensional Metal Oxide Semiconductors Based Ultrasensitive Potentiometric Biosensors. *ACS Nano* **2017,** *11* (5), 4710-4718.

50. (a) Chun, H. J.; Han, Y. D.; Park, Y. M.; Kim, K. R.; Lee, S. J.; Yoon, H. C., An Optical Biosensing Strategy Based on Selective Light Absorption and Wavelength Filtering from Chromogenic Reaction. *Materials (Basel)* **2018,** *11* (3); (b) Crosley, M. S.; Yip, W. T., Silica Sol-Gel Optical Biosensors: Ultrahigh Enzyme Loading Capacity on Thin Films via Kinetic Doping. *J Phys Chem B* **2017,** *121* (9), 2121-2126; (c) Evans, R. M.; Edwards, D. A., Receptor heterogeneity in optical biosensors. *J Math Biol* **2018,** *76* (4), 795-816; (d) Ahmed, N. B.; Masse, S.; Laurent, G.; Piquemal, J. Y.; Yepremian, C.; Brayner, R.; Coradin, T., Optical microalgal biosensors for aqueous contaminants using organically doped silica as cellular hosts. *Anal Bioanal Chem* **2018,** *410* (4), 1205-1216.

51. Ahmad, W.; Rana, N. F.; Riaz, S.; Ahmad, N. M.; Hameed, M.; Naeem, A.; Tahir, R., Chemical sensing of Benzo[a]pyrene using Corchorus depressus fluorescent flavonoids. *Nat Prod Res* **2018,** *32* (8), 968-971.

52. Boutilier, J.; Moulton, H. M., Surface Plasmon Resonance-Based Concentration Determination Assay: Label-Free and Antibody-Free Quantification of Morpholinos. *Methods Mol Biol* **2017,** *1565*, 251-263.

53. Whitesides, G., Whitesides, G.M. The origins and the future of microfluidics. Nature 442, 368-373. *Nature* **2006,** *442*, 368-73.

54. Srivastava, M.; Nirala, N. R.; Srivastava, S. K.; Prakash, R., A comparative Study of Aptasensor Vs Immunosensor for Label-Free PSA Cancer Detection on GQDs-AuNRs Modified Screen-Printed Electrodes. *Sci Rep* **2018,** *8* (1), 1923.

55. Abellan-Llobregat, A.; Jeerapan, I.; Bandodkar, A.; Vidal, L.; Canals, A.; Wang, J.; Morallon, E., A stretchable and screen-printed electrochemical sensor for glucose determination in human perspiration. *Biosens Bioelectron* **2017,** *91*, 885-891.

56. (a) Bakker, E.; Bhakthavatsalam, V.; Gemene, K. L., Beyond potentiometry: robust electrochemical ion sensor concepts in view of remote chemical sensing. *Talanta* **2008,** *75* (3), 629-35; (b) Cuartero, M.; Parrilla, M.; Crespo, G. A., Wearable Potentiometric Sensors for Medical Applications. *Sensors (Basel)* **2019,** *19* (2); (c) Ferreira, N. S.; Cruz, M. G. N.; Gomes, M.; Rudnitskaya, A., Potentiometric chemical sensors for the detection of paralytic shellfish toxins. *Talanta* **2018,** *181*, 380-384.

57. In *Genetically Modified Pest-Protected Plants: Science and Regulation*, Washington (DC), 2000.

58. An, L.; Wang, G.; Han, Y.; Li, T.; Jin, P.; Liu, S., Electrochemical biosensor for cancer cell detection based on a surface 3D micro-array. *Lab Chip* **2018,** *18* (2), 335-342.

59. (a) Brand, G. D.; Pires, D. A.; Furtado, J. R., Jr.; Cooper, A.; Freitas, S. M.; Bloch, C., Jr., Oligomerization affects the kinetics and thermodynamics of the interaction of a Bowman-Birk inhibitor with proteases. *Arch Biochem Biophys* **2017,** *618*, 9-14; (b) Ray, S.; Panjikar, S.; Anand, R., Structure Guided Design of Protein Biosensors for Phenolic Pollutants. *ACS Sens* **2017,** *2* (3), 411-418; (c) Tan, C. P.; Man, Y. C., Comparative differential scanning calorimetric analysis of vegetable oils: I. Effects of heating rate variation. *Phytochem Anal* **2002,** *13* (3), 129-41.

60. Damian, L., Isothermal Titration Calorimetry for Studying Protein–Ligand Interactions. *Methods in molecular biology (Clifton, N.J.)* **2013,** *1008*, 103-18.

61. Řezníček, M.; Szendiuch, I.; Reznicek, Z., Thermodynamic sensors new opportunities for measuring and control in industrial applications. **2010**.

62. (a) Bari, S. M. I.; Reis, L. G.; Nestorova, G. G., Calorimetric sandwich-type immunosensor for quantification of TNF-alpha. *Biosens Bioelectron* **2019,** *126*, 82-87; (b) Ihms, E. C.; Kleckner, I. R.; Gollnick, P.; Foster, M. P., Mechanistic Models Fit to Variable Temperature Calorimetric Data Provide Insights into Cooperativity. *Biophys J* **2017,** *112* (7), 1328-1338.

63. Davaji, B.; Lee, C. H., A paper-based calorimetric microfluidics platform for bio-chemical sensing. *Biosens Bioelectron* **2014,** *59*, 120-6.

64. Cali, K.; Tuccori, E.; Persaud, K. C., Gravimetric biosensors. *Methods Enzymol* **2020,** *642*, 435-468.

65. Ko, W.; Yim, C.; Jung, N.; Joo, J.; Jeon, S.; Seo, H.; Lee, S. S.; Park, J. C., A visible light-induced photocatalytic silver enhancement reaction for gravimetric biosensors. *Nanotechnology* **2011,** *22* (40), 405502.

66. (a) Nam, D. H.; Lee, J. O.; Sang, B. I.; Won, K.; Kim, Y. H., Silaffin peptides as a novel signal enhancer for gravimetric biosensors. *Appl Biochem Biotechnol* **2013,** *170* (1), 25-31; (b) Olivares, J.; Mirea, T.; Gordillo-Dagallier, L.; Marco, B.; Escolano, J. M.; Clement, M.; Iborra, E., Direct growth of few-layer graphene on AlN-based resonators for high-sensitivity gravimetric biosensors. *Beilstein J Nanotechnol* **2019,** *10*, 975-984.

67. (a) Kirste, R.; Rohrbaugh, N.; Bryan, I.; Bryan, Z.; Collazo, R.; Ivanisevic, A., Electronic Biosensors Based on III-Nitride Semiconductors. *Annu Rev Anal Chem (Palo Alto Calif)* **2015,** *8*, 149-69; (b) Mulla, M. Y.; Torsi, L.; Manoli, K., Electronic biosensors based on EGOFETs. *Methods Enzymol* **2020,** *642*, 403-433.

68. Hanson, C. W., 3rd; Thaler, E. R., Electronic nose prediction of a clinical pneumonia score: biosensors and microbes. *Anesthesiology* **2005,** *102* (1), 63-8.

69. Saha, S.; Sachdev, M.; Mitra, S. K., Recent advances in label-free optical, electrochemical, and electronic biosensors for glioma biomarkers. *Biomicrofluidics* **2023,** *17* (1), 011502.

70. (a) Ferreira, G. N.; da-Silva, A. C.; Tome, B., Acoustic wave biosensors: physical models and biological applications of quartz crystal microbalance. *Trends Biotechnol* **2009,** *27* (12), 689-97; (b) Fogel, R.; Limson, J.; Seshia, A. A., Acoustic biosensors. *Essays Biochem* **2016,** *60* (1), 101-10.

71. Lakshmanan, A.; Jin, Z.; Nety, S. P.; Sawyer, D. P.; Lee-Gosselin, A.; Malounda, D.; Swift, M. B.; Maresca, D.; Shapiro, M. G., Acoustic biosensors for ultrasound imaging of enzyme activity. *Nat Chem Biol* **2020,** *16* (9), 988-996.

72. (a) Wu, H.; Zu, H.; Wang, J. H.; Wang, Q. M., A study of Love wave acoustic biosensors monitoring the adhesion process of tendon stem cells (TSCs). *Eur Biophys J* **2019,** *48* (3), 249-260; (b) Zhang, Y.; Luo, J.; Flewitt, A. J.; Cai, Z.; Zhao, X., Film bulk acoustic resonators (FBARs) as biosensors: A review. *Biosens Bioelectron* **2018,** *116*, 1-15.

73. Faria, H. A. M.; Zucolotto, V., Label-free electrochemical DNA biosensor for zika virus identification. *Biosens Bioelectron* **2019,** *131*, 149-155.

74. Chirac, P. M., D.; Lepretre, F.; Isaac, S.; Glehen, O.; Figeac, M.; Villeneuve, L.; Peron, J.; Gibson, F.; Galateau-Salle, F.; Gilly, F. N.; Brevet, M., Genomic copy number alterations in 33 malignant peritoneal mesothelioma analyzed by comparative genomic hybridization array. *Hum Pathol* **2016,** *55*, 72-82.

75. (a) Ahmed, M. U.; Saito, M.; Hossain, M. M.; Rao, S. R.; Furui, S.; Hino, A.; Takamura, Y.; Takagi, M.; Tamiya, E., Electrochemical genosensor for the rapid detection of GMO using loop-mediated isothermal amplification. *Analyst* **2009,** *134* (5), 966-72; (b) Campuzano, S.; Yanez-Sedeno, P.; Pingarron, J. M., Electrochemical Genosensing of Circulating Biomarkers. *Sensors (Basel)* **2017,** *17* (4); (c) Cinti, S.; Volpe, G.; Piermarini, S.; Delibato, E.; Palleschi, G., Electrochemical Biosensors for Rapid Detection of Foodborne Salmonella: A Critical Overview. *Sensors (Basel)* **2017,** *17* (8).

76. Zhou, H.; Wu, Z. F.; Han, Q. J.; Zhong, H. M.; Peng, J. B.; Li, X.; Fan, X. L., Stable and Label-Free Fluorescent Probe Based on G-triplex DNA and Thioflavin T. *Anal Chem* **2018,** *90* (5), 3220-3226.

77. Thakkar, K. N., & Mody, H. M. , Recent advances in synthesis of quantum dots: an overview. *Journal of Nanoscience and Nanotechnology, 13(8), 5370-5388.* **2013**.

78. (a) Baqir, M. A.; Farmani, A.; Fatima, T.; Raza, M. R.; Shaukat, S. F.; Mir, A., Nanoscale, tunable, and highly sensitive biosensor utilizing hyperbolic metamaterials in the near-infrared range. *Appl Opt* **2018,** *57* (31), 9447-9454; (b) Andres-Penares, D.; Cros, A.; Martínez-Pastor, J. P.; Sánchez-Royo, J. F., Quantum size confinement in gallium selenide nanosheets: band gap tunability versus stability limitation. *Nanotechnology* **2017,** *28* (17), 175701.

79. Lu, S.; Wang, S.; Zhao, J.; Sun, J.; Yang, X., Fluorescence Light-Up Biosensor for MicroRNA Based on the Distance-Dependent Photoinduced Electron Transfer. *Anal Chem* **2017,** *89* (16), 8429-8436.

80. Segets, D.; Lucas, J. M.; Klupp Taylor, R. N.; Scheele, M.; Zheng, H.; Alivisatos, A. P.; Peukert, W., Determination of the quantum dot band gap dependence on particle size from optical absorbance and transmission electron microscopy measurements. *ACS Nano* **2012,** *6* (10), 9021-32.

81. (a) Alkahtani, M. H.; Alghannam, F.; Jiang, L.; Rampersaud, A. A.; Brick, R.; Gomes, C. L.; Scully, M. O.; Hemmer, P. R., Fluorescent nanodiamonds for luminescent thermometry in the biological transparency window. *Opt Lett* **2018,** *43* (14), 3317-3320; (b) Sharma, H.; Sidhu, J. S.; Hassen, W. M.; Singh, N.; Dubowski, J. J., Synthesis of a 3,4-Disubstituted 1,8-Naphthalimide-Based DNA Intercalator for Direct Imaging of Legionella pneumophila. *ACS Omega* **2019,** *4* (3), 5829-5838; (c) Tan, W.; Shi, Z. Y.; Smith, S.; Birnbaum, D.; Kopelman, R., Submicrometer intracellular chemical optical fiber sensors. *Science* **1992,** *258* (5083), 778-81.

82. (a) Pijeira, M. S. O.; de Menezes, A. S.; Fechine, P. B. A.; Shah, S. Q.; Ilem-Ozdemir, D.; Lopez, E. O.; Maricato, J. T.; Rosa, D. S.; Ricci-Junior, E.; Junior, S. A.; Alencar, L. M. R.; Santos-Oliveira, R., Folic acid-functionalized graphene quantum dots: Synthesis, characterization, radiolabeling with radium-223 and antiviral effect against Zika virus infection. *Eur J Pharm Biopharm* **2022,** *180*, 91-100; (b) Redondo-Fernandez, G.; Cigales Canga, J.; Soldado, A.; Ruiz Encinar, J.; Costa-Fernandez, J. M., Functionalized heteroatom-doped carbon dots for biomedical applications: A review. *Anal Chim Acta* **2023,** *1284*, 341874.

83. Xia, X., Fabrication of CdS quantum dots with egg white and application in the assay of hypochlorous acid and myeloperoxidase activity and inhibition. *Anal Methods* **2023,** *15* (34), 4260-4267.

84. Voronova, A.; Barras, A.; Plaisance, V.; Pawlowski, V.; Boukherroub, R.; Abderrahmani, A.; Szunerits, S., Anti-aggregation effect of carbon quantum dots on diabetogenic and beta-cell cytotoxic amylin and beta amyloid heterocomplexes. *Nanoscale* **2022,** *14* (39), 14683-14694.

85. (a) Kim, J.; Hwang, D. W.; Jung, H. S.; Kim, K. W.; Pham, X. H.; Lee, S. H.; Byun, J. W.; Kim, W.; Kim, H. M.; Hahm, E.; Ham, K. M.; Rho, W. Y.; Lee, D. S.; Jun, B. H., High-quantum yield alloy-typed core/shell CdSeZnS/ZnS quantum dots for bio-applications. *J Nanobiotechnology* **2022,** *20* (1), 22; (b) Gao, X.; Zhang, Y.; Fu, Z.; Cui, F., One step synthesis of ultra-high quantum yield fluorescent carbon dots for "on-off-on" detection of Hg(2+) and biothiols. *J Fluoresc* **2022,** *32* (5), 1921-1930; (c) Han, Y.; Kong, X.; Bao, R.; Yi, J.; Liu, L.; Gu, Y.; Yi, L., Synthesis of high quantum yield rhenium-doped carbonized polymer dots for dual sensing of Fe(3+) and Mo(6+) and anti-counterfeit ink applications. *Talanta* **2023,** *265*, 124913.

86. (a) Anju, S.; Ashtami, J.; Mohanan, P. V., Black phosphorus, a prospective graphene substitute for biomedical applications. *Mater Sci Eng C Mater Biol Appl* **2019,** *97*, 978-993; (b) Rohaizad, N.; Mayorga-Martinez, C. C.; Sofer, Z.; Pumera, M., 1T-Phase Transition Metal Dichalcogenides (MoS2, MoSe2, WS2, and WSe2) with Fast Heterogeneous Electron Transfer: Application on Second-Generation Enzyme-Based Biosensor. *ACS Appl Mater Interfaces* **2017,** *9* (46), 40697-40706.

87. Singh, H.; Singh, P.; Singh, R.; Sharma, J.; Singh, A. P.; Kumar, A.; Thakur, A., Composition dependent structural phase transition and optical band gap tuning in InSe thin films. *Heliyon* **2019,** *5* (11), e02933.

88. Alharshan, G. A.; Aboraia, A. M.; Uosif, M. A. M.; Sharaf, I. M.; Shaaban, E. R.; Saad, M.; H, A. L.; Elsenety, M. M., Optical Band Gap Tuning, DFT Understandings, and

Photocatalysis Performance of ZnO Nanoparticle-Doped Fe Compounds. *Materials (Basel)* **2023,** *16* (7).

89. (a) Pereira, P. F. S.; Santos, C. C.; Gouveia, A. F.; Ferrer, M. M.; Pinatti, I. M.; Botelho, G.; Sambrano, J. R.; Rosa, I. L. V.; Andres, J.; Longo, E., alpha-Ag(2-2x)Zn(x)WO(4) (0 </= x </= 0.25) Solid Solutions: Structure, Morphology, and Optical Properties. *Inorg Chem* **2017,** *56* (13), 7360-7372; (b) Toufanian, R.; Piryatinski, A.; Mahler, A. H.; Iyer, R.; Hollingsworth, J. A.; Dennis, A. M., Bandgap Engineering of Indium Phosphide-Based Core/Shell Heterostructures Through Shell Composition and Thickness. *Front Chem* **2018,** *6*, 567.

90. (a) Alivisatos, A. P., Semiconductor Clusters, Nanocrystals, and Quantum Dots. *Science* **1996,** *271* (5251), 933-937; (b) Diamantopoulos, N. C.; Barnasas, A.; Garoufalis, C. S.; Anyfantis, D. I.; Bouropoulos, N.; Poulopoulos, P.; Baskoutas, S., Band Gap Measurements of Nano-Meter Sized Rutile Thin Films. *Nanomaterials (Basel)* **2020,** *10* (12).

91. Chiu, C. H.; Chen, Y. T.; Shen, J. L., Quantum dots derived from two-dimensional transition metal dichalcogenides: synthesis, optical properties and optoelectronic applications. *Nanotechnology* **2023,** *34* (48).

92. (a) Almzargah, G. M.; Tohari, M. M., Tunable Switching between Slow and Fast Light in the Graphene Nanodisks (GND)-Quantum Dot (QD) Plasmonic Hybrid Systems. *Nanomaterials (Basel)* **2023,** *13* (5); (b) Furey, B. J.; Stacy, B. J.; Shah, T.; Barba-Barba, R. M.; Carriles, R.; Bernal, A.; Mendoza, B. S.; Korgel, B. A.; Downer, M. C., Two-Photon Excitation Spectroscopy of Silicon Quantum Dots and Ramifications for Bio-Imaging. *ACS Nano* **2022,** *16* (4), 6023-6033.

93. Rezapour, M. R. M., C. W.; Yun, J.; Ghassami, A.; Li, N.; Yu, S. U.; Hajibabaei, A.; Park, Y.; Kim, K. S., Graphene and Graphene Analogs toward Optical, Electronic, Spintronic, Green-Chemical, Energy-Material, Sensing, and Medical Applications. *ACS Appl Mater Interfaces* **2017,** *9 (29)*, 24393-24406.

94. Barbati, A. C.; Kirby, B. J., Electrokinetic measurements of thin Nafion films. *Langmuir* **2014,** *30* (8), 1985-93.

95. Abd-Elrahman, M. I.; Abu-Sehly, A. A.; Bakier, Y. M.; Hafiz, M. M., Thickness and optical constants calculation for chalcogenide-alkali metal Se(80)Te(8)(NaCl)(12) thin film. *Spectrochim Acta A Mol Biomol Spectrosc* **2017,** *184*, 243-248.

96. Akkerman, Q. A., Spheroidal Cesium Lead Chloride-Bromide Quantum Dots and a Fast Determination of Their Size and Halide Content. *Nano Lett* **2022,** *22* (20), 8168-8173.

97. Debellis, D.; Gigli, G.; Ten Brinck, S.; Infante, I.; Giansante, C., Quantum-Confined and Enhanced Optical Absorption of Colloidal PbS Quantum Dots at Wavelengths with Expected Bulk Behavior. *Nano Lett* **2017,** *17* (2), 1248-1254.

98. Watanabe, S.; Tamura, N.; Matsumoto, M., Lithography of self-assembled semiconductor quantum dots on templates fabricated from mixed Langmuir-Blodgett films. *J Oleo Sci* **2012,** *61* (5), 277-83.

99. Mullaugh, K. M.; Luther, G. W., 3rd, Spectroscopic determination of the size of cadmium sulfide nanoparticles formed under environmentally relevant conditions. *J Environ Monit* **2010,** *12* (4), 890-7.

100. (a) Liu, Y.; Yang, M.; Li, J.; Zhang, W.; Jiang, X., Plasma Treatment Conversion of Phenolic Compounds into Fluorescent Organic Nanoparticles for Cell Imaging. *Anal Chem* **2019,** *91* (10), 6754-6760; (b) Thakar, R.; Chen, Y.; Snee, P. T., Efficient emission from core/(doped) shell nanoparticles: applications for chemical sensing. *Nano Lett* **2007,** *7* (11), 3429-32.

101. Fang, Y., & Wu, L. , Recent advances in the synthesis of quantum dots. *Journal of Materials Chemistry C, 7(11), 3043-3055.* **2019**.

102. Shang, Y.; Ning, Z., Colloidal quantum-dots surface and device structure engineering for high-performance light-emitting diodes. *National Science Review* **2017,** *4* (2), 170-183.

103. Gazis, T. A.; Cartlidge, A. J.; Matthews, P. D., Colloidal III–V quantum dots: a synthetic perspective. *Journal of Materials Chemistry C* **2023,** *11* (12), 3926-3935.

104. Atchudan, R.; Edison, T.; Perumal, S.; Karthikeyan, D.; Lee, Y. R., Facile synthesis of zinc oxide nanoparticles decorated graphene oxide composite via simple solvothermal route and their photocatalytic activity on methylene blue degradation. *J Photochem Photobiol B* **2016,** *162*, 500-510.

105. Zak, A. K.; Razali, R.; Majid, W. H.; Darroudi, M., Synthesis and characterization of a narrow size distribution of zinc oxide nanoparticles. *Int J Nanomedicine* **2011,** *6*, 1399-403.

106. (a) Luo, J.; Wei, H.; Li, F.; Huang, Q.; Li, D.; Luo, Y.; Meng, Q., Microwave assisted aqueous synthesis of core-shell CdSe(x)Te(1-x)-CdS quantum dots for high performance sensitized solar cells. *Chem Commun (Camb)* **2014,** *50* (26), 3464-6; (b) Rajabi, H. R.; Naghiha, R.; Kheirizadeh, M.; Sadatfaraji, H.; Mirzaei, A.; Alvand, Z. M., Microwave assisted extraction as an efficient approach for biosynthesis of zinc oxide nanoparticles: Synthesis, characterization, and biological properties. *Mater Sci Eng C Mater Biol Appl* **2017,** *78*, 1109-1118.

107. Chikan, V.; McLaurin, E. J., Rapid Nanoparticle Synthesis by Magnetic and Microwave Heating. *Nanomaterials (Basel)* **2016,** *6* (5).

108. Ahmadian-Fard-Fini, S.; Salavati-Niasari, M.; Safardoust-Hojaghan, H., Hydrothermal green synthesis and photocatalytic activity of magnetic CoFe2O4–carbon quantum dots nanocomposite by turmeric precursor. *Journal of Materials Science: Materials in Electronics* **2017,** *28*.

109. Ahmed, M.; Guleria, A.; Rath, M. C.; Singh, A. K.; Adhikari, S.; Sarkar, S. K., Facile and green synthesis of CdSe quantum dots in protein matrix: tuning of morphology and optical properties. *J Nanosci Nanotechnol* **2014,** *14* (8), 5730-42.

110. (a) Li, Y.; Cui, R.; Zhang, P.; Chen, B. B.; Tian, Z. Q.; Li, L.; Hu, B.; Pang, D. W.; Xie, Z. X., Mechanism-oriented controllability of intracellular quantum dots formation: the role of glutathione metabolic pathway. *ACS Nano* **2013,** *7* (3), 2240-8; (b) edited by Edward, D. P., *Handbook of optical constants of solids*. Orlando : Academic Press, 1985.: 1985.

111. (a) Jin, G.; Jiang, L. M.; Yi, D. M.; Sun, H. Z.; Sun, H. C., The Influence of Surface Modification on the Photoluminescence of CdTe Quantum Dots: Realization of Bio-Imaging via Cost-Effective Polymer. *Chemphyschem* **2015,** *16* (17), 3687-94; (b) Liu, C.; Du, L.; Lin, Y.; Liang, J.; Liu, J.; Cao, Y. C., Graphite oxide-dispersed CdTe quantum dots nanocomposite for flexible display luminescent membranes. *Luminescence* **2017,** *32* (6), 964-969; (c) Lee, K. H.; Noesges, B. A.; McPherson, C.; Khan, F.; Brillson, L. J.; Winter, J. O., Oxidation of quantum dots encapsulated in block copolymer micelles as a function of polymer terminal charge. *Nanoscale* **2022,** *14* (32), 11779-11789.

112. Xia, P.; Shou, Q.; Wang, T.; Yang, G.; Li, H.; Li, Q.; Chen, Y.; Xie, T.; Huang, J.; Xing, X., Highly stable and recoverable humidity sensor using fluorescent quantum dot film. *Opt Lett* **2022,** *47* (11), 2674-2677.

113. Elumalai, D.; Rodríguez Fernández, B.; Kovtun, A.; Hidalgo, P.; Mendez, B.; Shaik, K.; Joshi, G.; Cuberes, T., Nanostructural Characterization of Luminescent Polyvinyl Alcohol/Graphene Quantum Dots Nanocomposite Films. *Nanomaterials* **2023,** *14*, 5.

114. Chen, T.; Chen, Y.; Li, Y.; Liang, M.; Wu, W.; Wang, Y., A Review on Multiple I-III-VI Quantum Dots: Preparation and Enhanced Luminescence Properties. *Materials* **2023,** *16* (14).

115. Che, N.; Yang, X.; Liu, Z.; Li, K.; Chen, X., Rapid detection of cell-free Mycobacterium tuberculosis DNA in tuberculous pleural effusion. *Journal of clinical microbiology* **2017,** *55* (5), 1526-1532.

116. (a) Tam, P. D., Genetically modified organism (GMO) detection by biosensor based on SWCNT material. *Current Applied Physics* **2015,** *15* (3), 397-401; (b) Cankar, K.; Stebih, D.; Dreo, T.; Zel, J.; Gruden, K., Critical points of DNA quantification by real-time PCR--effects of DNA extraction method and sample matrix on quantification of genetically modified organisms. *BMC Biotechnol* **2006,** *6*, 37.

117. Liu, J. L.; Ma, Y. C.; Yang, T.; Hu, R.; Yang, Y. H., A single nucleotide polymorphism electrochemical sensor based on DNA-functionalized Cd-MOFs-74 as cascade signal amplification probes. *Microchimica Acta* **2021,** *188* (8), 266.

118. Sandoval-Flores, G.; Alvarado-Reyna, S.; Elvir-Padilla, L. G.; Mendoza-Castillo, D. I.; Reynel-Avila, H. E.; Bonilla-Petriciolet, A., Kinetics, Thermodynamics, and Competitive Adsorption of Heavy Metals from Water Using Orange Biomass. *Water Environ Res* **2018,** *90* (12), 2114-2125.

119. Shimizu, S.; Matubayasi, N., Fluctuation adsorption theory: quantifying adsorbate-adsorbate interaction and interfacial phase transition from an isotherm. *Phys Chem Chem Phys* **2020,** *22* (48), 28304-28316.

120. Langmuir, I., The Adsorption of Gases on Plane Surfaces of Glass, Mica, and Platinum. *Journal of the American Chemical Society* **1918,** *40(9)*, 1361-1403.

121. Kalam, S.; Abu-Khamsin, S. A.; Kamal, M. S.; Patil, S., Surfactant Adsorption Isotherms: A Review. *ACS Omega* **2021,** *6* (48), 32342-32348.

122. Akhi, A. A.; Hasan, A.; Saha, N.; Howlader, S.; Bhattacharjee, S.; Dey, K.; Atique Ullah, A. K. M.; Bhuiyan, F. R.; Chakraborty, A. K.; Akhtar, U. S.; Shaikh, M. A. A.; Dey, B. K.; Bhattacharjee, S.; Ganguli, S., Ophiorrhiza mungos-Mediated Silver Nanoparticles as Effective and Reusable Adsorbents for the Removal of Methylene Blue from Water. *ACS Omega* **2024,** *9* (4), 4324-4338.

123. Bangari, R. S.; Yadav, A.; Sinha, N., Experimental and theoretical investigations of methyl orange adsorption using boron nitride nanosheets. *Soft Matter* **2021,** *17* (9), 2640-2651.

124. Lee, J. J.; Jeon, J. K., Isotherm, Kinetic and Thermodynamic Studies on Adsorption of Bromocresol Purple, Acid Red 66 and Acid Blue 40 Using Activated Carbon. *J Nanosci Nanotechnol* **2021,** *21* (7), 4104-4109.

125. Zhou, X.; Maimaitiniyazi, R.; Wang, Y., Some consideration triggered by misquotation of Temkin model and the derivation of its correct form. *Arabian Journal of Chemistry* **2022,** *15* (11), 104267.

126. Elahi, N.; Baghersad, M. H.; Kamali, M., Precise, direct, and rapid detection of Shigella Spa gene by a novel unmodified AuNPs-based optical genosensing system. *J Microbiol Methods* **2019,** *162*, 42-49.

127. Azadi, H.; Samiee, A.; Mahmoudi, H.; Jouzi, Z.; Khachak, P. R.; De Maeyer, P.; Witlox, F., Genetically modified crops and small-scale farmers: main opportunities and challenges. *Crit Rev Biotechnol* **2016,** *36* (3), 434-46.

128. Akinbo, O.; Obukosia, S.; Ouedraogo, J.; Sinebo, W.; Savadogo, M.; Timpo, S.; Mbabazi, R.; Maredia, K.; Makinde, D.; Ambali, A., Commercial Release of Genetically Modified Crops in Africa: Interface Between Biosafety Regulatory Systems and Varietal Release Systems. *Front Plant Sci* **2021,** *12*, 605937.

129. (a) Ermolli, M.; Prospero, A.; Balla, B.; Querci, M.; Mazzeo, A.; Van Den Eede, G., Development of an innovative immunoassay for CP4EPSPS and Cry1AB genetically modified protein detection and quantification. *Food Addit Contam* **2006,** *23* (9), 876-82; (b) Iqbal, A.; Ali, M. A.; Ahmed, S.; Hassan, S.; Shahid, N.; Azam, S.; Rao, A. Q.; Ali, Q.; Shahid, A. A., Engineered resistance and risk assessment associated with insecticidal and weeds resistant transgenic cotton using wister rat model. *Sci Rep* **2022,** *12* (1), 2518; (c) Liu, F.; Liu, Y.; Zou, J.; Zhang, L.; Zheng, H.; Luo, Y.; Wang, X.; Wang, L., Molecular Characterization and Efficacy Evaluation of Transgenic Maize Harboring cry2Ab-vip3A-cp4epsps for Insect Resistance and Herbicide Tolerance. *Plants (Basel)* **2023,** *12* (3).

130. (a) Amofah, G., Recommendations from a meeting on health implications of genetically modified organism (GMO). *Ghana Med J* **2014,** *48* (2), 123-5; (b) de Santis, B.; Stockhofe, N.; Wal, J. M.; Weesendorp, E.; Lalles, J. P.; van Dijk, J.; Kok, E.; De Giacomo, M.; Einspanier, R.; Onori, R.; Brera, C.; Bikker, P.; van der Meulen, J.; Kleter, G., Case studies on genetically modified organisms (GMOs): Potential risk scenarios and associated health indicators. *Food Chem Toxicol* **2018,** *117*, 36-65; (c) Ault, A., GMO controversy has adverse effects on UK research. *Nat Med* **2000,** *6* (4), 364.

131. Qaim, M., & Kouser, S. , Genetically modified crops and food security. *PLoS One, 8(6), e64879* **2013**.

132. Hielscher, S.; Pies, I.; Valentinov, V.; Chatalova, L., Rationalizing the GMO Debate: The Ordonomic Approach to Addressing Agricultural Myths. *Int J Environ Res Public Health* **2016,** *13* (5).

133. Van Eenennaam, A. L., & Young, A. E. , Prevalence and impacts of genetically engineered feedstuffs on livestock populations. *Journal of Animal Science, 92(10), 4255-4278* **2014**.

134. Domingo, J. L., & Giné Bordonaba, J. , A literature review on the safety assessment of genetically modified plants. *Environment International, 37(4), 734-742* **2011**.

135. Seetharam, S., Should the Bt brinjal controversy concern healthcare professionals and bioethicists? *Indian J Med Ethics* **2010,** *7* (1), 9-12.

136. Beeckman, D. S. A.; Rudelsheim, P., Biosafety and Biosecurity in Containment: A Regulatory Overview. *Front Bioeng Biotechnol* **2020,** *8*, 650.

137. Righelato, R., Food labels should state the benefits of GMOs. *Nature* **2002,** *419* (6905), 337.

138. Verma, C.; Nanda, S.; Singh, R.; Singh, R.; Mishra, S., A Review on Impacts of Genetically Modified Food on Human Health. *The Open Nutraceuticals Journal* **2011,** *4*, 3-11.

139. (a) Auxillos, J. Y.; Garcia-Ruiz, E.; Jones, S.; Li, T.; Jiang, S.; Dai, J.; Cai, Y., Multiplex Genome Engineering for Optimizing Bioproduction in Saccharomyces cerevisiae. *Biochemistry* **2019,** *58* (11), 1492-1500; (b) Botha, G. M.; Viljoen, C. D., Can GM sorghum impact Africa? *Trends Biotechnol* **2008,** *26* (2), 64-9; (c) Miller, H. I.; Silva, B., The flower industry gets the genetic engineering blues. *GM Crops Food* **2018,** *9* (2), 49-52.

140. Amaro-Blanco, I.; Fernandez-Moreno, P. T.; Osuna-Ruiz, M. D.; Bastida, F.; De Prado, R., Mechanisms of glyphosate resistance and response to alternative herbicide-based management in populations of the three Conyza species introduced in southern Spain. *Pest Manag Sci* **2018,** *74* (8), 1925-1937.

141. Komparic, A., The Ethics of Introducing GMOs into sub-Saharan Africa: Considerations from the sub-Saharan African Theory of Ubuntu. *Bioethics* **2015,** *29 (9)*, 604-12.

142. (a) Ju, L.; Deng, G.; Liang, J.; Zhang, H.; Li, Q.; Pan, Z.; Yu, M.; Long, H., Structural organization and functional divergence of high isoelectric point alpha-amylase genes in bread wheat (Triticum aestivum L.) and barley (Hordeum vulgare L.). *BMC Genet* **2019,** *20* (1), 25; (b) Smets, G.; Alcalde, E.; Andres, D.; Carron, D.; Delzenne, P.; Heise, A.; Legris, G.; Martinez Parrilla, M.; Verhaert, J.; Wandelt, C.; Ilegems, M.; Rudelsheim, P., The use of existing environmental networks for the post-market monitoring of GM crop cultivation in the EU. *Environ Sci Process Impacts* **2014,** *16* (7), 1754-63; (c) Tagliabue, G., European incoherence on GMO cultivation versus importation. *Nat Biotechnol* **2016,** *34* (7), 694-5; (d) Smets, G. A., E.; Andres, D.; Carron, D.; Delzenne, P.; Heise, A.; Legris, G.; Martinez Parrilla, M.; Verhaert, J.; Wandelt, C.; Ilegems, M.; Rudelsheim, P., The use of existing environmental networks for the post-market monitoring of GM crop cultivation in the EU. *Environ Sci Process*

Impacts **2014,** *16 (7)*, 1754-63; (e) Tagliabue, G., European incoherence on GMO cultivation versus importation. *Nat Biotechnol* **2016,** *34 (7)*, 694-5.

143. Oguchi, T.; Onishi, M.; Chikagawa, Y.; Kodama, T.; Suzuki, E.; Kasahara, M.; Akiyama, H.; Teshima, R.; Futo, S.; Hino, A.; Furui, S.; Kitta, K., Investigation of residual DNAs in sugar from sugar beet (Beta vulgaris L.). *Shokuhin Eiseigaku Zasshi* **2009,** *50* (1), 41-6.

144. ISAAA, ISAAA Brief No. 54. (ISAAA Brief No. 54. ISAAA:, Global Status of Commercialized Biotech/GM Crops in 2018: Biotech Crops Continue to Help Meet the Challenges of Increased Population and Climate Change. . *The International Service for the Acquisition of Agri-biotech Applications (ISAAA). Ithaca, (NY.)* **2018**.

145. James, C., Global status of commercialized biotech/GM crops: 2018. *ISAAA Brief* **(2018),** *No. 54.*

146. (a) Gaskell, G., Allum, N., Bauer, M. W., Durant, J., & Allansdottir, A., Worlds Apart? The Reception of Genetically Modified Foods in Europe and the U.S. *Science* **2000,** *290(5492)*, 1694-1697; (b) Lusk, J. L., & Rozan, A., Public Policy and Endogenous Beliefs: The Case of Genetically Modified Food. *Journal of Agricultural and Resource Economics* **2014,** *39(2)*, 113-130.

147. (a) Cabelkova, I.; Sanova, P.; Hlavacek, M.; Broz, D.; Smutka, L.; Prochazka, P., The moderating role of perceived health risks on the acceptance of genetically modified food. *Frontiers in Public Health* **2024,** *11*; (b) Krimsky, S., An Illusory Consensus behind GMO Health Assessment. *Science, Technology, and Human Values* **2015,** *40* (6), 883-914.

148. (a) Nicolia, A.; Manzo, A.; Veronesi, F.; Rosellini, D., An overview of the last 10 years of genetically engineered crop safety research. *Critical Reviews in Biotechnology* **2014,** *34* (1), 77-88; (b) Farias, D. F.; Viana, M. P.; de Oliveira, G. R.; Beneventi, M. A.; Soares, B. M.; Pessoa, C.; Pessoa, I. P.; Silva, L. P.; Vasconcelos, I. M.; de Sa, M. F.; Carvalho, A. F., Evaluation of cytotoxic and antimicrobial effects of two Bt Cry proteins on a GMO safety perspective. *Biomed Res Int* **2014,** *2014*, 810490; (c) Panchin, A. Y.; Tuzhikov, A. I., Published GMO studies find no evidence of harm when corrected for multiple comparisons. *Crit Rev Biotechnol* **2017,** *37* (2), 213-217.

149. (a) Panchin, A. Y. T., A. I. , Published GMO studies find no evidence of harm when corrected for multiple comparisons. *Crit Rev Biotechnol* **2017,** *37 (2)*, 213-217; (b) Farias, D. F. V., M. P.; de Oliveira, G. R.; Beneventi, M. A.; Soares, B. M.; Pessoa, C.; Pessoa, I. P.; Silva, L. P.; Vasconcelos, I. M.; de Sa, M. F.; Carvalho, A. F.,, Evaluation of cytotoxic and antimicrobial effects of two Bt Cry proteins on a GMO safety perspective. *Biomed Res Int 2014*

2014, *810490*; (c) Domingo, J. L., & Giné Bordonaba, J. , A literature review on the safety assessment of genetically modified plants. *Environment International* **2011,** *37(4)* (734-742).

150. Nicolia, A.; Manzo, A.; Veronesi, F.; Rosellini, D., An overview of the last 10 years of genetically engineered crop safety research. *Crit Rev Biotechnol* **2014,** *34* (1), 77-88.

151. Kuzma, J., & Vermaas, P., Regulation of genetically modified crops in the United States and the European Union: A comparative analysis. *Journal of Public Policy* **2008,** *28(1)*.

152. Aldemita, R. R.; Reano, I. M.; Solis, R. O.; Hautea, R. A., Trends in global approvals of biotech crops (1992-2014). *GM Crops Food* **2015,** *6* (3), 150-66.

153. (a) Arpaia, S.; Christiaens, O.; Giddings, K.; Jones, H.; Mezzetti, B.; Moronta-Barrios, F.; Perry, J. N.; Sweet, J. B.; Taning, C. N. T.; Smagghe, G.; Dietz-Pfeilstetter, A., Biosafety of GM Crop Plants Expressing dsRNA: Data Requirements and EU Regulatory Considerations. *Front Plant Sci* **2020,** *11*, 940; (b) Jaffe, G., Regulating transgenic crops: a comparative analysis of different regulatory processes. *Transgenic Res* **2004,** *13* (1), 5-19.

154. Holst-Jensen, A., Bertheau, Y., de Loose, M., & Grohmann, L. , Current status of genetically modified food detection methods: challenges and opportunities. *Analytical and bioanalytical chemistry, 403(5), 1233-1248.* **(2012)**.

155. Garibyan, L.; Avashia, N., Polymerase chain reaction. (1523-1747 (Electronic)).

156. Pallejà, A., Harrand, L., Iturriaga, E. A., & Rudi, K. , Next-generation sequencing in food safety: translating scientific advancements into practice. *Trends in Food Science & Technology* **2019,** *94, 109-123*.

157. Morisset, D., Stebih, D., Milavec, M., & Gruden, K. Žel, J. , Detection of genetically modified organisms-closing the gaps. *Nature biotechnology* **2013,** *31(7), 508-511*.

158. Zhang, D., & Li, J., Advances in mass spectrometry-based proteomic technologies for investigating genetically modified crops. *Trends in Food Science & Technology* **2018,** *81, 1-11*.

159. Dong, X.; Liu, Y.; Adcock, A. F.; Sheriff, K.; Liang, W.; Yang, L.; Sun, Y. P., Carbon-TiO(2) Hybrid Quantum Dots for Photocatalytic Inactivation of Gram-Positive and Gram-Negative Bacteria. *Int J Mol Sci* **2024,** *25* (4).

160. Zhang, S., Sun, Y., Liu, Y., Fu, Z., Ultrasensitive and Selective Genosensing Detection of Breast Cancer BRCA1 Gene Using CdSe Quantum Dots as Luminescent Labels. *Sensors and Actuators B: Chemicals* **2017,** *251*, 96-103.

161. O'Connor, S.; Al Hassan, L.; Brennan, G.; McCarthy, K.; Silien, C.; Liu, N.; Kennedy, T.; Ryan, K.; O'Reilly, E., Cadmium selenide sulfide quantum dots with tuneable emission

profiles: An electrochemiluminescence platform for the determination of TIMP-1 protein. *Bioelectrochemistry* **2022,** *148*, 108221.

162. (a) Yang, J.; Liu, H.; Huang, Y.; Li, L.; Zhu, X.; Ding, Y., One-step hydrothermal synthesis of near-infrared emission carbon quantum dots as fluorescence aptamer sensor for cortisol sensing and imaging. *Talanta* **2023,** *260*, 124637; (b) Wu, J.; Lu, Q.; Wang, H.; Huang, B., Passivator-Free Microwave-Hydrothermal Synthesis of High Quantum Yield Carbon Dots for All-Carbon Fluorescent Nanocomposite Films. *Nanomaterials (Basel)* **2022,** *12* (15).

163. Kiczor, A.; Mergo, P., Synthesis of CdSe Quantum Dots in Two Solvents of Different Boiling Points for Polymer Optical Fiber Technology. *Materials (Basel)* **2023,** *17* (1).

164. Fan, D.; Ren, X.; Wang, H.; Wu, D.; Zhao, D.; Chen, Y.; Wei, Q.; Du, B., Ultrasensitive sandwich-type photoelectrochemical immunosensor based on CdSe sensitized La-TiO2 matrix and signal amplification of polystyrene@Ab2 composites. *Biosens Bioelectron* **2017,** *87*, 593-599.

165. Liu, Y., Bai, B., Wei, H., Tian, Z., Tian, Y., A quantum Dot Fluorescence Turn-On Probe for Sensitive and Selective DNA Detection. *Chemistry - A Europeaan Journal* **2013,** *19* (27), 8806-8810.

166. Oh, S.-D.; Duong, H.; Rhee, J., Simple and sensitive progesterone detection in human serum using a CdSe/ZnS quantum dot-based direct binding assay. *Analytical biochemistry* **2015,** *483*.

167. Hu, X., Zhang, G., Cao, S., Highly Sensitive and Selective Electrochemical Detection of miRNA-21 Using a Molecular Beacon Probe and Target-Recycled CdSe Quantum Dots. *Analytical Chemistry* **2015,** *87*, 5947-5953.

168. Fang, Y.; Gao, N.; Tian, X.; Zhou, J.; Zhang, H.-F.; Gao, J.; He, X.-P.; Wen, Q.; Jia, L.-J.; Jin, H., Effect of P450 oxidoreductase polymorphisms on the metabolic activities of ten cytochrome P450s varied by polymorphic CYP genotypes in human liver microsomes. *Cellular Physiology and Biochemistry* **2018,** *47* (4), 1604-1616.

169. Huang, Y.-H. Y., H.-Y.; Huang, S.-W.; Ou, G.; Hsu, Y.-F.; Hsu, M.-J., Interleukin-6 induces vascular endothelial growth factor-C expression via Src-FAK-STAT3 signaling in lymphatic endothelial cells. *PLoS One* **2016,** *11 (7)* (e0158839).

170. Chen, D.; Lei, H.; Zhu, C.; Chen, X.; Tian, H.; Fang, W.; Qin, H.; Peng, X., Epitaxial Integration of Multiple CdSe Quantum Dots in a Colloidal CdS Nanoplatelet. *J Am Chem Soc* **2022,** *144* (19), 8444-8448.

171. Meysam, S., Recent Advances in Quantum Dots-Based Biosensors. In *Quantum Dots*, Jagannathan, T., Ed. IntechOpen: Rijeka, 2022; p Ch. 7.

172. Gupta, J.; Rajamani, P., Size- and surface functionalization-driven molecular interaction of CdSe quantum dots with jack bean urease: multispectroscopic, thermodynamic, and AFM approach. *Environ Sci Pollut Res Int* **2023,** *30* (16), 48300-48322.

173. Li, J.; Yang, Y.; Zhu, A.; Li, L.; Liu, X.; Xie, X., Improved detection and recognition of glycoproteins using fluorescent polymers with a molecular imprint based on glycopeptides. *Mikrochim Acta* **2021,** *188* (12), 439.

174. Liu, H.; Jing, Y.; Yu, X.; Pang, D.; Zhang, Z., Construction of CdSe/ZnS quantum dot microarray in a microfluidic chip. *Science China Chemistry* **2012,** *55*.

175. Vijian, D.; Chinni, V.; Lee, S.; Lertanantawong, B.; Surareungchai, W., Non-protein coding RNA-based genosensor with quantum dots as electrochemical labels for attomolar detection of multiple pathogens. *Biosensors & bioelectronics* **2015,** *77*, 805-811.

176. Liu, Z.; Zhou, J.; Wang, X.; Zhao, J.; Zhao, P.; Ma, Y.; Zhang, S.; Huo, D.; Hou, C.; Ren, K., Graphene oxide mediated CdSe quantum dots fluorescent aptasensor for high sensitivity detection of fluoroquinolones. *Spectrochimica Acta Part A: Molecular and Biomolecular Spectroscopy* **2024,** *305*, 123497.

177. Davoodi, M.; Davar, F.; Mandani, S.; Rezaei, B.; Shalan, A., CdSe Quantum Dot Nanoparticles: Synthesis and Application in the Development of Molecularly Imprinted Polymer-Based Dual Optical Sensors. *Industrial & Engineering Chemistry Research* **2021,** *60*.

178. Sapsford, K.; Pons, T.; Medintz, I.; Mattoussi, H., Biosensing with Luminescent Semiconductor Quantum Dots. *Sensors* **2006,** *6*.

179. Qiu, X.; Xu, J.; Cardoso Dos Santos, M.; Hildebrandt, N., Multiplexed Biosensing and Bioimaging Using Lanthanide-Based Time-Gated Forster Resonance Energy Transfer. *Acc Chem Res* **2022,** *55* (4), 551-564.

180. Soldado, A.; Barrio, L. C.; Diaz-Gonzalez, M.; de la Escosura-Muniz, A.; Costa-Fernandez, J. M., Advances in quantum dots as diagnostic tools. *Adv Clin Chem* **2022,** *107*, 1-40.

181. Salmi, A.; Rouabhi, R., Toxicology Study of the Toxicity of Cadmium Selenide (CdSe) on a Model Bio Indicator Helix aspersa. *Archives of Environmental Protection* **2018,** *2018*.

182. Gomes, S.; Vieira, C.; Almeida, D.; Santos-Mallet, J.; Menna-Barreto, R.; Cesar, C.; Feder, D., CdTe and CdSe Quantum Dots Cytotoxicity: A Comparative Study on Microorganisms. *Sensors* **2011,** *00*, 11664-11678.

183. Abdoos, H., A critical review on quantum dots: From synthesis toward applications in electrochemical biosensors for determination of disease-related biomolecules. *Talanta* **2020,** *224*.

184. Ozkan-Ariksoysal, D., Chapter 5 - Electrochemical DNA biosensors based on quantum dots. In *Electroanalytical Applications of Quantum Dot-Based Biosensors*, Uslu, B., Ed. Elsevier: 2021; pp 155-184.

185. Clift, M.; Stone, V., Quantum Dots: An Insight and Perspective of Their Biological Interaction and How This Relates to Their Relevance for Clinical Use. *Theranostics* **2012,** *2*, 668-80.

186. Ren, L.; Wang, L.; Rehberg, M.; Stoeger, T.; Zhang, J.; Chen, S., Applications and Immunological Effects of Quantum Dots on Respiratory System. *Frontiers in Immunology* **2022,** *12*.

187. Luo, H.; Kebede, B.; McLaurin, E.; Chikan, V., Rapid Induction and Microwave Heat-Up Syntheses of CdSe Quantum Dots. *ACS Omega* **2018,** *3*, 5399-5405.

188. Pacheco Coello, R.; Pestana Justo, J.; Factos Mendoza, A.; Santos Ordonez, E., Comparison of three DNA extraction methods for the detection and quantification of GMO in Ecuadorian manufactured food. *BMC Res Notes* **2017,** *10* (1), 758.

189. Muhammad, F.; Tahir, M.; Zeb, M.; Kalasad, M.; Mohd Said, S.; Sarker, M.; Mohd Sabri, M. F.; Ali, S., Synergistic enhancement in the microelectronic properties of poly-(dioctylfluorene) based Schottky devices by CdSe quantum dots. *Scientific Reports* **2020,** *10*.

190. García-Alegría, A. M.; Anduro-Corona, I.; Pérez-Martínez, C. J.; Guadalupe Corella-Madueño, M. A.; Rascón-Durán, M. L.; Astiazaran-Garcia, H., Quantification of DNA through the NanoDrop Spectrophotometer: Methodological Validation Using Standard Reference Material and Sprague Dawley Rat and Human DNA. *Int J Anal Chem* **2020,** *29* (8896738).

191. (a) Medintz, I.; Uyeda, H.; Goldman, E.; Mattoussi, H., Medintz, I.L., Uyeda, H.T., Goldman, E.R. & Mattoussi, H. Quantum dot bioconjugates for imaging, labelling and sensing. Nat. Mater. 4, 435-446. *Nature materials* **2005,** *4*, 435-46; (b) Wei, Y. P.; Liu, X. P.; Mao, C. J.; Niu, H. L.; Song, J. M.; Jin, B. K., Highly sensitive electrochemical biosensor for streptavidin detection based on CdSe quantum dots. *Biosens Bioelectron* **2018,** *103*, 99-103.

192. (a) Phukan, P.; Saikia, D., Optical and Structural Investigation of CdSe Quantum Dots Dispersed in PVA Matrix and Photovoltaic Applications. *International Journal of Photoenergy* **2013,** *2013*; (b) Chu, V. H.; Ha Lien, N. T.; Le Tien, H.; Vu, D.; Hong Nhung, T.; Lien, V. T. K., Synthesis and optical properties of water soluble CdSe/CdS quantum dots for biological applications. *Advances in Natural Sciences: Nanoscience and Nanotechnology* **2012,** *3*.

193. Kumar, A.; Kumar, P., Cytotoxicity of quantum dots: Use of quasiSMILES in development of reliable models with index of ideality of correlation and the consensus modelling. *J Hazard Mater* **2021,** *402*, 123777.

194. (a) Barandiaran, I.; Gutierrez, J.; Etxeberria, H.; Tercjak, A.; Kortaberria, G., Tuning photoresponsive and dielectric properties of PVA/CdSe films by capping agent change. *Composites Part A: Applied Science and Manufacturing* **2019,** *118*, 194-201; (b) Muheddin, D. Q.; Aziz, S. B.; Mohammed, P. A., Variation in the Optical Properties of PEO-Based Composites via a Green Metal Complex: Macroscopic Measurements to Explain Microscopic Quantum Transport from the Valence Band to the Conduction Band. *Polymers (Basel)* **2023,** *15* (3).

195. Jedidi, A.; Markovits, A.; Minot, C.; Bouzriba, S.; Abderraba, M., Modeling localized photoinduced electrons in rutile-TiO2 using periodic DFT+U methodology. *Langmuir* **2010,** *26* (21), 16232-8.

196. (a) Ayorinde, K., *Towards Semiconductor Nanorods With Nickel/Iron Cocatalyst. Towards Semiconductor Nanorods With Nickel/Iron Cocatalyst*. 2023; (b) Zheng, D.; Wang, Q.; Gao, F.; Wang, Q.; Qiu, W.; Gao, F., Development of a novel electrochemical DNA biosensor based on elongated hexagonal-pyramid CdS and poly-isonicotinic acid composite film. *Biosens Bioelectron* **2014,** *60*, 167-74; (c) Song, J.; Dai, Z.; Guo, W.; Li, Y.; Wang, W.; Li, N.; Wei, J., Preparation of CdTe/CdS/SiO2 core/multishell structured composite nanoparticles. *J Nanosci Nanotechnol* **2013,** *13* (10), 6924-7.

197. (a) Rezanejade Bardajee, G.; Hooshyar, Z.; Rezanezhad, H.; Guerin, G., Optical properties of water-soluble CdTe quantum dots passivated by a biopolymer based on poly((2-dimethylaminoethyl) methacrylate) grafted onto kappa-carrageenan. *ACS Appl Mater Interfaces* **2012,** *4* (7), 3517-25; (b) Xu, J.; Wang, C.; Leblanc, R. M., Surface chemistry and photophysical properties of a diacetylene-peptide derivative capped quantum dots Langmuir monolayer. *Colloids Surf B Biointerfaces* **2009,** *70* (2), 163-8; (c) Zukowski, K.; Kosman, J.; Juskowiak, B., Light-Induced Oxidase Activity of DNAzyme-Modified Quantum Dots. *Int J Mol Sci* **2020,** *21* (21).

198. Koca, M.; Arici, C.; Muglu, H.; Vurdu, C. D.; Kandemirli, F.; Zalaoglu, Y.; Yildirim, G., Quantum chemical calculations and interpretation of electronic transitions and spectroscopic characteristics belonging to 1-(3-Mesityl-3-methylcyclobutyl)-2-(naphthalene-1-yloxy)ethanone. *Spectrochim Acta A Mol Biomol Spectrosc* **2015,** *137*, 899-912.

199. Farzin, L.; Sadjadi, S.; Sheini, A.; Mohagheghpour, E., A nanoscale genosensor for early detection of COVID-19 by voltammetric determination of RNA-dependent RNA polymerase (RdRP) sequence of SARS-CoV-2 virus. *Mikrochim Acta* **2021,** *188* (4), 121.

200. Dhas, N.; Pastagia, M.; Sharma, A.; Khera, A.; Kudarha, R.; Kulkarni, S.; Soman, S.; Mutalik, S.; Barnwal, R. P.; Singh, G.; Patel, M., Organic quantum dots: An ultrasmall nanoplatform for cancer theranostics. *J Control Release* **2022,** *348*, 798-824.

201. (a) Kyaw, H. M. A.; Ishak, M. N.; Mohd Noor, A. F.; Go, K.; Matsuda, A.; Yaacob, K. A., CdSe nanostructured thin film by electrophoretic deposition for quantum dots sensitized solar cell. *Nanotechnology* **2024**; (b) Ming, S. K.; Taylor, R. A.; McNaughter, P. D.; Lewis, D. J.; Leontiadou, M. A.; O'Brien, P., Tunable structural and optical properties of CuInS(2) colloidal quantum dots as photovoltaic absorbers. *RSC Adv* **2021,** *11* (35), 21351-21358.

202. (a) Raju, G. S. R.; Varaprasad, G. L.; Lee, J. H.; Park, J. Y.; Chodankar, N. R.; Ranjith, K. S.; Pavitra, E.; Huh, Y. S.; Han, Y. K., A Novel and Cost-Effective CsVO(3) Quantum Dots for Optoelectronic and Display Applications. *Nanomaterials (Basel)* **2022,** *12* (16); (b) Zhang, H., Quantum dot-A10 RNA aptamer-doxorubicin conjugate. In *Molecular Imaging and Contrast Agent Database (MICAD)*, Bethesda (MD), 2004; (c) Zhang, H., (64)Cu-1,4,7,10-Tetraazacyclododecane-1,4,7,10-tetraacetic acid-quantum dot-vascular endothelial growth factor. In *Molecular Imaging and Contrast Agent Database (MICAD)*, Bethesda (MD), 2004.

203. (a) Islam, M. R.; Bach, L. G.; Vo, T. S.; Lee, D. C.; Lim, K. T., Controlled synthesis, optical properties and cytotoxicity studies of CdSe-poly(lactic acid) multifunctional nanocomposites by ring-opening polymerization. *J Nanosci Nanotechnol* **2014,** *14* (8), 6251-5; (b) Peng, J.; Liu, S.; Wang, L.; Liu, Z.; He, Y., Study on the interaction between CdSe quantum dots and chitosan by scattering spectra. *J Colloid Interface Sci* **2009,** *338* (2), 578-83.

204. (a) Schroder, S. D.; Wallberg, J. H.; Kroll, J. A.; Maroun, Z.; Vaida, V.; Kjaergaard, H. G., Intramolecular Hydrogen Bonding in Methyl Lactate. *J Phys Chem A* **2015,** *119* (37), 9692-702; (b) Martins, F. T.; Guimaraes, F. F.; Honorato, S. B.; Ayala, A. P.; Ellena, J., Vibrational and thermal analyses of multicomponent crystal forms of the anti-HIV drugs lamivudine and zalcitabine. *J Pharm Biomed Anal* **2015,** *110*, 76-82; (c) Jeyavijayan, S., Molecular structure, spectroscopic (FTIR, FT-Raman, 13C and 1H NMR, UV), polarizability and first-order hyperpolarizability, HOMO-LUMO analysis of 2,4-difluoroacetophenone. *Spectrochim Acta A Mol Biomol Spectrosc* **2015,** *136 Pt B*, 553-66; (d) Debus, R. J., FTIR studies of metal ligands, networks of hydrogen bonds, and water molecules near the active site Mn(4)CaO(5) cluster in Photosystem II. *Biochim Biophys Acta* **2015,** *1847* (1), 19-34.

205. Nguyen, T. T.; Nguyen, P. H.; Tran, T. H.; Minh, T. N., Existence of both blue-shifting hydrogen bond and Lewis acid-base interaction in the complexes of carbonyls and thiocarbonyls with carbon dioxide. *Phys Chem Chem Phys* **2011,** *13* (31), 14033-42.

206. (a) Lim, C. S.; Jang, D. S.; Yu, S. M.; Lee, J. J., Analysis of the Properties of Modified Asphalt Binder by FTIR Method. *Materials (Basel)* **2022,** *15* (16); (b) Bhagyasree, J. B.; Varghese, H. T.; Panicker, C. Y.; Van Alsenoy, C.; Al-Saadi, A. A.; Dolezal, M.; Samuel, J., Spectroscopic (FT-IR, FT-Raman), first order hyperpolarizability, NBO analysis, HOMO and LUMO analysis of 5-tert-Butyl-6-chloro-N-[(4-(trifluoromethyl)phenyl]pyrazine-2-carboxamide. *Spectrochim Acta A Mol Biomol Spectrosc* **2015,** *137*, 193-206; (c) Dalton, P. D.; Jefferson, A.; Hong, Y.; Chirila, T. V.; Vijayasekaran, S.; Tahija, S. G., The use of Fourier transform infrared spectrometry for monitoring the retention of polymers in the vitreous humour. *Biomed Mater Eng* **1995,** *5* (3), 185-93.

207. Singh, R.; Yadav, R. A., Raman and IR studies and DFT calculations of the vibrational spectra of 2,4-Dithiouracil and its cation and anion. *Spectrochim Acta A Mol Biomol Spectrosc* **2014,** *130*, 188-97.

208. (a) Dizdarevic, A.; Maric, M.; Shahzadi, I.; Ari Efiana, N.; Matuszczak, B.; Bernkop-Schnurch, A., Imine bond formation as a tool for incorporation of amikacin in self-emulsifying drug delivery systems (SEDDS). *Eur J Pharm Biopharm* **2021,** *162*, 82-91; (b) Fatima, R.; Sharma, M.; Dhiman, A.; Arora, A.; Mudila, H.; Prasher, P., Targeted delivery of fenamates with aminated starch. *Ther Deliv* **2023,** *14* (3), 183-192; (c) Furutani, Y.; Kawanabe, A.; Jung, K. H.; Kandori, H., FTIR spectroscopy of the all-trans form of Anabaena sensory rhodopsin at 77 K: hydrogen bond of a water between the Schiff base and Asp75. *Biochemistry* **2005,** *44* (37), 12287-96.

209. (a) Ray, B.; Agarwal, S.; Lohani, N.; Rajeswari, M. R.; Mehrotra, R., Structural, conformational and thermodynamic aspects of groove-directed-intercalation of flavopiridol into DNA. *J Biomol Struct Dyn* **2016,** *34* (11), 2518-35; (b) Kahn, T. R.; Fong, K. K.; Jordan, B.; Lek, J. C.; Levitan, R.; Mitchell, P. S.; Wood, C.; Hatcher, M. E., An FTIR investigation of flanking sequence effects on the structure and flexibility of DNA binding sites. *Biochemistry* **2009,** *48* (6), 1315-21; (c) Lindqvist, M.; Graslund, A., An FTIR and CD study of the structural effects of G-tract length and sequence context on DNA conformation in solution. *J Mol Biol* **2001,** *314* (3), 423-32.

210. Patel, A.; Dwivedi, A.; Dwivedi, N., Theoretical Study of Dependence of Wavelength on Size of Quantum Dot. *International Journal for Scientific Research & Development 2321-0613* **2016,** *4*, 1158-1159.

211. Jin, W.; Costa-Fernandez, J.; Pereiro, R.; Sanz-Medel, A., Surface-modified CdSe quantum dots as luminescent probes for cyanide determination. *Analytica Chimica Acta* **2004,** *522*, 1-8.

212. (a) Wang, X. J.; Wang, H. Z.; Sun, B. W.; Han, W. J., [Adsorption properties of thiocyanate anion on granular Mg/Al mixed oxides]. *Huan Jing Ke Xue* **2012,** *33* (9), 3182-8; (b) Li, G.; Xiao, P.; Webley, P., Binary adsorption equilibrium of carbon dioxide and water vapor on activated alumina. *Langmuir* **2009,** *25* (18), 10666-75.

213. (a) Abdel-Latif, A.; Osman, G., Comparison of three genomic DNA extraction methods to obtain high DNA quality from maize. *Plant Methods* **2017,** *13* (1), 1; (b) Tamari, F.; Hinkley, C. S.; Ramprashad, N., A comparison of DNA extraction methods using Petunia hybrida tissues. *J Biomol Tech* **2013,** *24* (3), 113-8; (c) Carey, S. J.; Becklund, L. E.; Fabre, P. P.; Schenk, J. J., Optimizing the lysis step in CTAB DNA extractions of silica-dried and herbarium leaf tissues. *Appl Plant Sci* **2023,** *11* (3), e11522.

214. Lucena-Aguilar, G.; Sánchez-López, A. M.; Barberán-Aceituno, C.; Carrillo-Ávila, J. A.; López-Guerrero, J. A.; Aguilar-Quesada, R., DNA Source Selection for Downstream Applications Based on DNA Quality Indicators Analysis. (1947-5543 (Electronic)).

215. Wang, C.; Cheng, N.; Zhu, L.; Xu, Y.; Huang, K.; Zhu, P.; Zhu, S.; Fu, W.; Xu, W., Colorimetric biosensor based on a DNAzyme primer and its application in logic gate operations for DNA screening. *Anal Chim Acta* **2017,** *987*, 111-117.

216. Goris, J.; Konstantinidis, K. T.; Klappenbach, J. A.; Coenye, T.; Vandamme, P.; Tiedje, J. M., DNA-DNA hybridization values and their relationship to whole-genome sequence similarities. *Int J Syst Evol Microbiol* **2007,** *57* (Pt 1), 81-91.

217. Yang, S.; Berdine, G., Normality tests. *The Southwest Respiratory and Critical Care Chronicles* **2021,** *9*, 87-90.

218. Shapiro, S. S.; Wilk, M. B.; Chen, H. J., A Comparative Study of Various Tests of Normality. *Journal of the American Statistical Association* **1968,** *63*, 1343-1372.

219. Feng, L.; Zou, C.; Wang, Z.; Zhu, L., Robust Comparison of Regression Curves. *Test* **2014,** *24*.

220. Vélez, J.; Correa, J., A modified Q-Q plot for large sample sizes. *Comunicaciones en Estadística* **2015,** *8*, 163.

221. (a) Amir, H.; Subramanian, V.; Sornambikai, S.; Ponpandian, N.; Viswanathan, C., Nitrogen-enhanced carbon quantum dots mediated immunosensor for electrochemical detection of HER2 breast cancer biomarker. *Bioelectrochemistry* **2024,** *155*, 108589; (b) Das, P. K.; Adil, O.; DeGregorio, A. P.; Sumita, M.; Shamsi, M. H., Pseudouridine-modified RNA probe for label-free electrochemical detection of nucleic acids on 2D MoS(2) nanosheets. *Analyst* **2024,** *149* (4), 1310-1317.

222. Bhardwaj, A.; Hreibi, A.; Liu, C.; Heo, J.; Blondy, J. M.; Gérôme, F., High temperature stable PbS quantum dots. *Optics Express* **2013,** *21*, 24922-8.

223. Amollo, T. A.; Mola, G. T.; Nyamori, V. O., Reduced graphene oxide-germanium quantum dot nanocomposite: electronic, optical and magnetic properties. *Nanotechnology* **2017,** *28* (49), 495703.

224. Chibisov, A. K.; Slavnova, T. D.; Gorner, H., Effect of macromolecules and Triton X-100 on the triplet of aggregated chlorophyll in aqueous solution. *J Photochem Photobiol B* **2003,** *72* (1-3), 11-6.

225. (a) Nandwani, Y.; Kaur, A.; Bansal, A. K., Generation of Ophthalmic Nanosuspension of Prednisolone Acetate Using a Novel Technology. *Pharm Res* **2021,** *38* (2), 319-333; (b) Sahana, D. K.; Mittal, G.; Bhardwaj, V.; Kumar, M. N., PLGA nanoparticles for oral delivery of hydrophobic drugs: influence of organic solvent on nanoparticle formation and release behavior in vitro and in vivo using estradiol as a model drug. *J Pharm Sci* **2008,** *97* (4), 1530-42.

226. Zaini, M. S.; Liew, J. Y. C.; Paiman, S.; Tee, T. S.; Kamarudin, M. A., Solvent-Dependent Photoluminescence Emission and Colloidal Stability of Carbon Quantum dots from Watermelon Peels. *J Fluoresc* **2023**.

227. Bahari, N.; Hashim, N.; Abdan, K.; Md Akim, A.; Maringgal, B.; Al-Shdifat, L., Role of Honey as a Bifunctional Reducing and Capping/Stabilizing Agent: Application for Silver and Zinc Oxide Nanoparticles. *Nanomaterials (Basel)* **2023,** *13* (7).

228. Malik, M. A.; Batterjee, M. G.; Kamli, M. R.; Alzahrani, K. A.; Danish, E. Y.; Nabi, A., Polyphenol-Capped Biogenic Synthesis of Noble Metallic Silver Nanoparticles for Antifungal Activity against Candida auris. *J Fungi (Basel)* **2022,** *8* (6).

229. (a) Medina-Lopez, D.; Liu, T.; Osella, S.; Levy-Falk, H.; Rolland, N.; Elias, C.; Huber, G.; Ticku, P.; Rondin, L.; Jousselme, B.; Beljonne, D.; Lauret, J. S.; Campidelli, S., Interplay of structure and photophysics of individualized rod-shaped graphene quantum dots with up to 132 sp(2) carbon atoms. *Nat Commun* **2023,** *14* (1), 4728; (b) Garcia-Millan, T.; Swift, T. A.; Morgan, D. J.; Harniman, R. L.; Masheder, B.; Hughes, S.; Davis, S. A.; Oliver, T. A. A.; Galan, M. C., Small variations in reaction conditions tune carbon dot fluorescence. *Nanoscale* **2022,** *14* (18), 6930-6940.

230. (a) Aghajamali, M.; Vieira, M. A.; Firouzi-Haji, R.; Cui, K.; Cho, J. Y.; Bergren, A. J.; Hassanzadeh, H.; Meldrum, A., Synthesis and properties of multi-functionalized graphene quantum dots with tunable photoluminescence and hydrophobicity from asphaltene and its oxidized and reduced derivatives. *Nanoscale Adv* **2022,** *4* (19), 4080-4093; (b) Gao, D.; Zhang,

Y.; Wu, K.; Min, H.; Wei, D.; Sun, J.; Yang, H.; Fan, H., One-step synthesis of ultrabright amphiphilic carbon dots for rapid and precise tracking lipid droplets dynamics in biosystems. *Biosens Bioelectron* **2022,** *200*, 113928.

231. Li, C.; Li, N.; Yang, L.; Liu, L.; Zhang, D., Synthesis of fluorescent carbon dots by B/P doping and application for Co(2+) and methylene blue detection. *Spectrochim Acta A Mol Biomol Spectrosc* **2024,** *309*, 123824.

232. (a) Kong, Q.; Zhang, H.; Wang, P.; Lan, Y.; Ma, W.; Shi, X., NiCo bimetallic and the corresponding monometallic organic frameworks loaded CMC aerogels for adsorbing Cu(2+): Adsorption behavior and mechanism. *Int J Biol Macromol* **2023,** *244*, 125169; (b) He, H.; Zhu, Z. Q.; Liu, J.; Zhu, Y. N.; Yan, Q. M.; Liu, Y.; Mo, N.; Xuan, H. L.; Wei, W. Y., [Removal of Pb(2+) from Aqueous Solution by Magnesium-Calcium Hydroxyapatite Adsorbent]. *Huan Jing Ke Xue* **2019,** *40* (9), 4081-4090.

Appendices

Appendix A: A.1: Ethics Approval Letter

THE UNIVERSITY OF ZAMBIA
DIRECTORATE OF RESEARCH AND GRADUATE STUDIES

Great East Road Campus | P.O. Box 32379 | Lusaka10101 | Tel: +260-211-290 258/291 777
Fax: (+260)-211-290 258/253 952 | E-**mail**: director.drgs@unza.zm | Website: www.unza.zm

APPROVAL OF STUDY

IORG No. 0005376
NASRECREC IRB No. 00006465
REF NO. NASREC: 2023-DEC-006

14th October, 2024

Mr. Happy Mabo
The University of Zambia
P.O. Box 32379
LUSAKA

Dear Mr. Mabo

RE: "ROOM TEMPERATURE AND NITROGEN-FREE SYNTHESIS OF AQUEOUS AND HIGHLY LUMINESCENT AND STABLE CdSe QUANTUM DOTS FOR RAPID GENOSENSING OF 5-ENOLPYRUVYLSHIKIMATE-3-PHOSPHATE SYNTHASE (CP4EPSPS) DNA SEGMENT IN GM CEREAL"

Reference is made to your protocol captioned above. The NASREC resolved to approve this study and your participation as Principal Investigator for a period of one year.

REVIEW TYPE	ORDINARY REVIEW	APPROVAL NO. NASREC-2023-DEC-006
Approval and Expiry Date	Approval Date: 14th October, 2024	Expiry Date: 13th October, 2025
Protocol Version and Date	Version - Nil.	13th October, 2025
Information Sheet, Consent Forms and Dates	• English.	To be provided
Consent form ID and Date	Version - Nil	To be provided
Recruitment Materials	Nil	Nil
Other Study Documents	Questionnaire.	

Specific conditions will apply to this approval. As Principal Investigator it is your responsibility to ensure that the contents of this letter are adhered to. If these are not adhered to, the approval may be suspended. Should the study be suspended, study sponsors and other regulatory authorities will be informed.

CONDITIONS OF APPROVAL

- No participant may be involved in any study procedure prior to the study approval or after the expiration date.

- All unanticipated or Serious Adverse Events (SAEs) must be reported to NASREC within 5 days.

- All protocol modifications must be approved by NASREC prior to implementation unless they are intended to reduce risk (but must still be reported for approval). Modifications will include any change of investigator/s or site address.

- All protocol deviations must be reported to NASREC within 5 working days.

- All recruitment materials must be approved by NASREC prior to being used.

- Principal investigators are responsible for initiating Continuing Review proceedings. NASREC will only approve a study for a period of 12 months.

- It is the responsibility of the PI to renew his/her ethics approval through a renewal application to NASREC.

- Where the PI desires to extend the study after expiry of the study period, documents for study extension must be received by NASREC at least 30 days before the expiry date. This is for the purpose of facilitating the review process. Documents received within 30 days after expiry will be labelled "late submissions" and will incur a penalty fee of K500.00. No study shall be renewed whose documents are submitted for renewal 30 days after expiry of the certificate.

- Every 6 (six) months a progress report form supplied by The University of Zambia Natural and Applied Sciences Research Ethics Committee as an IRB must be filled in and submitted to us. There is a penalty of K500.00 for failure to submit the report.

- When closing a project, the PI is responsible for notifying, in writing or using the Research Ethics and Management Online (REMO), both NASREC and the National Health Research Authority (NHRA) when ethics certification is no longer required for a project.

- In order to close an approved study, a Closing Report must be submitted in writing or through the REMO system. A Closing Report should be filed when data collection has ended and the study team will no longer be using human participants or animals or secondary data or have any direct or indirect contact with the research participants or animals for the study.
- Filing a closing report (rather than just letting your approval lapse) is important as it assists NASREC in efficiently tracking and reporting on projects. Note that some funding agencies and sponsors require a notice of closure from the IRB which had approved the study and can only be generated after the Closing Report has been filed.

- A reprint of this letter shall be done at a fee.

- All protocol modifications must be approved by NASREC by way of an application for an amendment prior to implementation unless they are intended to reduce risk (but must still be reported for approval). Modifications will include any change of investigator/s or site address or methodology and methods. Many modifications entail minimal risk adjustments to a protocol and/or consent form and can be made on an Expedited basis (via the IRB Chair). Some examples are: format changes, correcting spelling errors, adding key personnel, minor changes to questionnaires, recruiting and changes, and so forth. Other, more substantive changes, especially those that may alter the risk-benefit ratio, may require Full Board review. In all cases, except where noted above regarding subject safety, any changes to any protocol document or procedure must first be approved by NASREC before they can be implemented.

Should you have any questions regarding anything indicated in this letter, please do not hesitate to get in touch with us at the above indicated address.

On behalf of NASREC, we would like to wish you all the success as you carry out your study.

Yours faithfully,

Dr. Mususu Kaonda

VICE-CHAIRPERSON THE UNIVERSITY OF ZAMBIA NATURAL AND APPLIED SCIENCES RESEARCH ETHICS COMMITTEE - IRB

CC: Director, Directorate of Research, Innovation and Development
Assistant Director (Research), Directorate of Research, Innovation and Development
Assistant Registrar (Research), Directorate of Research, Innovation and Development

Appendix B: B.1: Adsorption Isotherm Studies of CdSe QDs

B.1.1 Effect of PVA Concentration on Properties of CdSe QDs

To study the effect of the concentration of the stabilizer, PVA, different concentrations of 0.00 M, 3.21×10^{-5} M, 6.42×10^{-5} M, 9.63×10^{-5} M and 1.28×10^{-4} M, were used and it was observed that the 0.13 g, 0.26 g and 0.39 g amounts gave better luminescent CdSe QDs. In this procedure used to synthesize the CdSe QDs, it was observed that in the reactions where there was no PVA added and the ones where very large amounts of PVA of 1.60×10^{-4} M and above were used, the obtained particles had a red luminescence as can be seen from Figure B.1, below. This phenomenon could be attributed to the critical micelle concentration of polyvinyl alcohol[224].

The synthesis of CdSe QDs involves the nucleation and growth of CdSe nanoscale particles from precursor ions in the presence of stabilizing agents. In the case of CdSe QDs synthesized from Cd^{2+} stabilized by citrate ions, in pH 12, and sodium selenosulphite mixed with sodium borohydride, polyvinyl alcohol (PVA) affected the size of the resulting particles and the fluorescence intensity of the particles[225].

PVA is a water-soluble polymer that can be used as a stabilizing agent in the synthesis of nanoparticles. PVA has a high affinity for the surfaces of nanoparticles, and it can form a protective layer around the particles, preventing their agglomeration and controlling their growth. The concentration of PVA in the reaction mixture can affect the size of the resulting nanoparticles, as well as their surface properties and colloidal stability[226].

In the synthesis of CdSe QDs from Cd^{2+} stabilized by citrate ions, under controlled pH, and sodium selenosulphite mixed with sodium borohydride, the addition of PVA can lead to smaller particle sizes. This is because PVA can act as a capping agent, controlling the growth of the nanoparticles by inhibiting the deposition of additional CdSe atoms onto the existing particles[227]. This results in the formation of smaller particles with a narrower size distribution[228].

At the same time, the size of the nanoparticles can also affect their fluorescence properties. Smaller particles tend to exhibit higher fluorescence quantum yields due to their larger surface area-to-volume ratio, which enhances the radiative recombination of electron-hole pairs. Therefore, the addition of PVA can enhance the fluorescence intensity of the CdSe QDs[229].

However, the effect of PVA on the fluorescence intensity of the CdSe QDs is not a straightforward relationship. The concentration of PVA can affect the surface properties of the

particles, such as their charge and hydrophobicity, which can impact the colloidal stability of the particles and their interaction with other molecules in the solution[230].

Therefore, the optimal concentration of PVA for enhancing the fluorescence intensity of the CdSe QDs may depend on its critical micelle concentration, the specific synthetic conditions and the desired properties of the resulting particles[231].

In summary, the addition of PVA affected the size of the CdSe QDs synthesized from Cd^{2+} stabilized by citrate ions, in pH 12, and sodium selenosulphite mixed with sodium borohydride, and this in turn affected the fluorescence intensity of the particles, as was observed in the QDs synthesized, as shown in Figure B.1 (b), below. The optimal concentration of PVA for enhancing the fluorescence intensity depend on the specific synthetic conditions and the desired properties of the resulting QDs.


a)

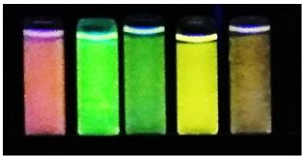
b)

Figure B.1: CdSe-QDs solutions in, from left to right, synthesised using 0.00 M, 3.21×10^{-5} M, 6.42×10^{-5} M, 9.63×10^{-5} M and 1.28×10^{-4} M of PVA a) in ordinary light and b) under UV-light at 366 nm.

B2.2 Surface Modification of CdSe QDs with Thiourea

The surface chemistry of the synthesised CdSe QDs was changed through modification with thiourea. The QDs were surface modified with thiourea in order to provide them with the needed ligands for functionalization with glutaraldehyde which in turn helped to provided appendages for immobilization of the oligonucleotides used as capture probes. The initial concentrations of the thiourea used in the experiments carried out; the equilibrium concentrations and the amounts bound onto CdSe QDs are given in Table B.1.

Table B.1: Concentration of Thiourea (TU) and the amount bound onto the CdSe QDs

Initial concentration of TU (mg mL^{-1})	Thiourea concentration at equilibrium (C_e)-CdSe-QDs@TU (mg g^{-1})	Bound TU onto CdSe-QDs (mg mL^{-1})
0.0540	0.0330	0.0210
0.1100	0.0870	0.0230
0.1600	0.1360	0.0240
0.2200	0.1927	0.0273
0.2700	0.2440	0.0260

0.3300	0.3039	0.0261
0.3800	0.3538	0.0262
0.4300	0.4036	0.0264
0.4900	0.4636	0.0264
0.5400	0.5135	0.0265

The Langmuir and Freundlich isotherm models were used to explain the equilibrium data obtained from the experiments and also determine the maximum binding capacity.

The linearized equation (9) of the Langmuir isotherm model was used to compute the values shown in Table B.2, from which the Langmuir plot was done, giving $R^2 = 0.99902$ given in Table B.3, which showed that the experimental adsorption data fitted very well into the Langmuir model. This suggests that the adsorption process of thiourea onto the synthesised CdSe QDs was of the monolayer type and therefore the adsorption process was homogeneous. The Langmuir plots are shown in Figure B.2 and Figure B.3 below.

Table B.2: The Equilibrium adsorption capacities of Thiourea (TU) onto the CdSe QDs based on the Langmuir equation.

Thiourea concentration at equilibrium (C_e) – CdSe-QDs@TU (mg mL^{-1})	$(Q_mK_LC_e)/(1+K_LC_e)$ (mg/g) CdSe-QDs@TU (Qe)
0.0330	0.0084
0.0870	0.0092
0.1360	0.0096
0.1927	0.01092
0.2440	0.0104
0.3039	0.01044
0.3538	0.01048
0.4036	0.01056
0.4636	0.01056
0.5135	0.0106

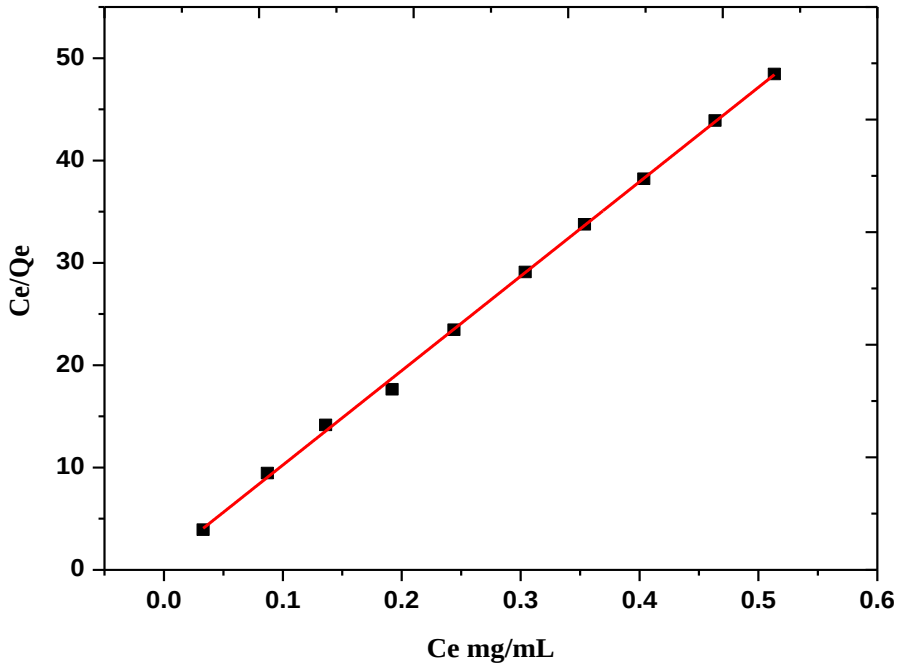

Figure B.2: Langmuir adsorption isotherm plot of Ce/Qe against Ce CdSe QDs@TU

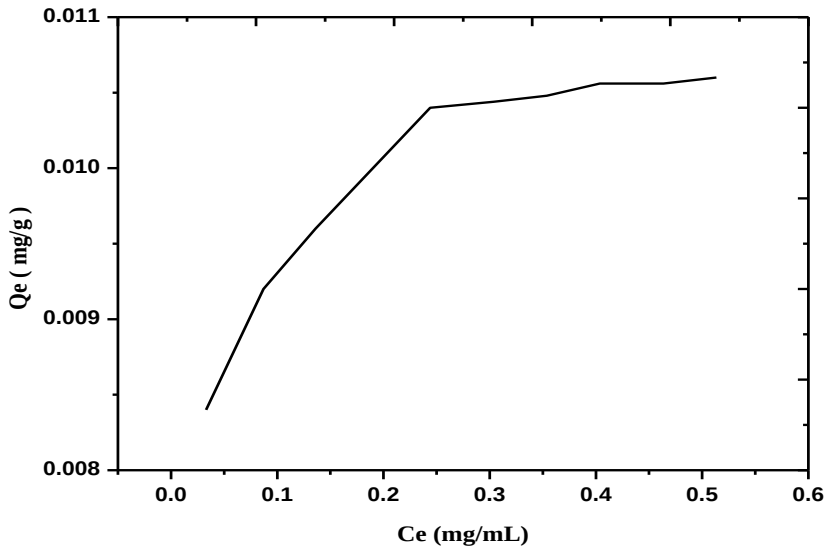

Figure B.3: Langmuir adsorption isotherm plot of Qe against Ce CdSe QDs@TU

The Freundlich's plot between $\ln Q_e$ against $\ln C_e$ gives a straight line with slope 1/n and intercept ln K_F, as represented in Figure B.4.

The Freundlich isotherm model gave $R^2 = 0.8119$, indicating that the adsorption process could not have taken place through a multilayer process. This result is confirmed by the n value of 0.0872, indicating that the adsorption was unfavourable.

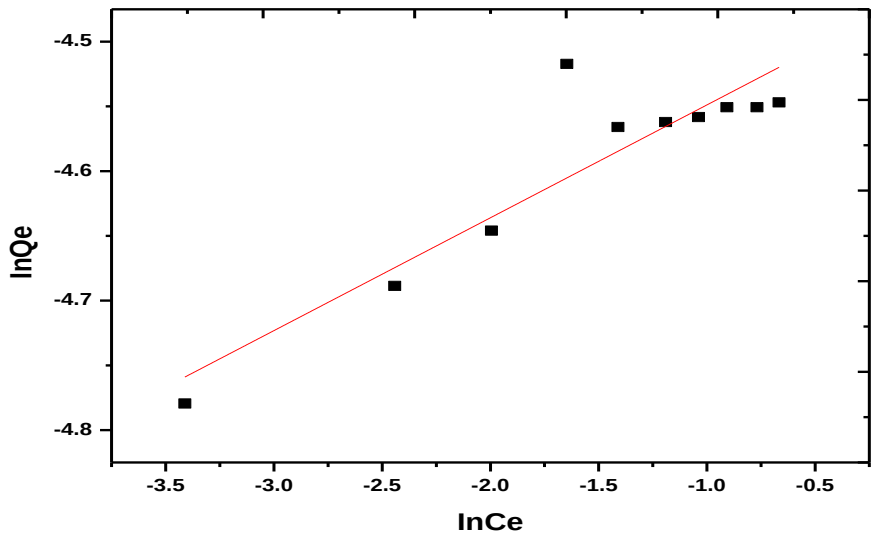

Figure B.4: Freundlich adsorption isotherm plot of In Qe against In Ce CdSe QDs@TU

Both the Langmuir and the Freundlich isotherms were used to analyse the adsorption behaviour of the CdSe QDs with respect to a surface modifier, thiourea.

The Langmuir isotherm assumes that the adsorption sites are homogeneous and that there is maximum adsorption capacity. The Freundlich isotherm, on the other hand, assumes that the adsorption sites are heterogeneous and that the adsorption strength decreases with increasing coverage.

As earlier alluded to, the values of R^2 = 0.99902 for the Langmuir model indicates that the adsorption behaviour of the modifying particles was homogenous and of a monolayer type. Both models have their own assumptions and limitations, and the choice of the model should be based on the specific characteristics of the system being studied, and in this case seeing that thiourea has a high tendency to donate its proton, leaving the sulphur atom with a lone pair of electrons, it is very easy to have an electrostatic bond forming between the partially positively charged atom of cadmium in the CdSe molecule with then now negatively charged atom of sulphur in the thiourea[232].

However, this does not prevent formation of van deer Waals forces among the molecules of CdSe QDs and thiourea.

Therefore, the Freundlich isotherm could not be used to describe the adsorption of thiourea onto CdSe QDs, because the actual properties of CdSe and that of thiourea might not necessarily conform to the accessions made by this model.

Table B.3: Langmuir and Freundlich model parameters

Type of model	Langmuir					Freundlich			
Parameter	Q_m(mg/g)	K_L(mL/mg)	R_L	R^2	R	n	K_f	R^2	R
Value	0.0108	0.9727	0.6556	0.99902	0.99956	0.0872	0.0115	0.8119	0.91258

Appendix C: C.1: Schematic diagram shows CdSe QDs synthesis, surface modification, functionalization, immobilization with the oligonucleotide capture probe and detection of target ssDNA analyte.

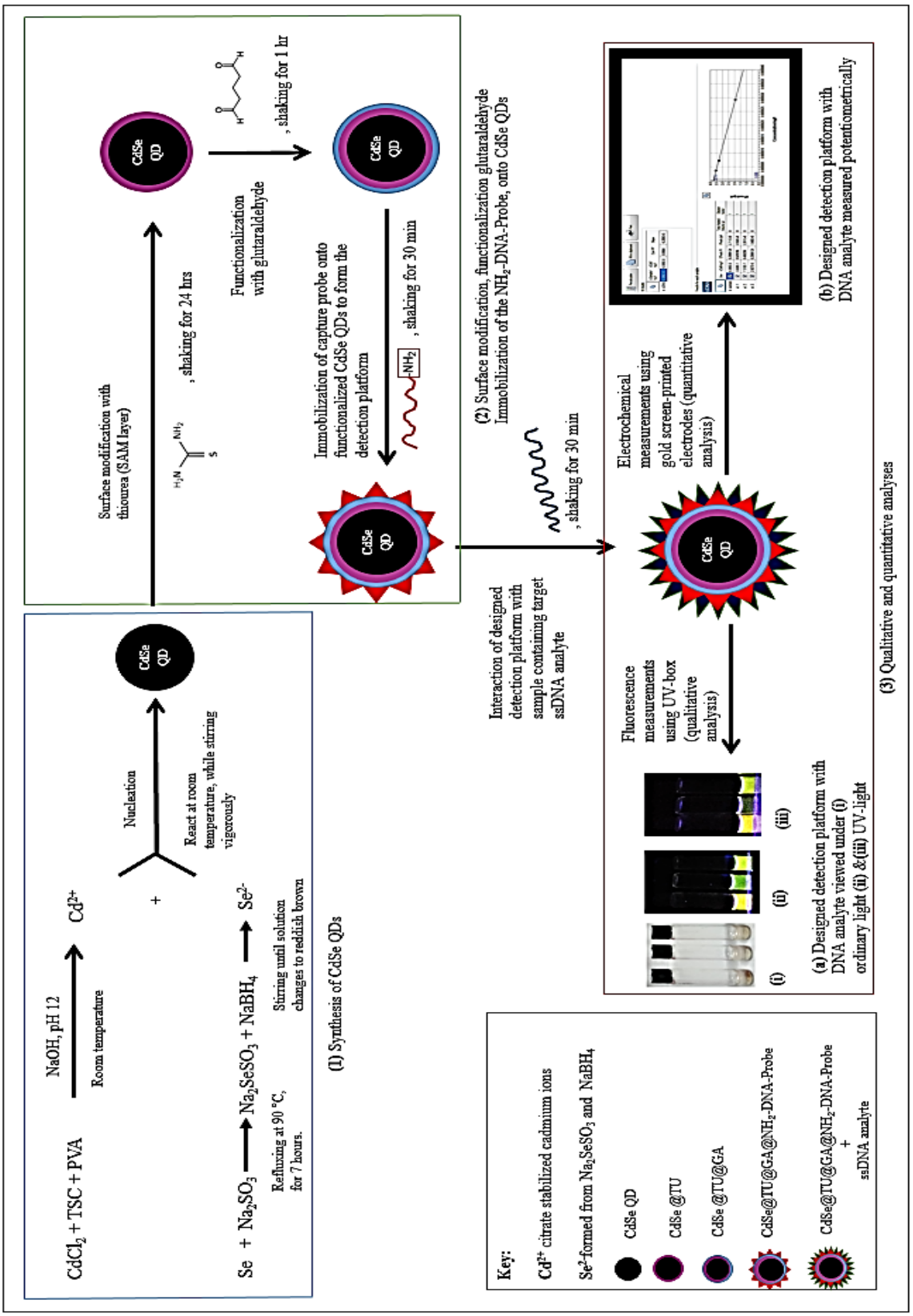

Appendix D: D.1: Sample calculation for the radius, R, of CdSe QDs, using Brus equation.

$$E_g = [E_{bulk} + \frac{h^2}{8R^2}\left(\frac{1}{m_e^*} + \frac{1}{m_h^*}\right) - \frac{1.8e^2}{4\pi\varepsilon_0\varepsilon_r R}]$$

Given values:

E_g = 3.43 eV

E_{bulk} = 1.78 eV

m_e^* = 0.13 m_0

m_h^* = 0.45 m_0

ε_r = 10 (for CdSe)

h = 6.626 × 10^{-34} J s

e = 1.602 × 10^{-19} C

ε_0 = 8.854 × 10^{-12} F/m

where, (m_0 = 9.11 × 10^{-31} kg)

Using the Brus equation (3), the following steps are taken:

Step 1: Converting eV to J:

ΔE = E_g - E_{bulk}

= 3.43 eV - 1.74 eV

= 1.690 eV

= 1.690 eV × 1.602 × 10^{-19} J/eV

= 2.707 × 10^{-19} J

Step 2: Calculating $\left(\frac{1}{m_e^*} + \frac{1}{m_h^*}\right)$:

m_e^* = 0.13 × 9.11 × 10^{-31} kg

= 1.1843 × 10^{-31} kg

m_h^* = 0.45 × 9.11 × 10^{-31} kg

= 4.0995 × 10^{-31} kg

$$= \left(\frac{1}{m_e^*} + \frac{1}{m_h^*}\right)$$

$$= \left(\frac{1}{1.1843 \times 10^{-31}} + \frac{1}{4.0995 \times 10^{-31}}\right)$$

= (8.444 × 10^{30} + 2.439 × 10^{30})

= 1.088 × 10^{31} kg

Step 3: Calculating confinement term coefficient $\left(\frac{h^2}{8}\right)$:

$= [\ \frac{(6.626 \times 10^{-34})^2}{8}]$

$= \left(\frac{4.390 \times 10^{-67}}{8}\right)$

$= 5.488 \times 10^{-68}$

$= 5.488 \times 10^{-68} \times 1.088 \times 10^{31}$

$= 5.971 \times 10^{-37}$

Step 4: Calculating Coulomb term coefficient $\left(\frac{1.8e^2}{4\pi\varepsilon_0\varepsilon_r}\right)$:

$= \frac{1.8e^2}{4\pi\varepsilon_0\varepsilon_r}$

$= \left[\frac{1.8 \times (1.602 \times 10^{-19})^2}{\left(4 \times \left(\frac{22}{7}\right) \times (8.854 \times 10^{-12}) \times 10\right)}\right]$

$= \left(\frac{4.620 \times 10^{-38}}{1.113 \times 10^{-9}}\right)$

$= 4.151 \times 10^{-29}$

Step 5: Writing the Brus equation:

$\Delta E = \left[\left(\frac{5.971 \times 10^{-37}}{R^2}\right) - \left(\frac{4.151 \times 10^{-29}}{R}\right)\right]$

Step 6: Substituting ΔE:

2.707×10^{-19} J$= \left[\left(\frac{5.971 \times 10^{-37}}{R^2}\right) - \left(\frac{4.151 \times 10^{-29}}{R}\right)\right]$

Step 7: Multiplying through by R^2:

$2.707 \times 10^{-19}\ R^2 = 5.971 \times 10^{-37} - (4.151 \times 10^{-29})\ R$

Step 8: Rearranging to a quadratic equation:

$2.707 \times 10^{-19}R^2 + 4.151 \times 10^{-29}R - 5.971 \times 10^{-37} = 0$

Step 9: Solving the quadratic equation:

Using the quadratic formula:

$R = \left(\frac{-b \mp \sqrt{(b^2 - 4ac)}}{2a}\right)$

a = 2.707×10^{-19}

b = 4.151×10^{-29}

c = -5.971×10^{-37}

$$= \left[\left(\frac{-\left(4.151 \times 10^{-29}\right) \mp \sqrt{((4.151 \times 10^{-29})^2) - [4 \times (2.707 \times 10^{-19}) \times (-5.971 \times 10^{-37})]}}{2 \times (2.707 \times 10^{-19})}\right)\right]$$

$$= \left[\left(\frac{-\left(4.151 \times 10^{-29}\right) \mp \sqrt{(1.723 \times 10^{-57}) - (-1.144 \times 10^{-54})}}{2 \times (2.707 \times 10^{-19})}\right)\right]$$

$$= \left[\left(\frac{-\left(4.151 \times 10^{-29}\right) \mp \sqrt{(1.146 \times 10^{-54})}}{2 \times (2.707 \times 10^{-19})}\right)\right]$$

$$= \left[\left(\frac{-\left(4.151 \times 10^{-29}\right) \mp (8.051 \times 10^{-28})}{2 \times (2.707 \times 10^{-19})}\right)\right]$$

$$= \left[\left(\frac{-\left(4.151 \times 10^{-29}\right) \mp (8.051 \times 10^{-28})}{5.414 \times 10^{-19}}\right)\right]$$

$$= \left(\frac{7.636 \times 10^{-28}}{5.414 \times 10^{-19}}\right)$$

$= 1.410 \times 10^{-9}$ nm

= 1.410 nm

Therefore the radius, R, is 1.410 nm, meaning that the average diameter of the CdSe QDs is approximately 2.82 nm.

Appendix E: E.1: Local Purchase Order List for the Purchased Oligonucleotides Used in the Design of the GM Cereal Detection Platform

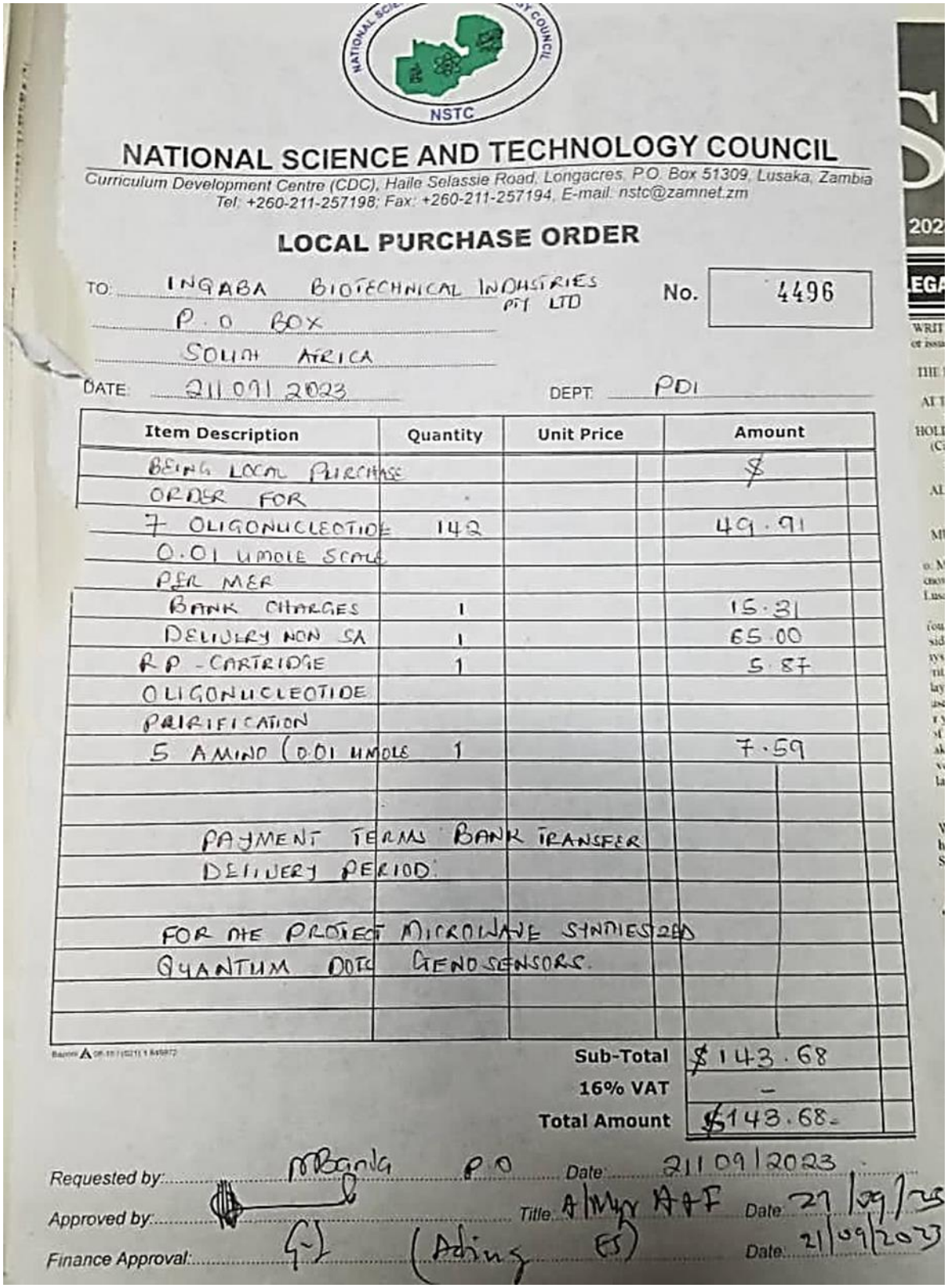

NATIONAL SCIENCE AND TECHNOLOGY COUNCIL

Curriculum Development Centre (CDC), Haile Selassie Road, Longacres, P.O. Box 51309, Lusaka, Zambia
Tel: +260-211-257198; Fax: +260-211-257194, E-mail: nstc@zamnet.zm

LOCAL PURCHASE ORDER

TO: INQABA BIOTECHNICAL INDUSTRIES PTY LTD
P. O BOX
SOUTH AFRICA

No. 4496

DATE: 21/09/2023 DEPT: PDI

Item Description	Quantity	Unit Price	Amount
BEING LOCAL PURCHASE ORDER FOR			$
7 OLIGONUCLEOTIDE 142 0.01 UMOLE SCALE PER MER			49.91
BANK CHARGES	1		15.31
DELIVERY NON SA	1		65.00
RP - CARTRIDGE OLIGONUCLEOTIDE PURIFICATION	1		5.87
5 AMINO (0.01 UMOLE	1		7.59
PAYMENT TERMS BANK TRANSFER			
DELIVERY PERIOD:			
FOR THE PROJECT MICROWAVE SYNTHESIZED QUANTUM DOTS GENOSENSORS.			
		Sub-Total	$143.68
		16% VAT	-
		Total Amount	$143.68

Requested by: MBanda P O Date: 21/09/2023

Approved by: Title: A/MGR A&F Date: 21/09/23

Finance Approval: (Acting ES) Date: 21/09/2023

Appendix E: E.2: Commercial Invoice for Purchase of Oligonucleotides Used in the Design of the GM Cereal Detection Platform

inqaba biotec™

Africa's Genomics Company

Inqaba Biotechnical Industries (Pty) Ltd

Co. Reg. No: 2001/011245/07
VAT No: 4150197251

Commercial Invoice

Exporter

Inqaba Biotechnical Industries (Pty) Ltd
(IBS007)
PostNet Suite #017
Private Bag X12
Menlo Park, Gauteng
0102
South Africa
+27 12 343 5829
info@inqababiotec.co.za

inqaba biotec™
Inqaba Biotechnical Industries (Pty) Ltd
Co. Reg. No. 2001/011245/07
VAT No: 4150197251

Export References

Date:	**19.10.2023**
Invoice #:	**SCIN03992**
Exporter #:	**20053405**
Incoterms:	**DAP**

Reason:
For Sales Purpose, Permanent Export, Sold Product

Packaging Type

Padded envelope in a DHL flyer bag

Storage and Notes

Keep at room temperature.
NON HAZARDOUS
NON INFECTIOUS

Consignee

University of Zambia (UNZ005), Happy Mabo
Natural Sciences, Department of Chemistry
Natural Sciences Buildings
Lusaka 260
Zambia
/ +260 977661213
hy.mb00@yahoo.com
ATT: Happy Mabo

Notify Party

University of Zambia (UNZ005), Happy Mabo
Natural Sciences, Department of Chemistry
Natural Sciences Buildings
Lusaka 260
Zambia
/ +260 977661213
hy.mb00@yahoo.com

Code	Description	Quantity	Unit Price	Commercial Value
	IT23269ZA0753559 / S2306539			
IB OL0001	7 Oligonucleotide, 0.01 umole scale, per mer	142.0	$ 0.35	$ 49.91
IB OM0021	5' Amino (0.01 umole)	1.0	$ 7.59	$ 7.59
IB PU0001	RP-cartridge oligonucleotide purification	1.0	$ 5.87	$ 5.87
			Shipment Sub-Total	$ 63.37
			Freight Charges	$ 80.31
			Total	$ 143.68

I/We hereby certify that the information on this invoice is true and correct and that the contents of this shipment are as above stated.
inqaba biotec™:

Signature of Exporter

Date 2023/10/19

PostNet Suite #017, Private Bag X12, Menlo Park, 0102, South Africa • Phone: +27 12 343 5829 • Fax: +27 86 677 8409
Email: info@inqababiotec.co.za • Website: http://www.inqababiotec.co.za

Page: 1 / 1

Appendix E: E.3: Packaging List Notice for the Purchased Oligonucleotides Used in the Design of the GM Cereal Detection Platform

Africa's Genomics Company

Inqaba Biotechnical Industries (Pty) Ltd

Co. Reg. No: 2001/011245/07
VAT No: 4150197251

Packing List

Exporter

Inqaba Biotechnical Industries (Pty) Ltd
(IBS007)
PostNet Suite #017
Private Bag X12
Menlo Park, Gauteng
0102
South Africa
+27 12 343 5829
info@inqababiotec.co.za

Inqaba Biotechnical Industries (Pty) Ltd
Co. Reg. No. 2001/011245/07
VAT No: 4150197251

Export References

Date:	19.10.2023
Invoice #:	SCIN03992
Exporter #:	20053405
Incoterms:	DAP

Reason:
For Sales Purpose, Permanent Export, Sold Product

Packaging Type

Padded envelope in a DHL flyer bag

Storage and Notes

Keep at room temperature.
NON HAZARDOUS
NON INFECTIOUS

Consignee

University of Zambia (UNZ005), Happy Mabo
Natural Sciences, Department of Chemistry
Natural Sciences Buildings
Lusaka 260
Zambia
/ +260 977661213
hy.mb00@yahoo.com
ATT: Happy Mabo

Packing Information

1 box with 48 x 38 x 1 CM and 1 KG

Total 1 boxes
Total weight: 1kG

Packing Information

Reference	Code	Description	Quantity
	BOX NUMBER DHL flyer bag		
IT23269ZA0753559 SA2023/156806	IB OL0001	7 Oligonucleotide, REF#1059655	1.0

I/We hereby certify that the information on this packing list is true and correct and that the contents of this shipment are as above stated.
inqaba biotec™:

Signature of Exporter

2023/10/19
Date